II. Searching for fingerprints of brain cognitive activity.

Włodzisław Duch

Neurocognitive Laboratory,
Center of Modern Interdisciplinary Technologies,
Dept. of Informatics, Faculty of Physics, Astronomy & Informatics,
Nicolaus Copernicus University

Google: W. Duch

BRANDY, 26-27 June, Val del Sol

On the threshold of a dream …

How to recognize specific activity changes of the brain networks?

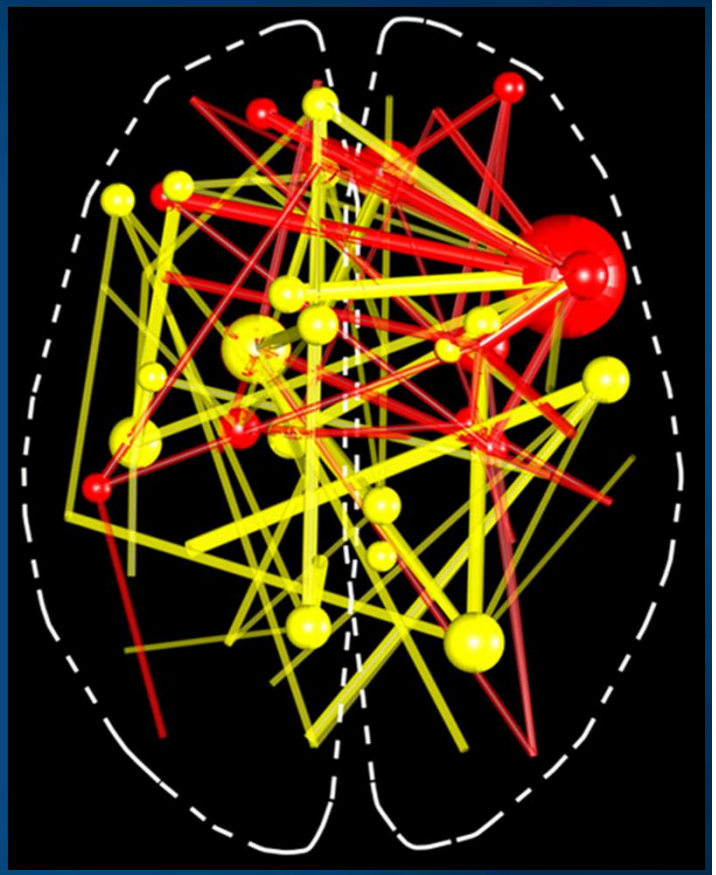

- Dynamic functional brain networks.
- Simulation of brain networks.
- EEG/MEG microstates.
- Spectral fingerprints.
- Simulation of brain networks.
- Conclusions.

Final goal: Use your brain to the max!
Optimization of brain processes?

Duch W. (2012) Mind-Brain Relations, Geometric Perspective and Neurophenomenology, American Philosophical Association Newsletter 12(1), 1-7.

Possible form of Brain Fingerprints

fMRI: BFP is based on **V(X,t)** voxel intensity of fMRI BOLD signal changes, contrasted between task and reference activity or resting state.
EEG: spatial, spatio-temporal, ERP maps/shapes, coherence, various phase synchronization indices.

1. **Spatial/Power**: direct localization/reconstruction of sources.
2. **Spatial/Synch**: changes in functional graph network structure.
3. **Spectral fingerprinting** (MEG, EEG), localized power distributions.
4. **EEG** microstates, sequences & transitions, dynamics in ROI space.
5. **Frequency/Power**: ERS/ERD smoothed patterns E(X,t,f).
6. **EEG decomposition into components:** ICA, CCA, tensor, RP ...
7. **ERP power maps**: spatio-temporal averaged energy distributions.
8. Model-based: **The Virtual Brain**, integrating EEG/neuroimaging data.

Neuroplastic changes of connectomes and functional connections as results of training for optimization of brain processes.

Dynamic functional brain networks

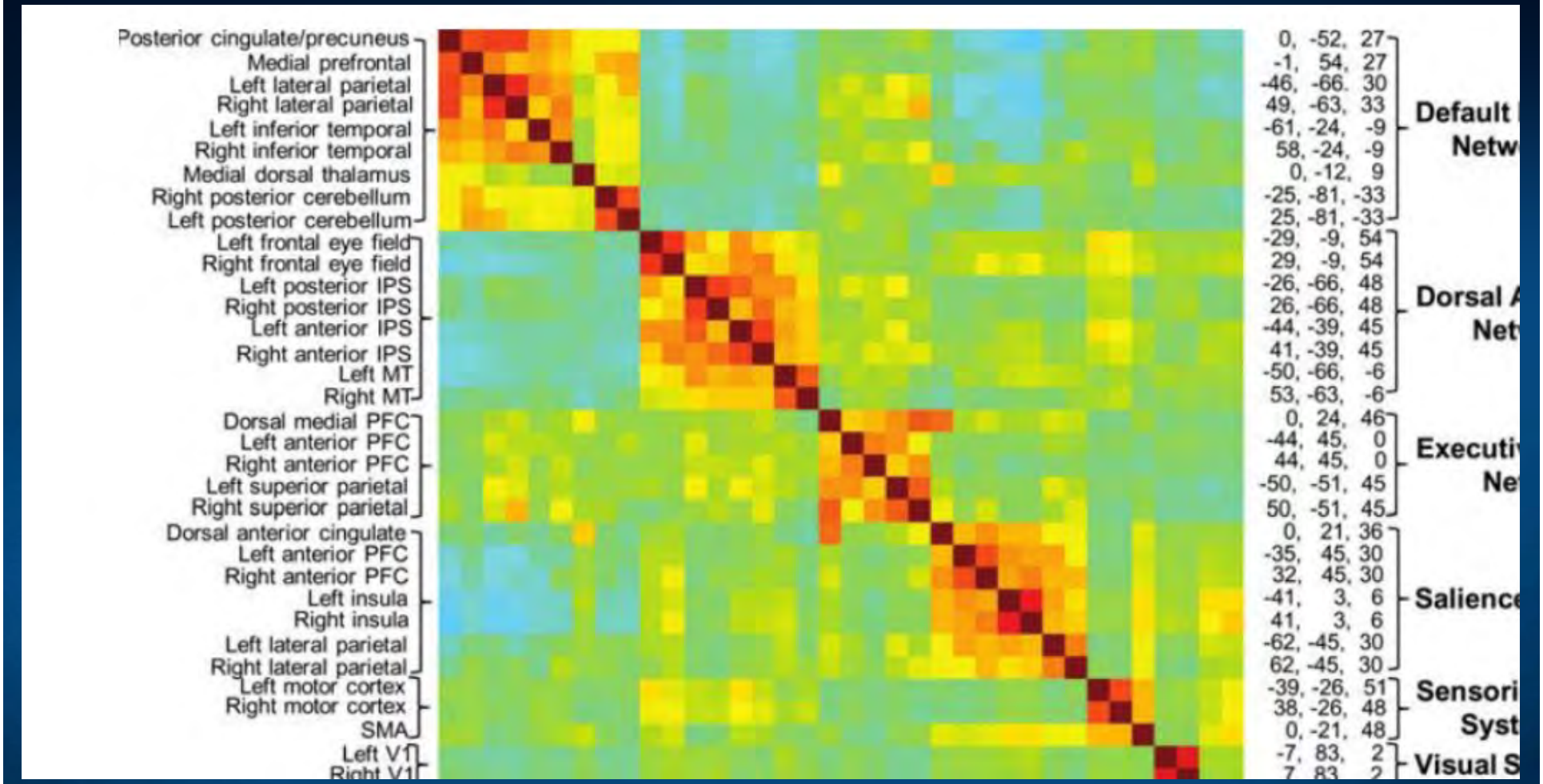

Correlation matrix representing resting-state functional connectivity between selected brain regions Shows stronger connectivity for 7 large-scale brain networks: default mode (DM), dorsal attention (DAT), executive control network (FPN, CON), salience (SAL), sensorimotor (SOM), visual (VSN), auditory (ASN). Switching DMN ⇔ Salience ⇔ FPN

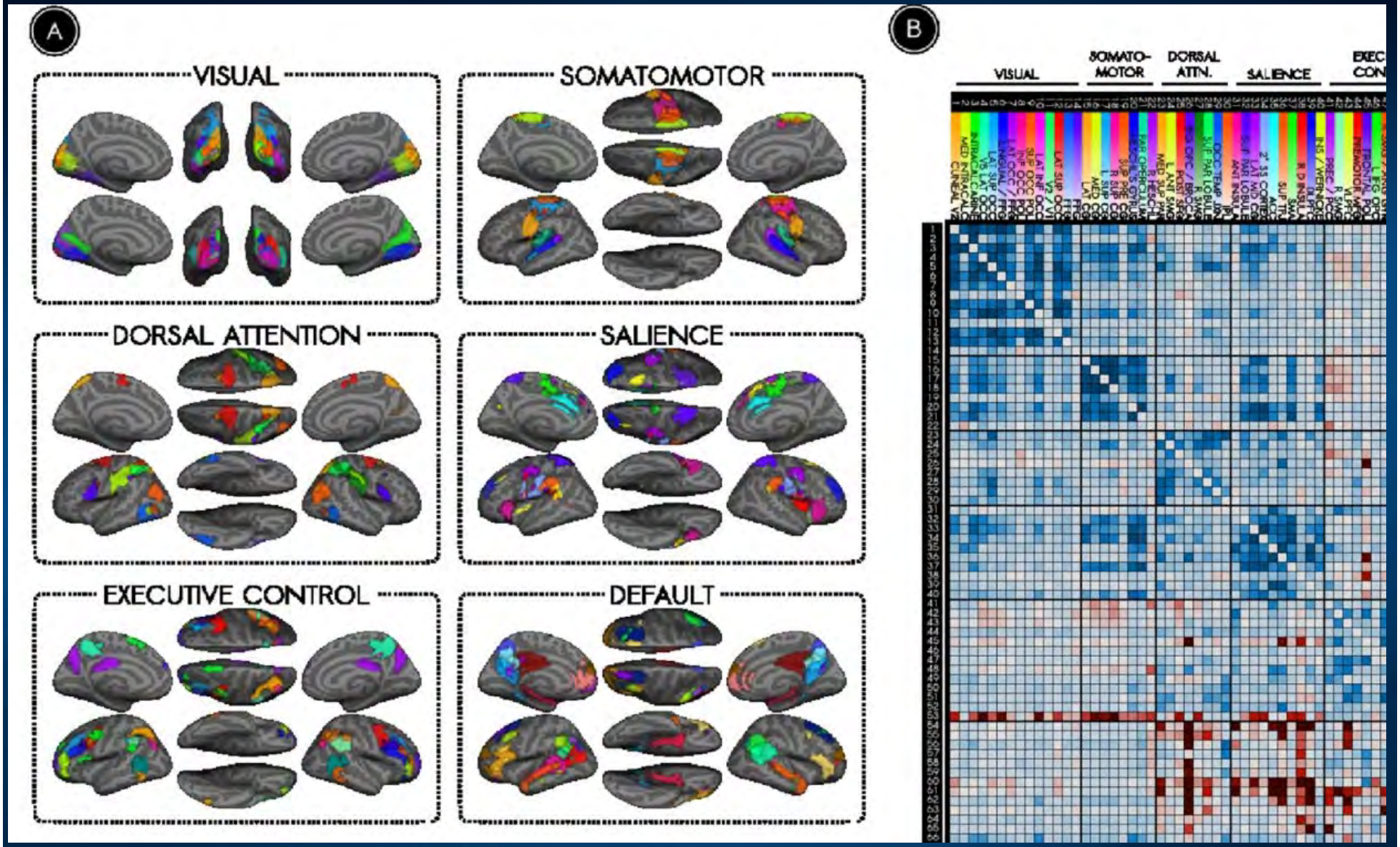

Ciric et.al. (2017). Contextual connectivity: A framework for understanding the intrinsic dynamic architecture of large-scale functional brain networks. *Scientific Reports* 7, 6537

Ciric et.al. (2017). Contextual connectivity: A framework for understanding the intrinsic dynamic architecture of large-scale functional brain networks. *Scientific Reports*.

Correlations of 6 canonical networks.

Perception,
Action-attention
DMN (Default Mode Network)

Each has up to 10 different network connectivity states (NC-states), rather stable for single subjects, ex.
DMN has usually 7-9.

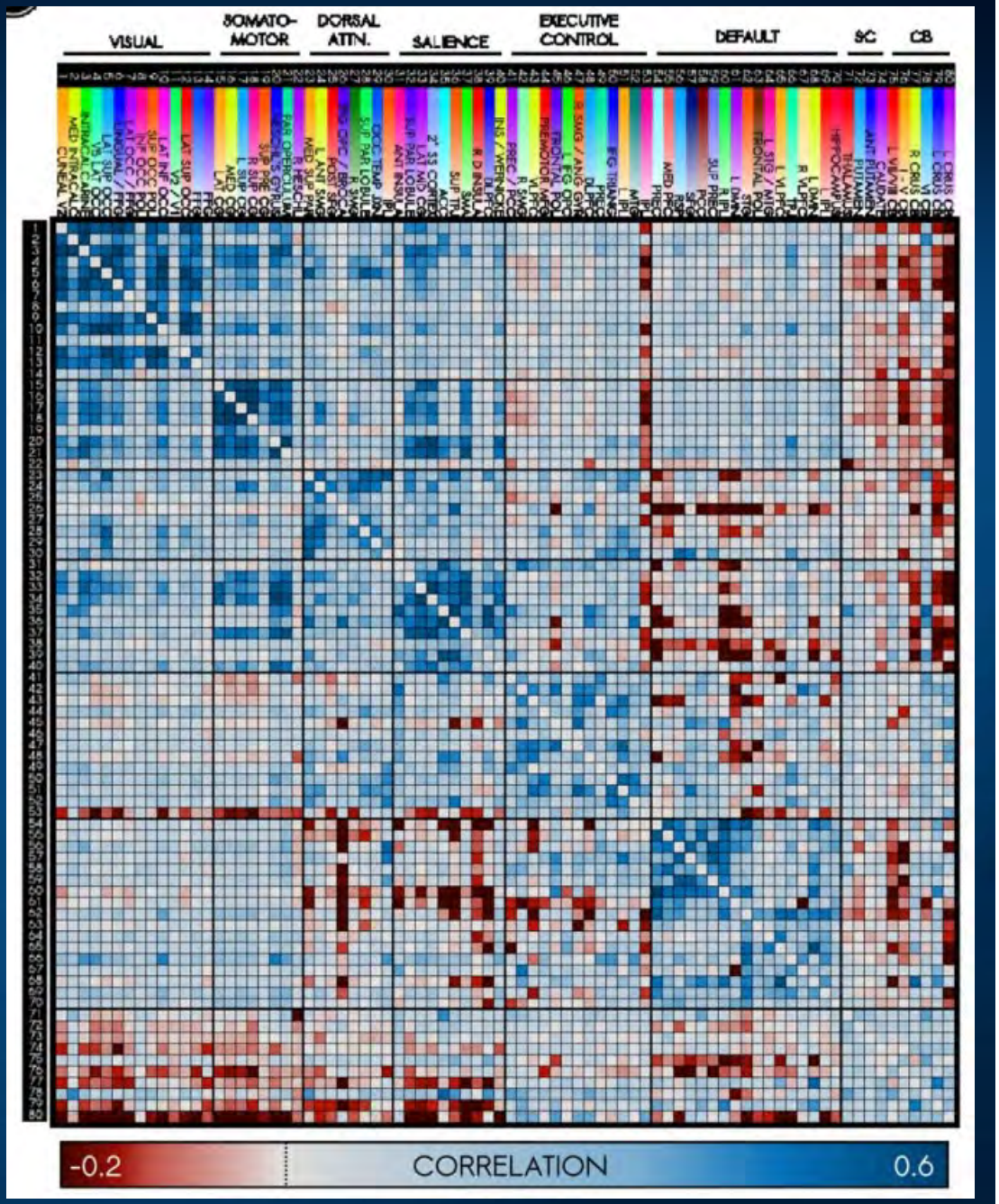

DMN time-averaged baseline.
Between-network allegiances (prob. that nodes are in the same community). Rim colors = canonical networks, rim length = greater allegiance to other networks, size of connections = strength of between-network allegiances.
DMN1: weak within-network allegiance strong to DAT, SAL, and VIS.

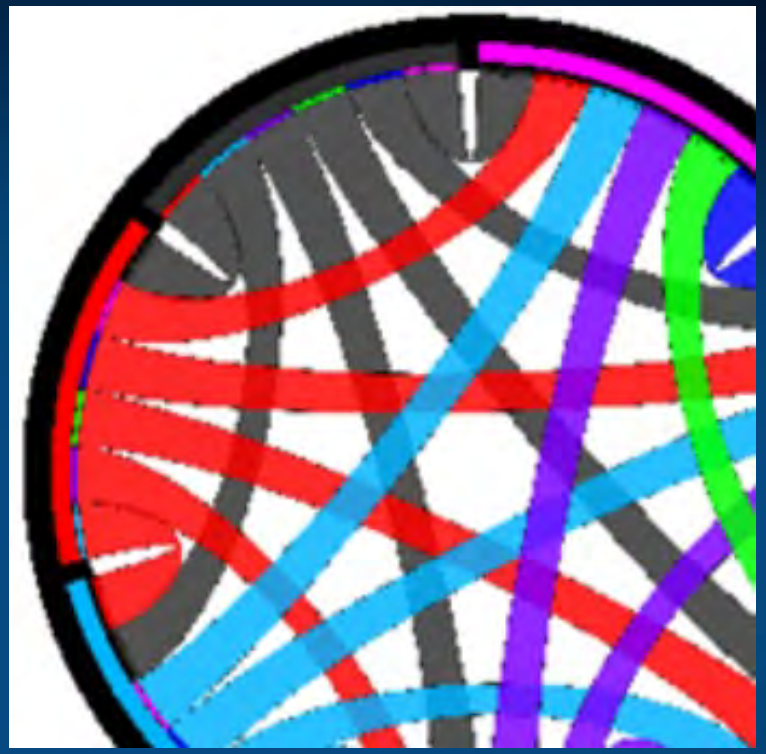

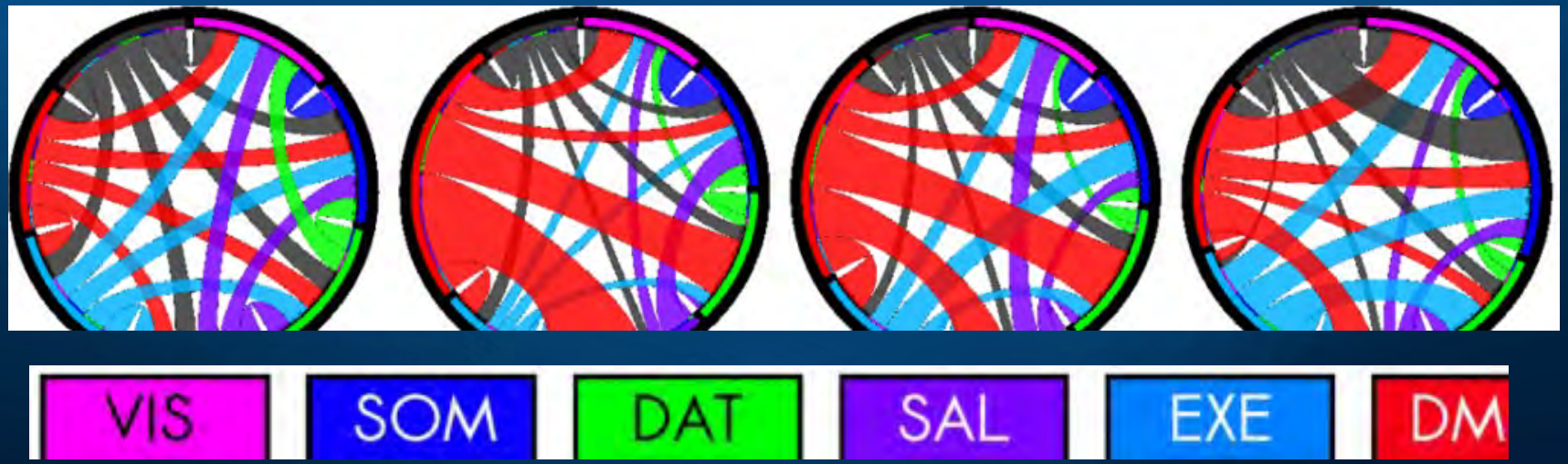

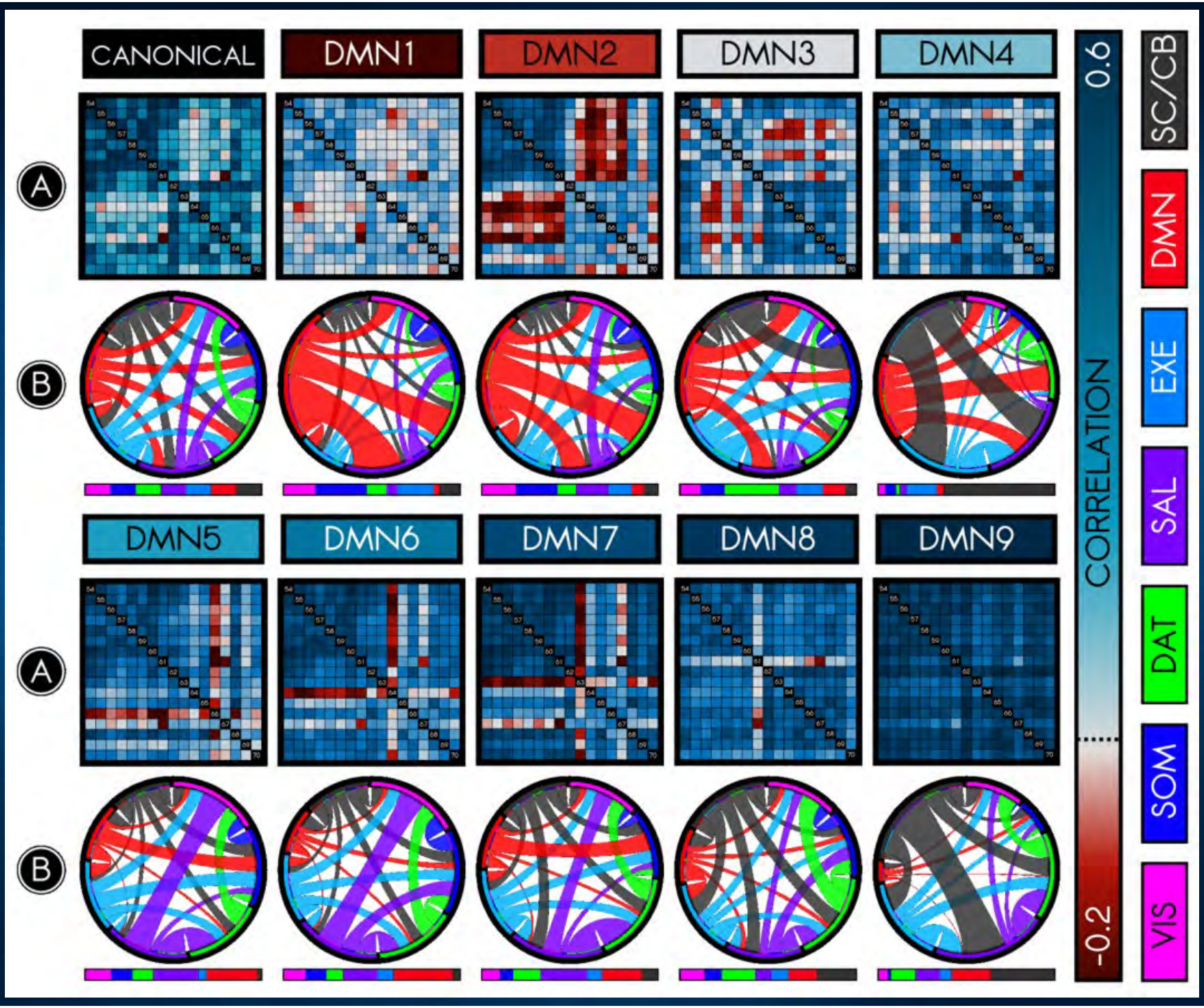
CANONICAL
DMN1
DMN2
DMN3
DMN4
DMN5
DMN6
DMN7
DMN8
DMN9
A
B
A
B
CORRELATION
0.6
-0.2
SC/CB
DMN
EXE
SAL
DAT
SOM
VIS

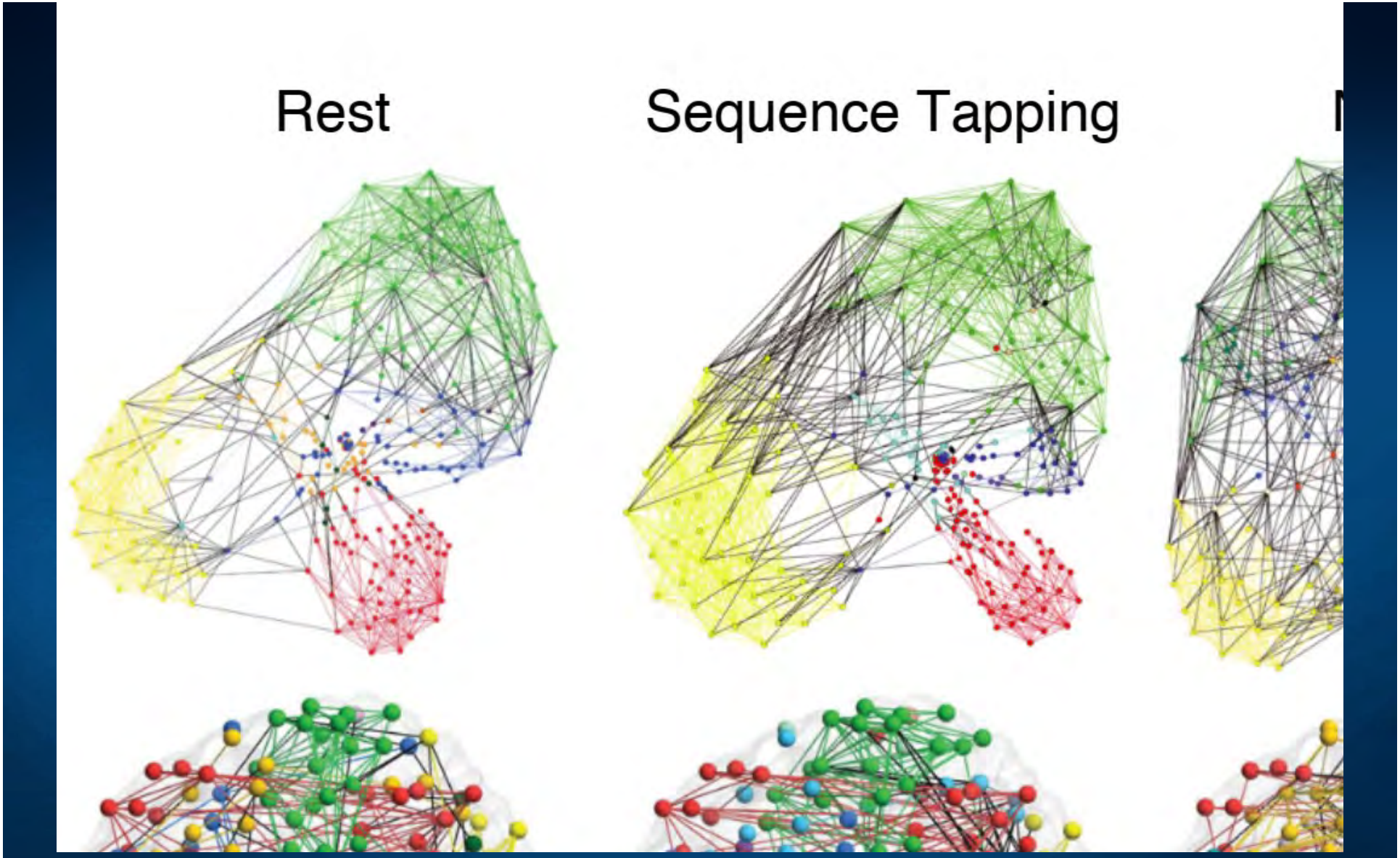

Color edges = within-module connections, black edges = between-module connections. Cohen and D'Esposito (2016). The segregation and integration of distinct brain networks and their relationship to cognition.
J. of Neurosci, 36(48):12083–12094

Questions

Global Neuronal Workspace Theory (Deahene et al. 1998): brain processes underlying effortful tasks require two main computational spaces:

- a set of specialized and modular perceptual, motor, memory, evaluative, and attentional processors;
- a unique global workspace composed of distributed and heavily interconnected neurons with long-range axons.

Workspace neurons are mobilized in effortful tasks for which the specialized processors (Kahneman's System 1) do not suffice (System 2), mobilize or suppress contribution of specific processor neurons.

1. Can the whole-brain network properties change during performance?
2. Do modularity, path length, global, local efficiency and other network measures dependent on the cognitive load?

Finc, K., Bonna, K., Lewandowska, M., Wolak, T., Nikadon, J., Dreszer, J., Duch W, Kühn, S. (2017). Transition of the functional brain network related to increasing cognitive demands. Human Brain Mapping, 38(7), 3659–3674.

Cognitive load on whole-brain network

35 participants (17 females; Mean age = 22.6 ± 3.1; 19-31).

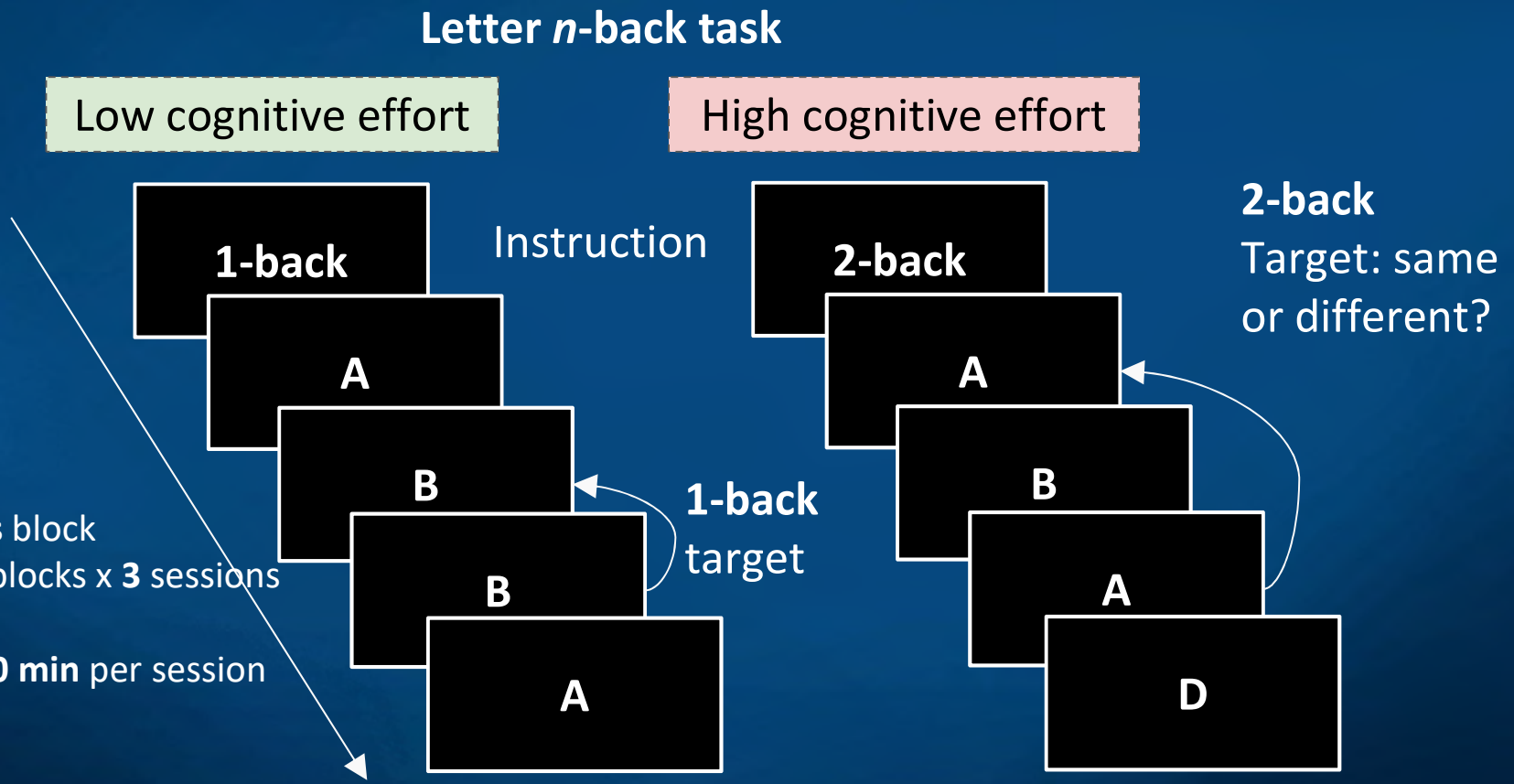

Finc et al, Human Brain Mapping, 2017

Human connectome and MRI/fMRI

Node definition (parcelation)

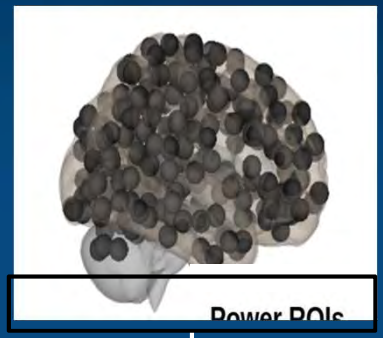

Signal extraction

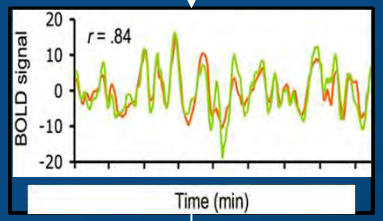

Correlation calculation

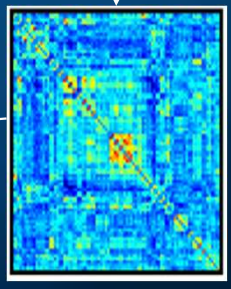

Correlation matrix

Binary matrix

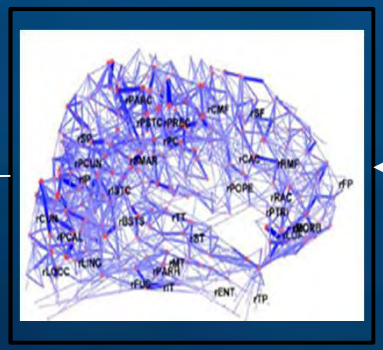

Whole-brain graph

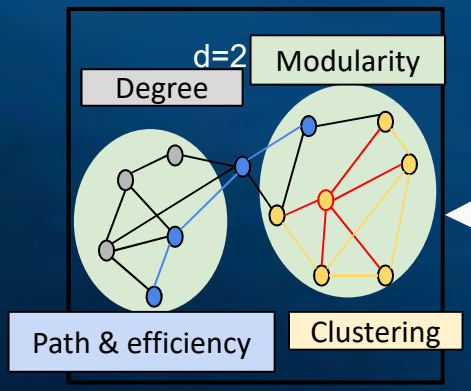

Graph theory

Structural connectivity

Functional connectivity

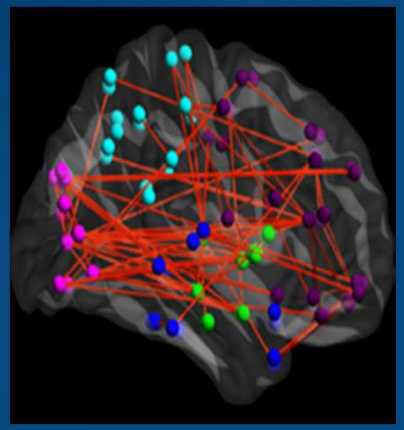

Many toolboxes available for such analysis.

Bullmore & Sporns (2009)

Data workflow

Two experimental conditions: 1-back, 2-back

Node definition

Anatomical parcellation (**90** nodes)

Functional parcellation (**264** nodes)

Weighted correlation matrices

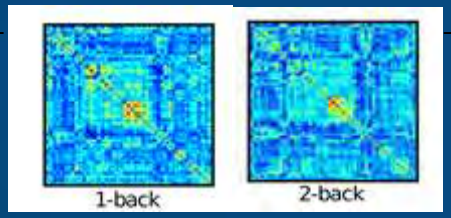

Fisher's *z*-scores

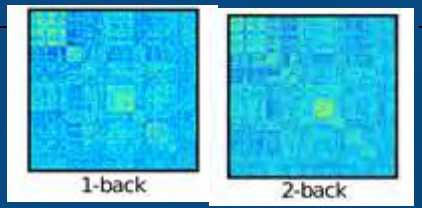

Binary correlation matrices

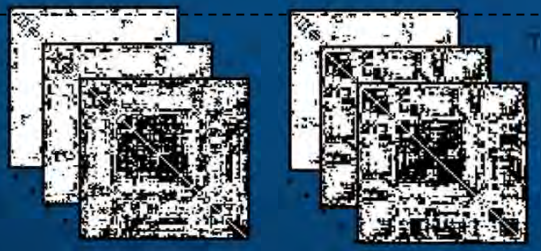

Threshold (0.01 - 0.6)

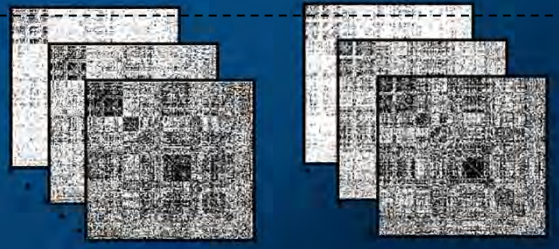

global efficiency | **local efficiency** | **modularity**

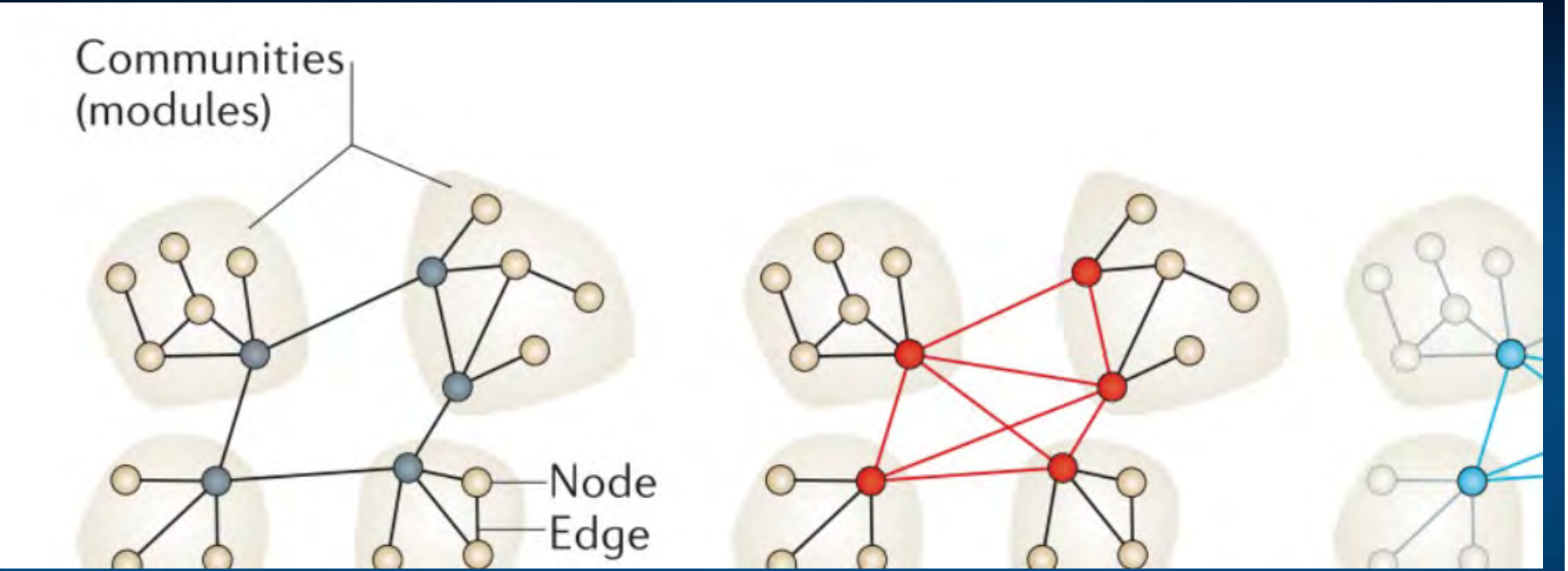

Network neuroscience is focused on identifying network structures. Hubs, rich club and core of the network. Hubs connect modules via long-distance connections. Hubs are also often densely interconnected forming so called ’rich club’ or integrated core.

Bullmore and Sporns (2012) The economy of brain network organization. Nature Reviews Neuroscience, 13(5):336.

Brain modules and cognitive processes

Simple and more difficult tasks, requiring the whole-brain network reorganization.

Left: 1-back

Right: 2-back

Average over 35 participants.

Left and midline sections.

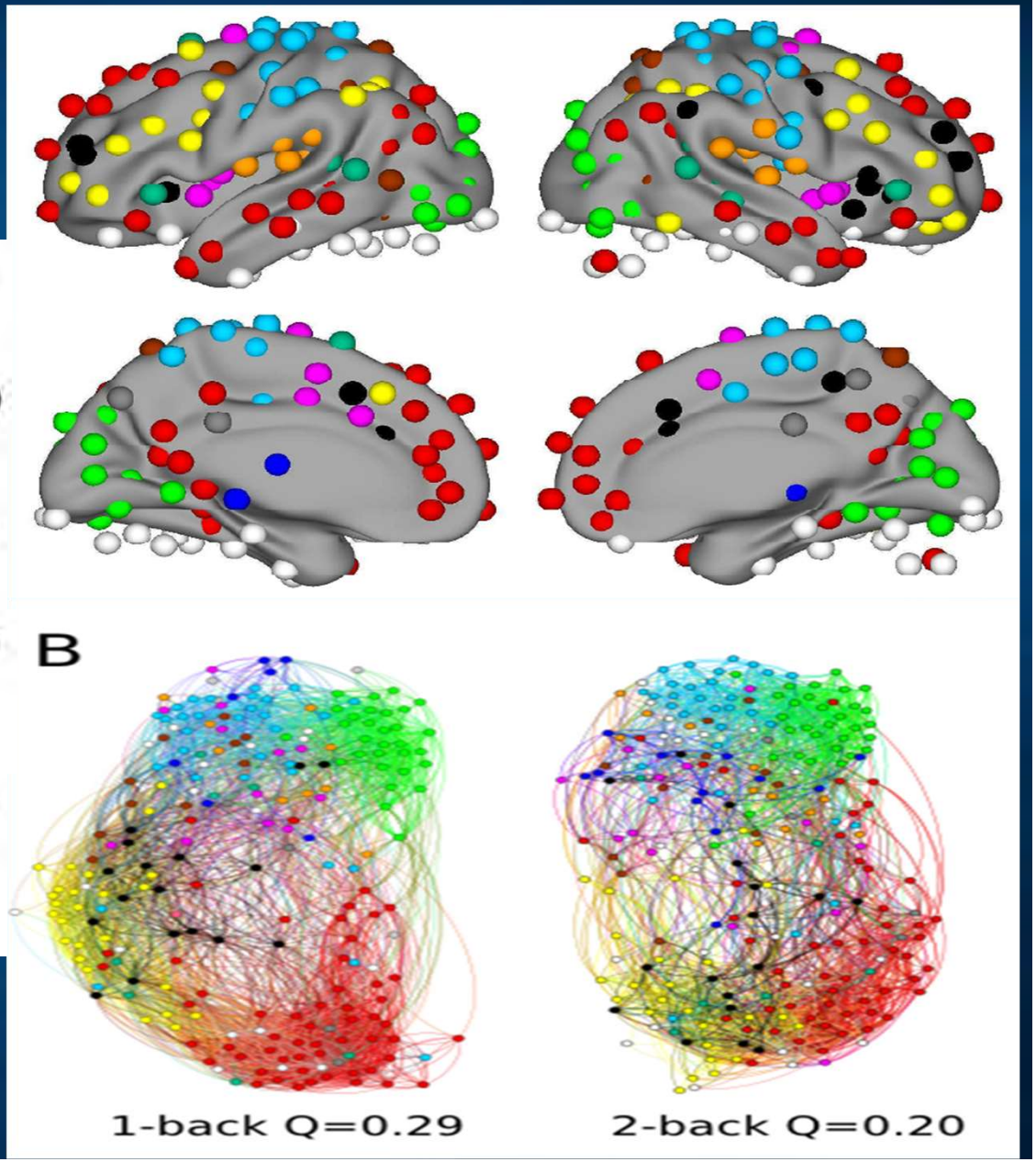

K. Finc et al, HBM (2017).

Brain modules and cognitive processes

Simple and more difficult tasks, requiring the whole-brain network reorganization.

Left: 1-back local hubs

Right: 2-back local hubs

Average over 35 *participants.*

Dynamical change of the landscape of attractors, depending on the cognitive load. Less local (especially in DMN), more global binding (especially in PFC).

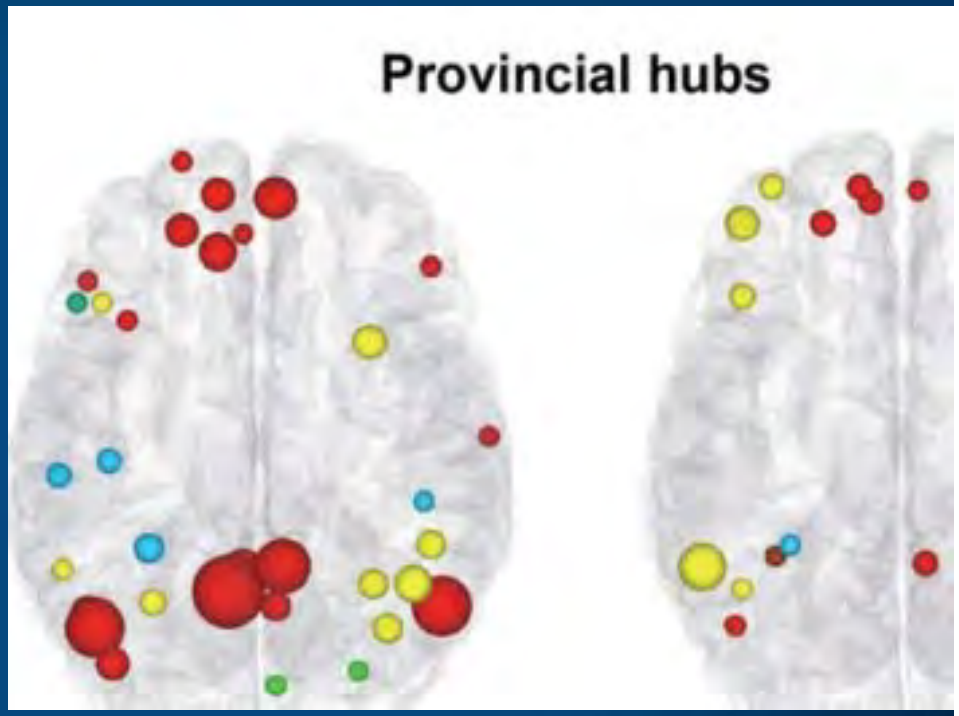

K. Finc et al, HBM (2017).

Brain modules and cognitive processes

Simple and more difficult tasks, requiring the whole-brain network reorganization.

Left: 1-back connector hubs

Right: 2-back connector hubs

Average over 35 *participants.*

Dynamical change of the landscape of attractors, depending on the cognitive load – System 2 (Khaneman).
DMN areas engaged in global binding!

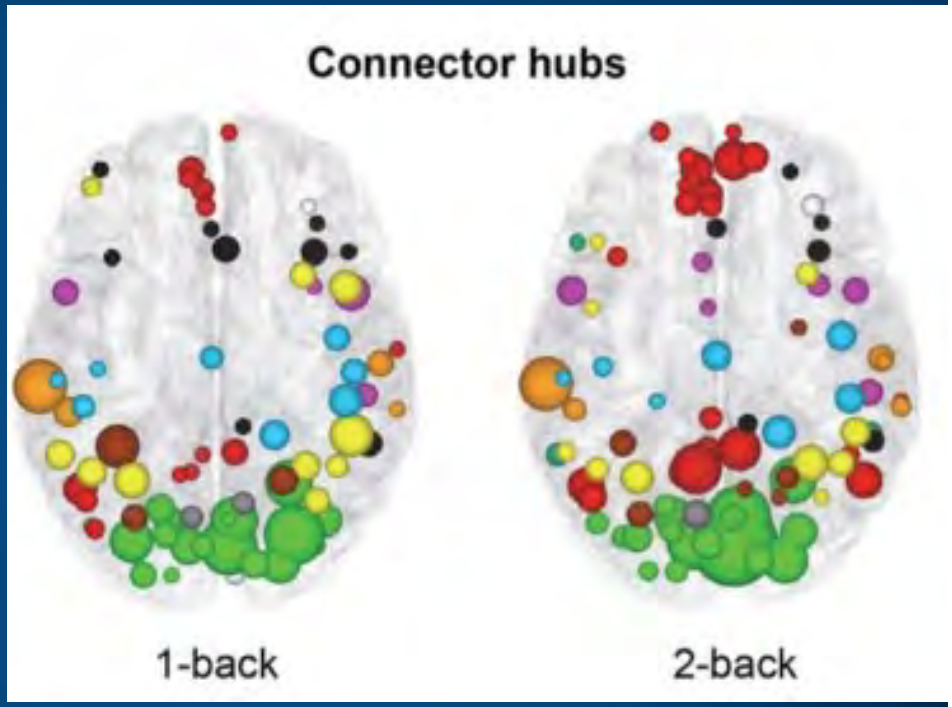

K. Finc et al, HBM (2017).

Changes in modularity

Modularity metric: fraction of within-community edges in the network minus such fraction for randomly connected network with unchanged community structure.

Parcellation
AAL, 90 ROI

Parcellation
264 ROI
functional

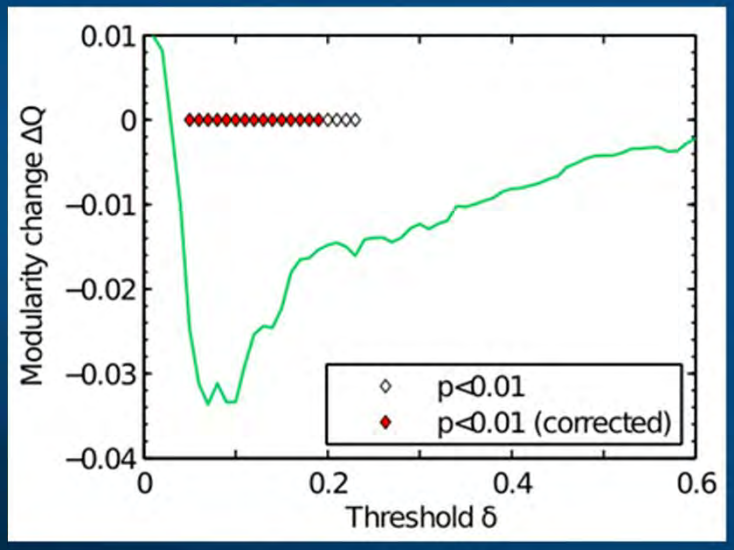

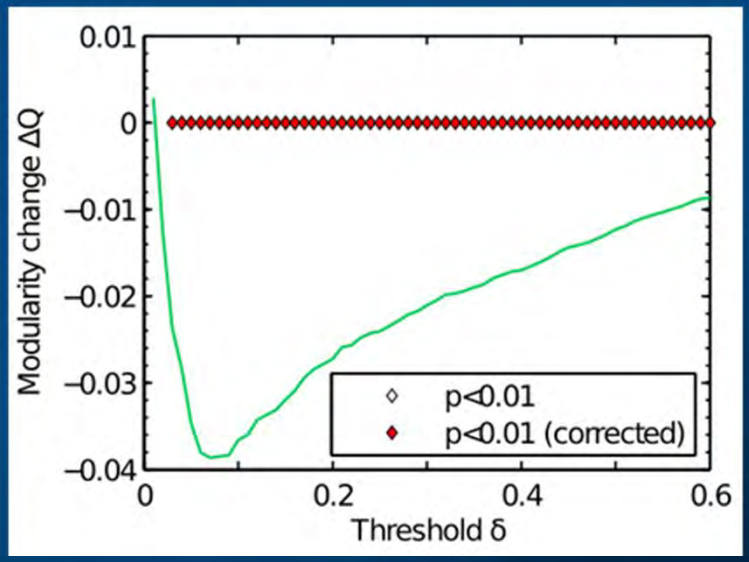

Modularity for both parcellations significantly decreases for thresholds ~0.1.
Coarse parcellation washes out many effects, especially strong correlations.

Finc et al, Human Brain Mapping, 2017

Changes in efficiency

Global efficiency ~ inverse of characteristic path length
Local efficiency ~ clustering coefficient (Latora & Marchiori, 2001).

Parcellation
AAL, 90 ROI

Parcellation
264 ROI
functional

Global efficiency

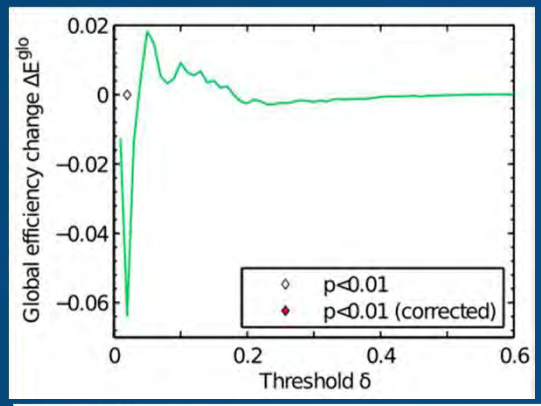

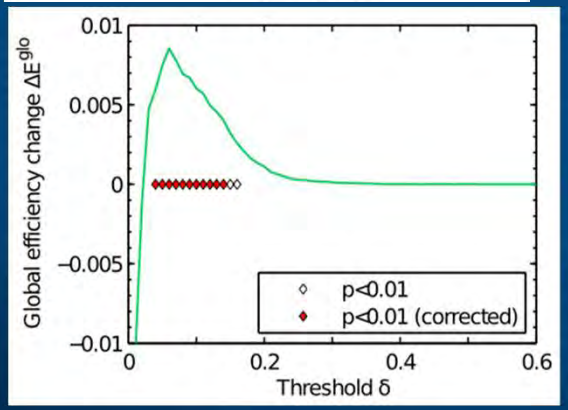

Local efficiency

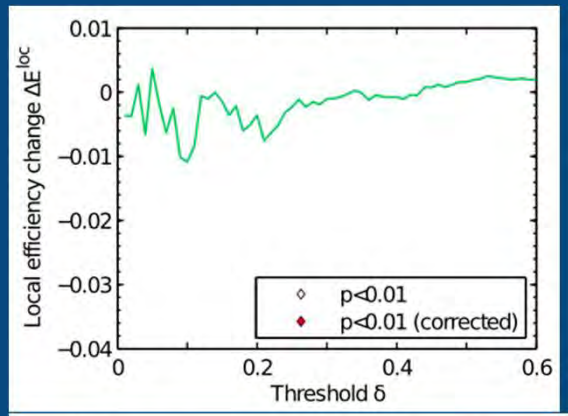

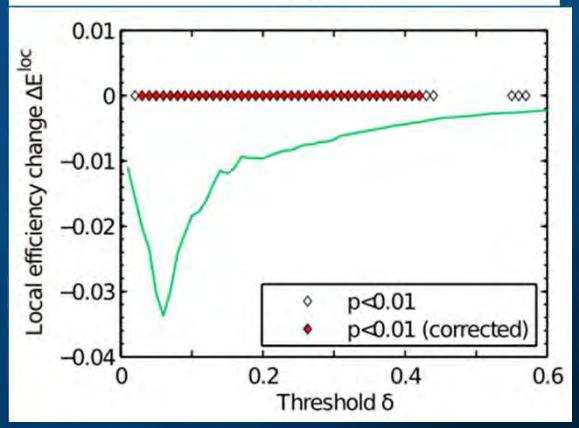

Finc et al, Human Brain Mapping, 2017

Cognitive load

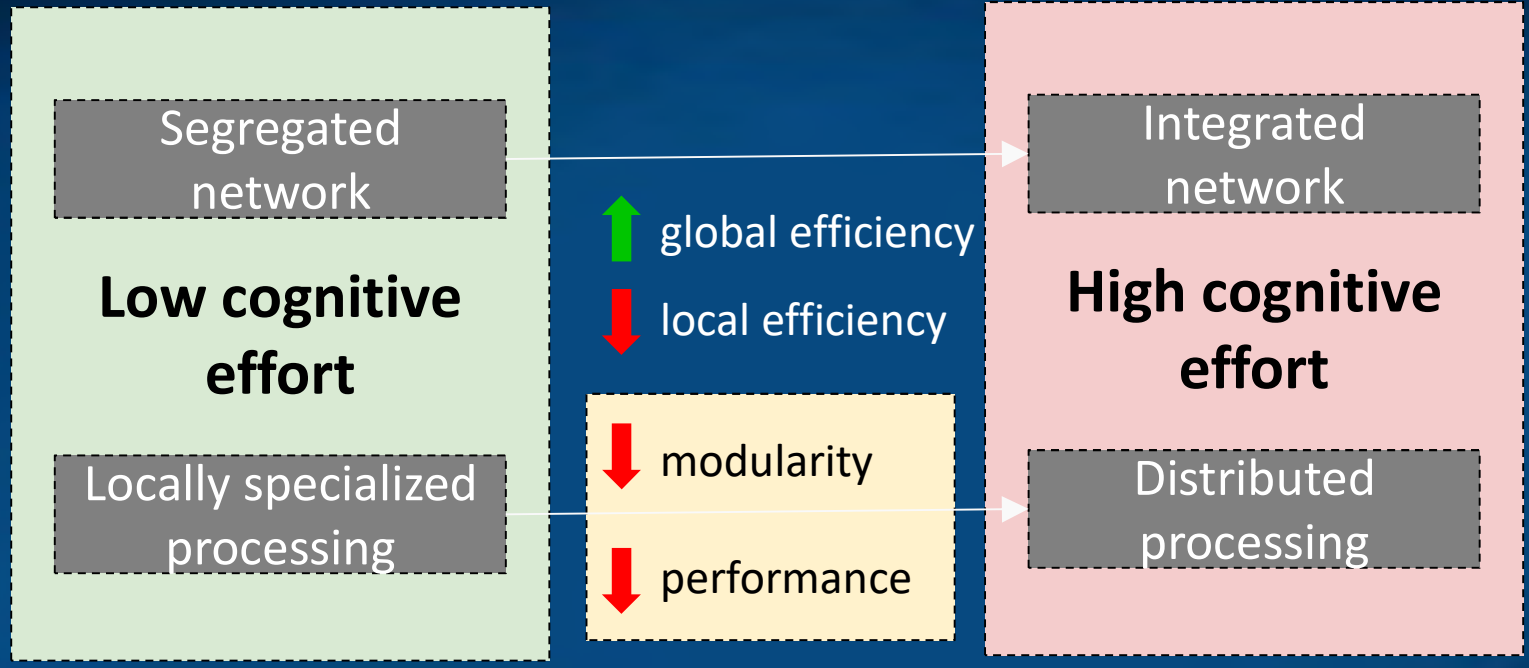

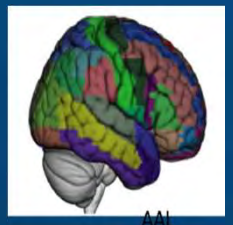

≠

Parcellation into 264 regions (10 mm spheres) shows subnetworks more precisely than for 90 regions; only a small subgroup of neurons in each ROI is strongly correlated.

Resting state/cognitive performance

Characteristic path length λ	Intellectual performance
Modularity	Working memory performance
Modularity	Working memory capacity

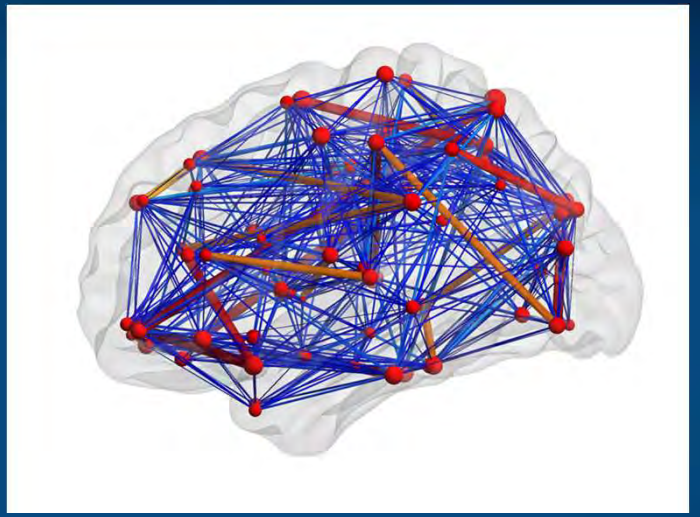

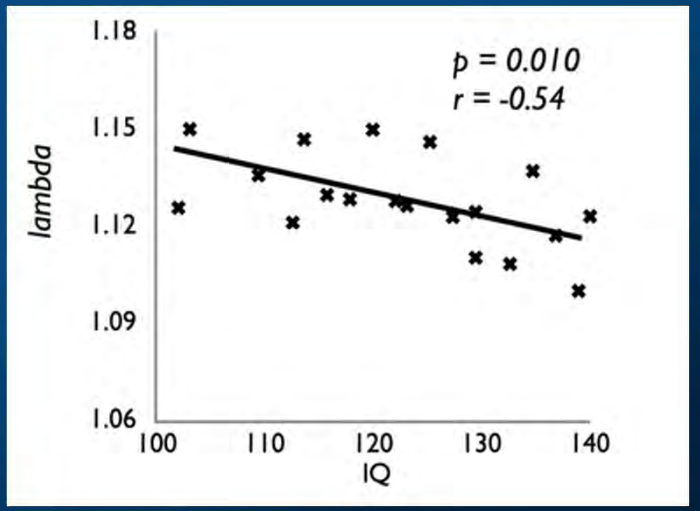

Network modularity ⇔ higher working memory capacity and performance.

High connectivity within modules and sparse connections between modules increases effective cooperation of brain regions, is associated with higher IQ.

van den Heuvel *et al.* (2009) | Stevens *et al.* (2012)

Working memory training

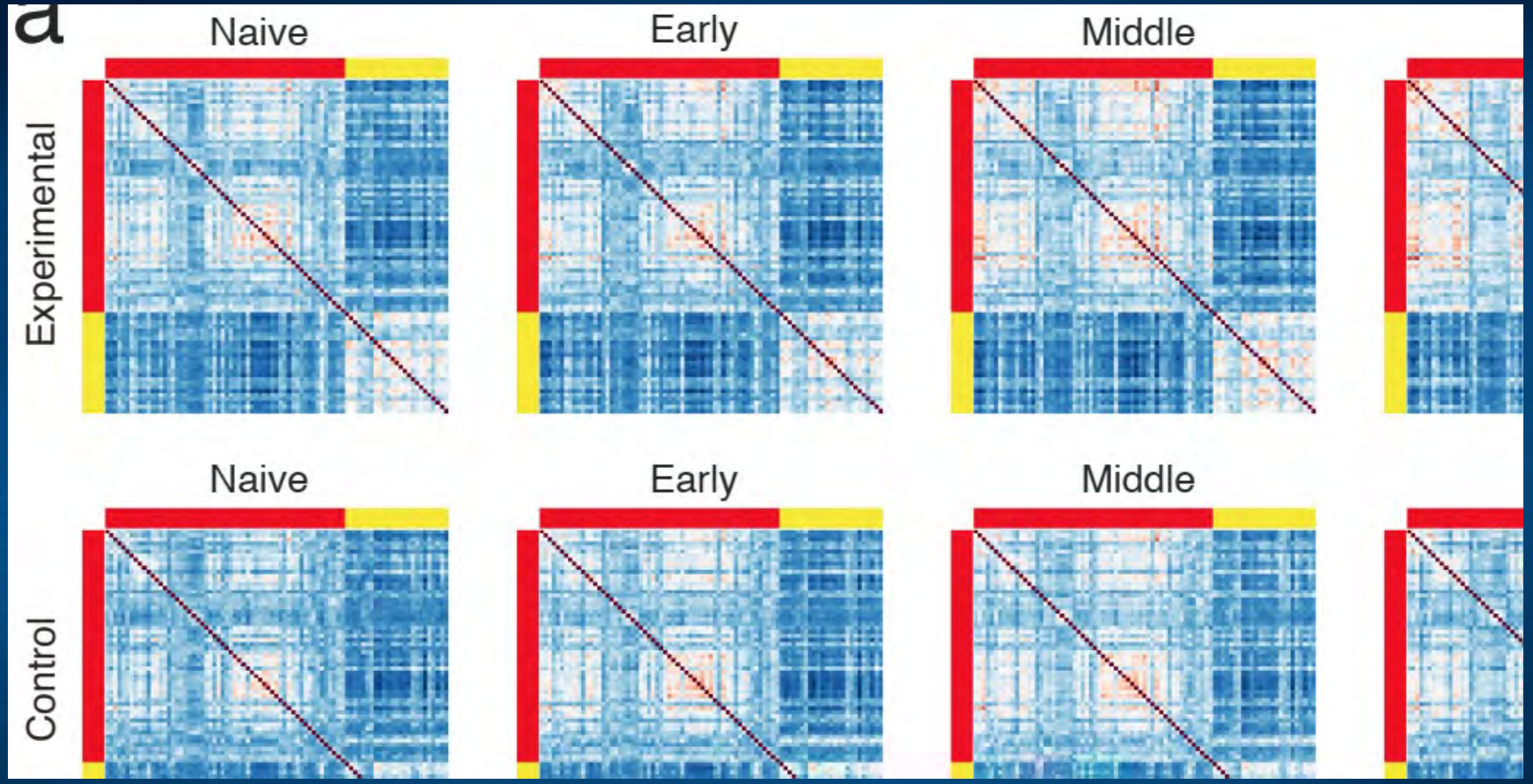

6-week training, dual n-back task, c**hanges in module allegiance of fronto-parietal and default-mode networks.** Each matrix element represents the probability that the pair of nodes is assigned to the same community.

Segregation of task-relevant DMN and FPN regions is a result of training and complex task automation.

Working memory training

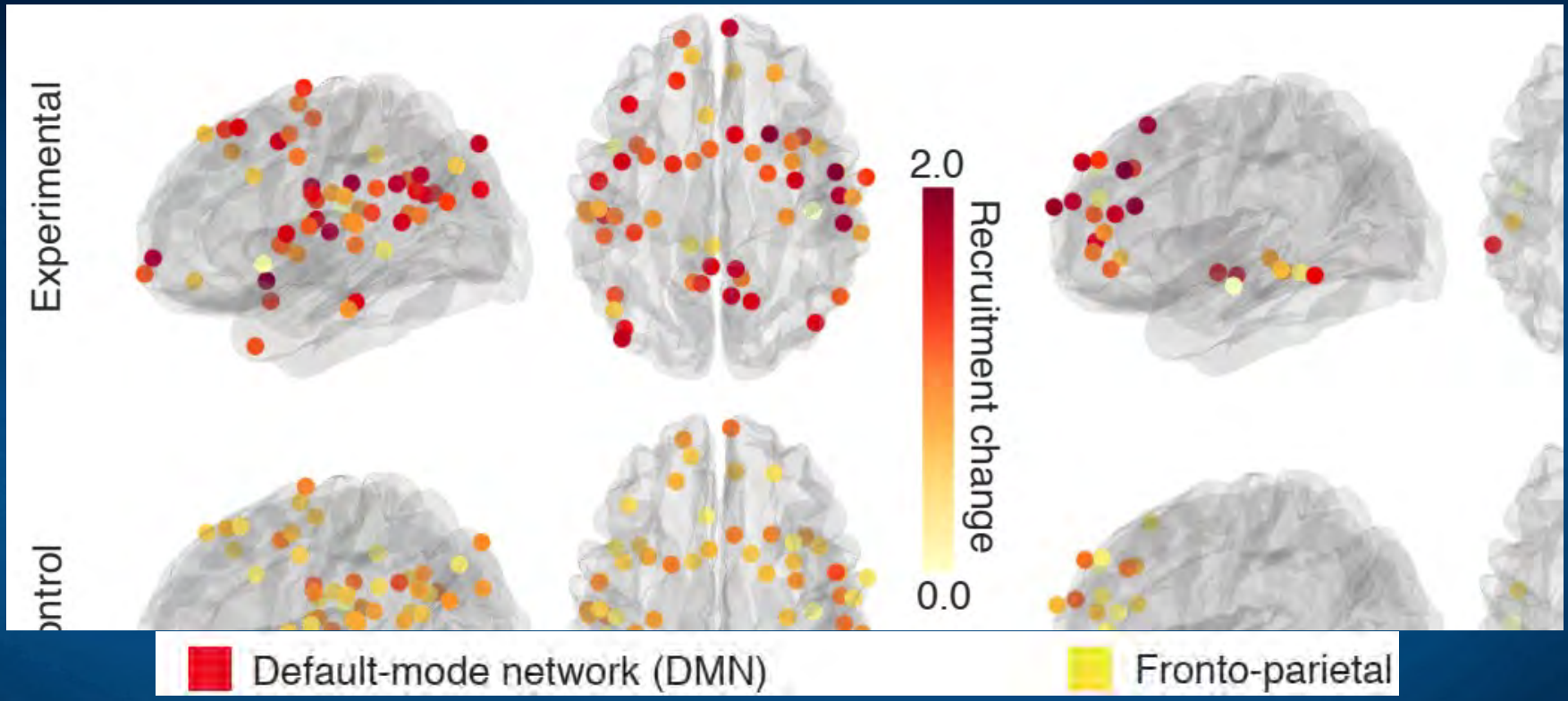

Recruitment changes from the ‘Naive’ to the ‘Late’ stage of training.

Both control and experimental groups exhibited increase of the DMN recruitment but FPN recruitment only increased in experimental group.

No consistent changes in FPN-DMN networks integration was noticed.

Deaf vs. Control

Edge-wise functional network differences visualized in the brain space (A). Connections that are significantly stronger (red) or weaker (blue) in deaf adults. Edge thickness reflects t-test statistic strength. (B) Chord diagram representing the number of significant edges between different large-scale networks.

Red bands represent edges with stronger functional connectivity in the deaf compared to hearing control, while blue bands represent edges with weaker functional connectivity. (Bonna, Finc, Szwed et al, in review).

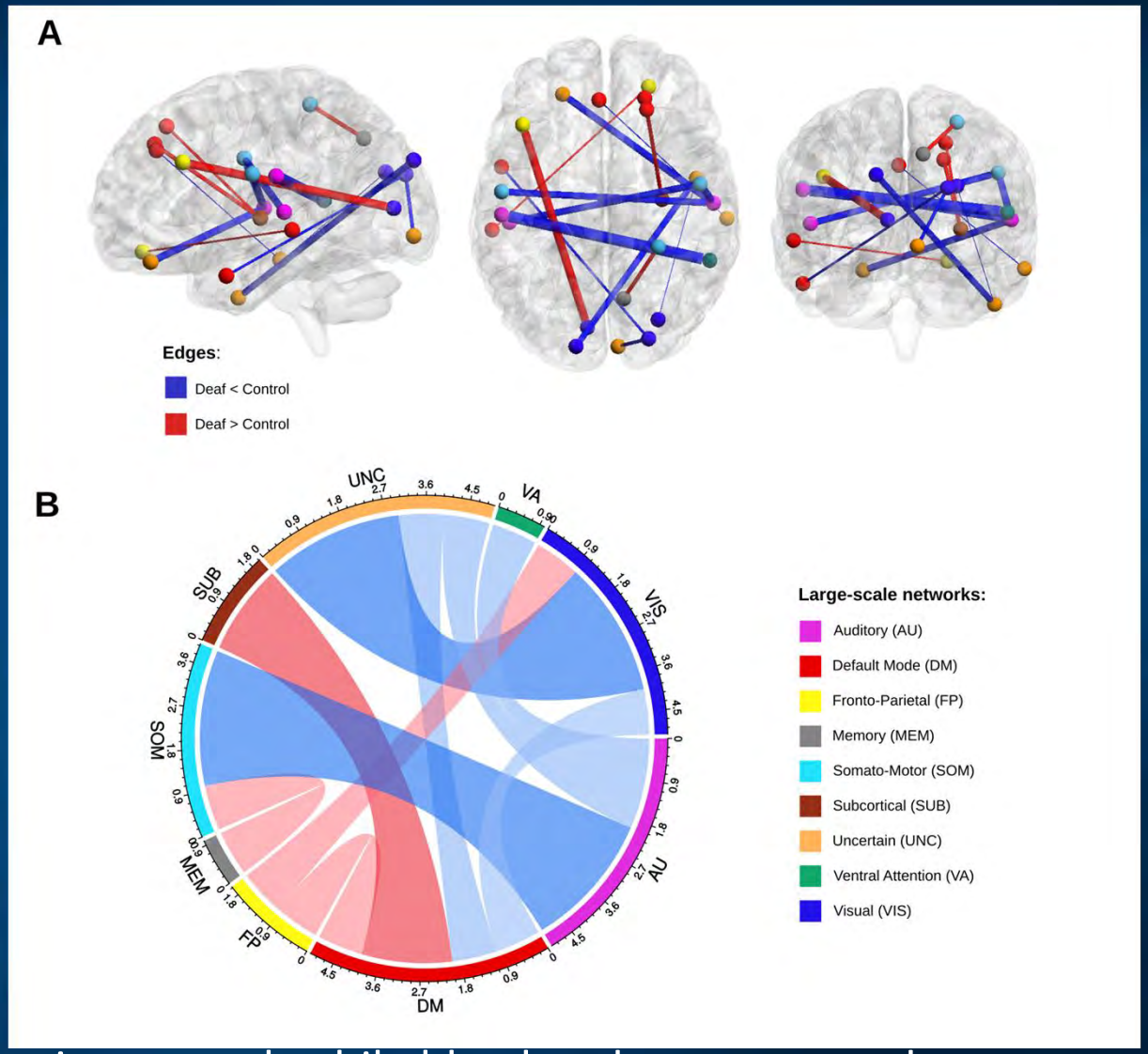

Deaf-Control

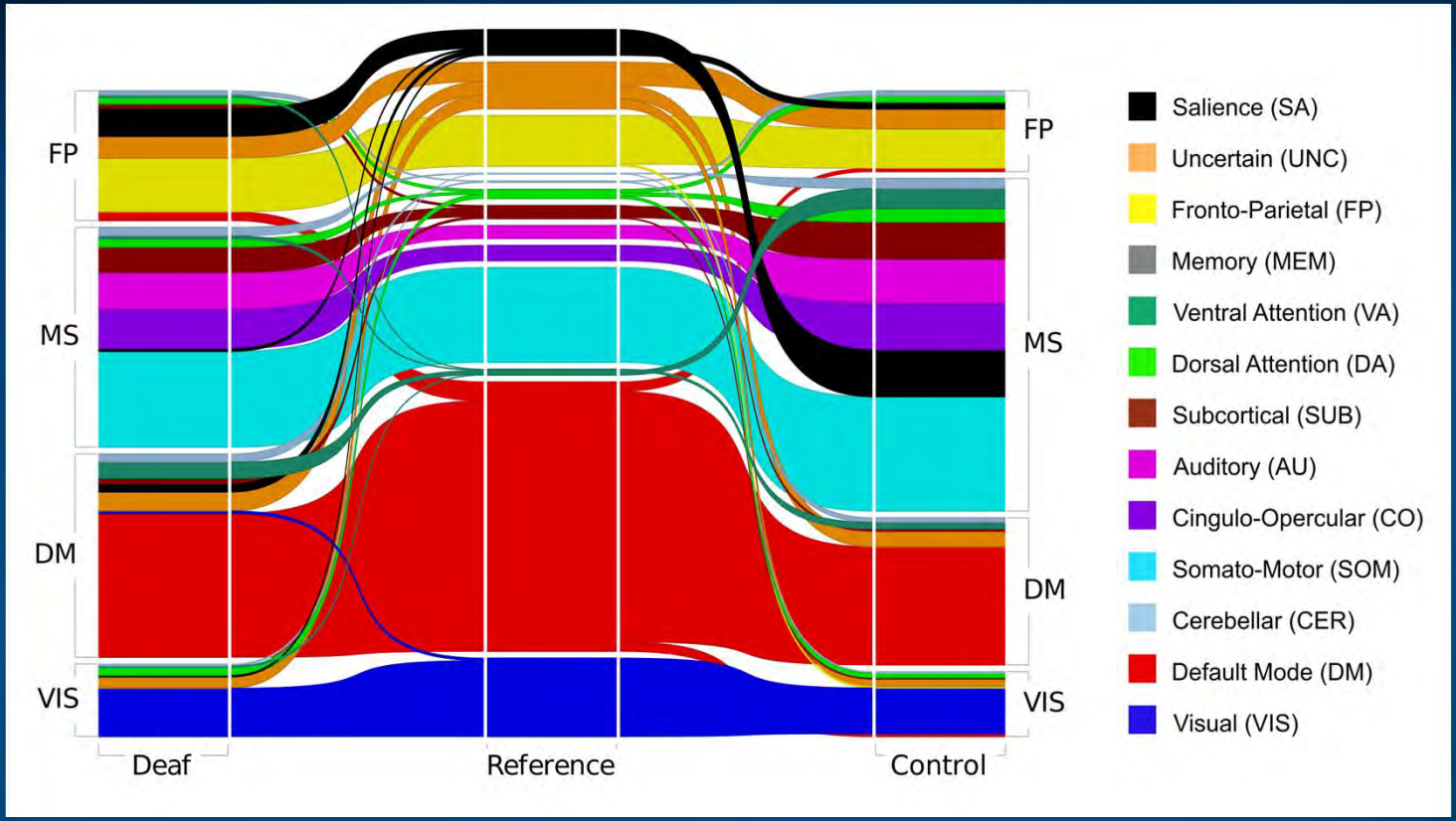

Modular organization of mean functional networks in deaf (left) vs control group (right) and reference network division into large-scale brain systems (Power et al., 2011). Salience nodes (black) are part of fronto-parietal (FP) module in deaf group but fall into multi-system (MS) module in control group. Also ventral-attention nodes (dark green) are part of MS module in control group but in deaf group they are part of default mode module (DM).

EEG/MEG Microstates

Microstates

Lehmann et al. EEG microstate duration and syntax in acute, medication-naïve, first-episode schizophrenia. Psychiatry Research Neuroimaging, 2005

Khanna et al. Microstates in Resting-State EEG. *Neuroscience and Biobehavioral Reviews*, 2015

4-7 states 60-150 ms

Symbolic dynamics.

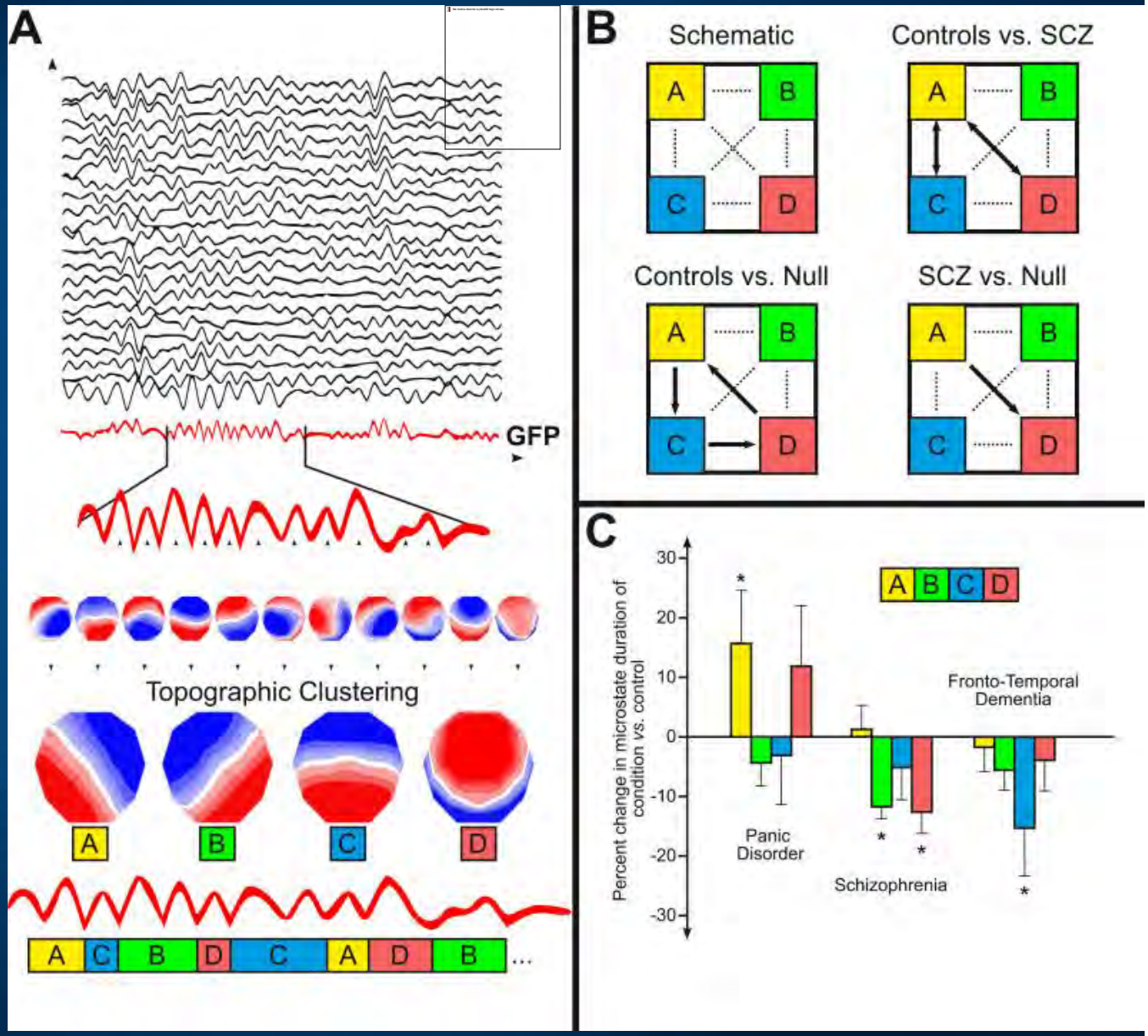

Yuan .. Bodurka, 2015

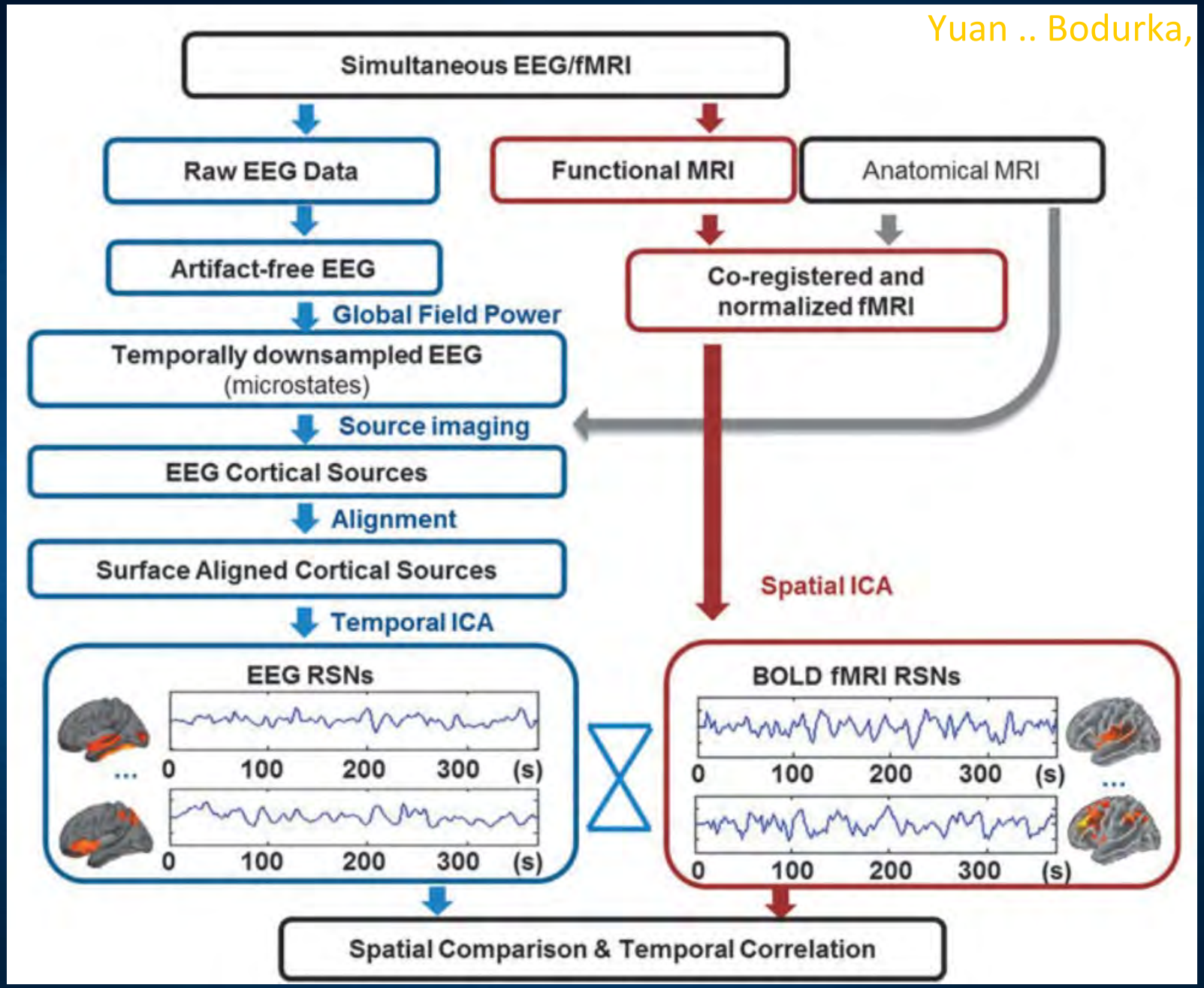

8 large networks from BOLD-EEG

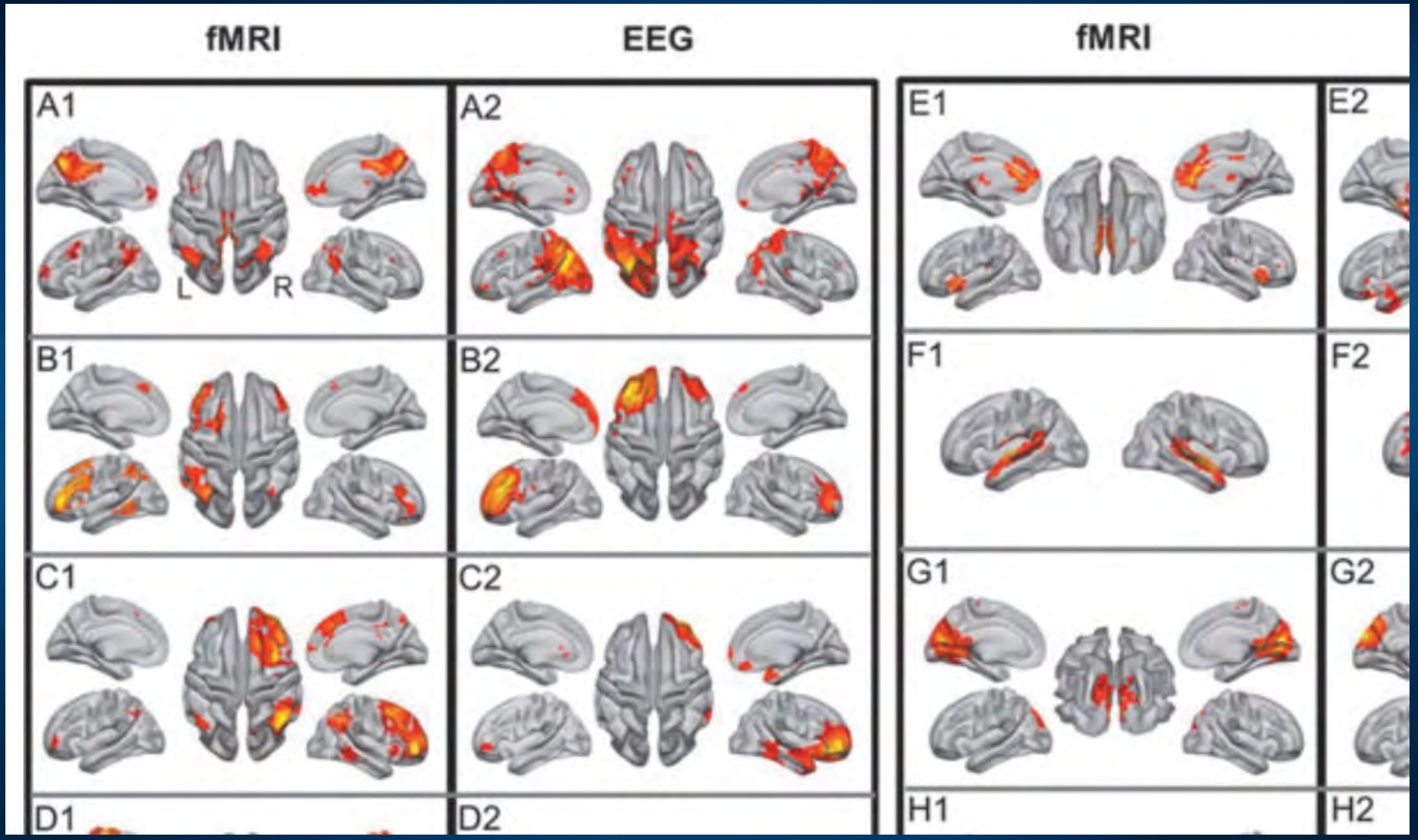

DMN, FP (frontoparietal)-left, right, sensorimotor, ex, control, auditory, visual (medial), (H) visual (lateral). Yuan … Bodurka (2015)

14 networks from BOLD-EEG

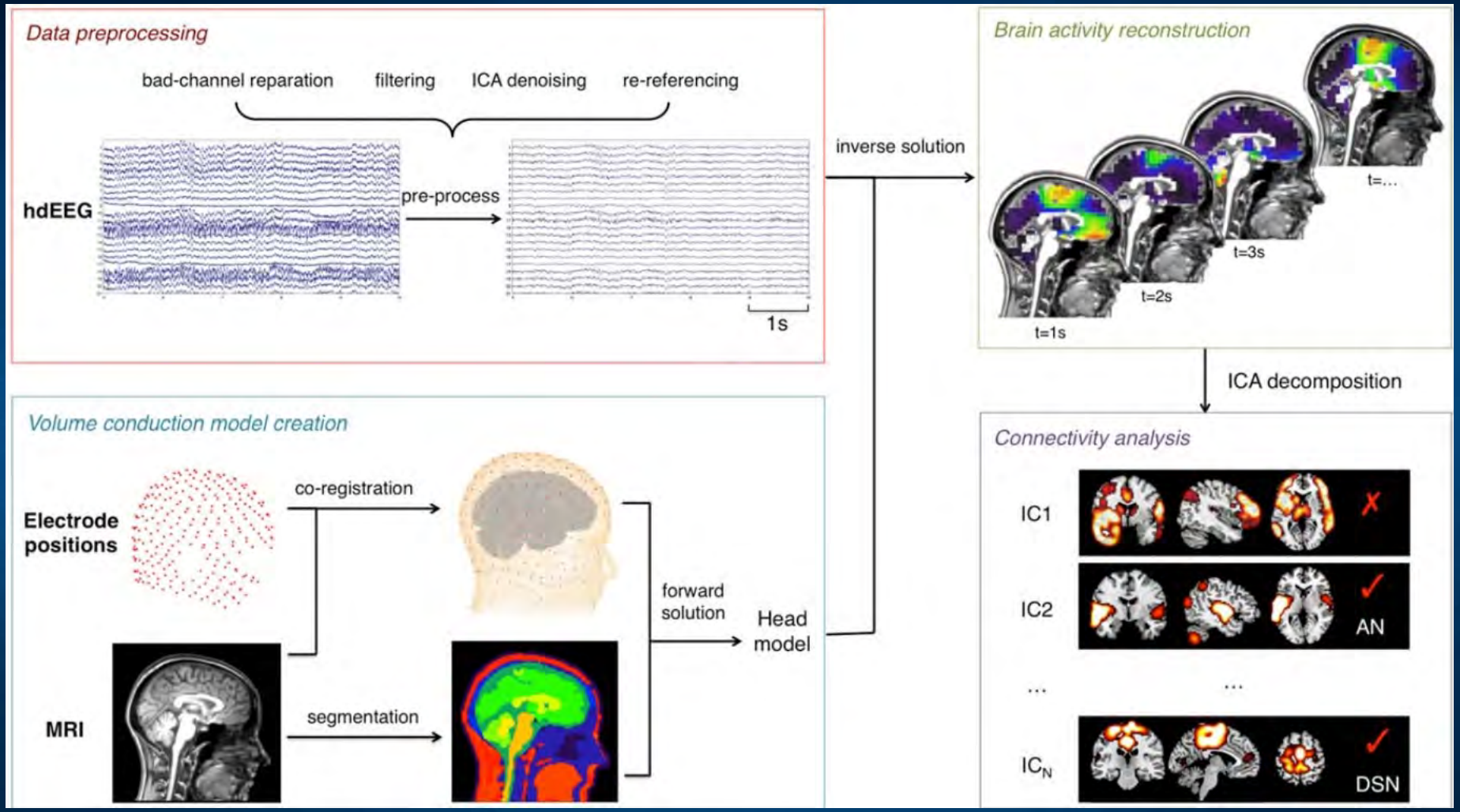

Liu et al. Detecting large-scale networks in the human brain. HBM (2017; 2018).

Microstates sources

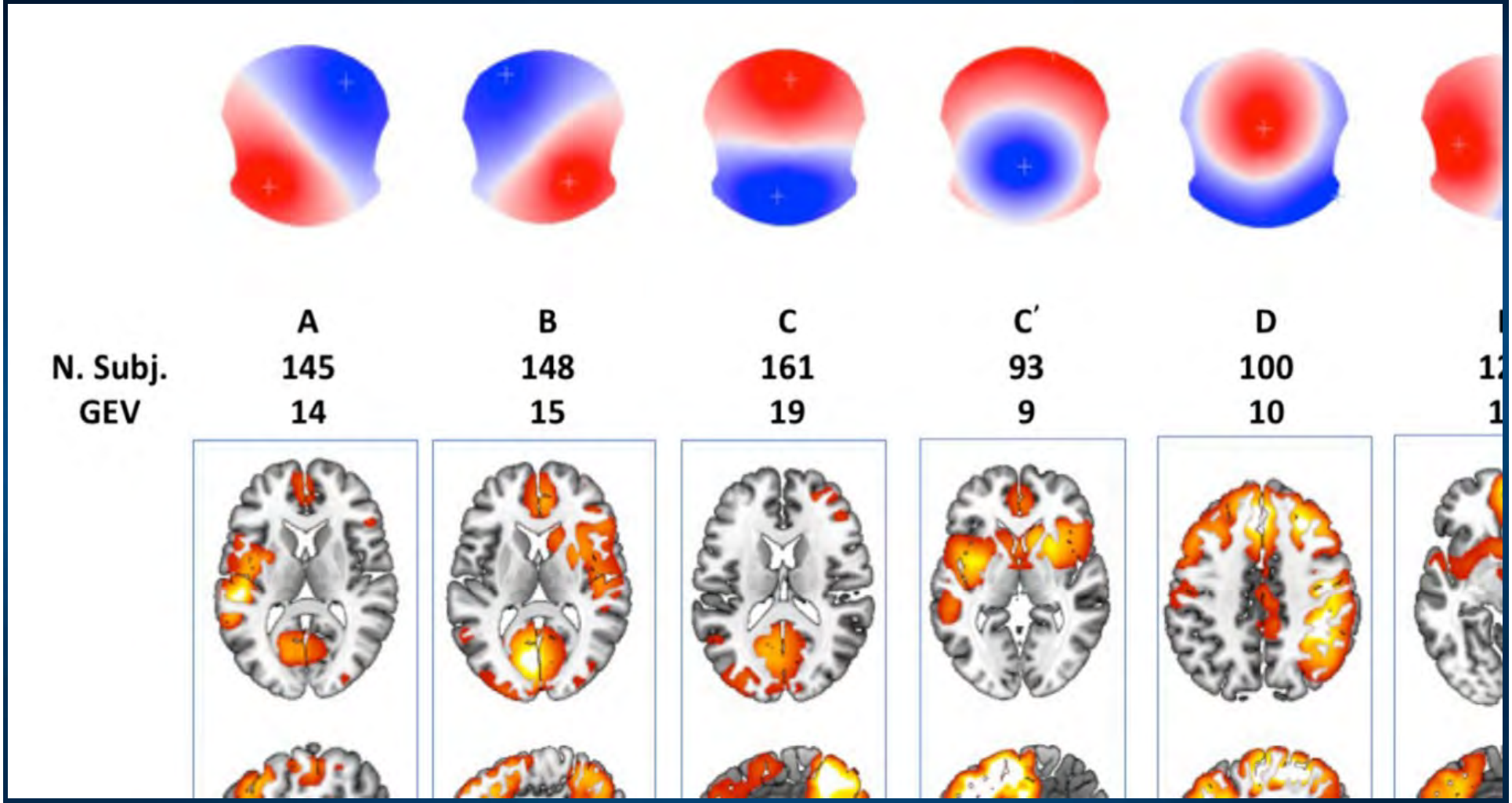

Michel, C. M., & Koenig, T. (2018). EEG microstates as a tool for studying the temporal dynamics of whole-brain neuronal networks: A review. *NeuroImage*, *180*, 577–593. https://doi.org/10.1016/j.neuroimage.2017.11.062

Checkerboard reversal, 5 microstates

M1 => V1

M2 => V2

M3=>Para-hippocampal

M4=>BA7, left PC, precuneus

M5=>dACC

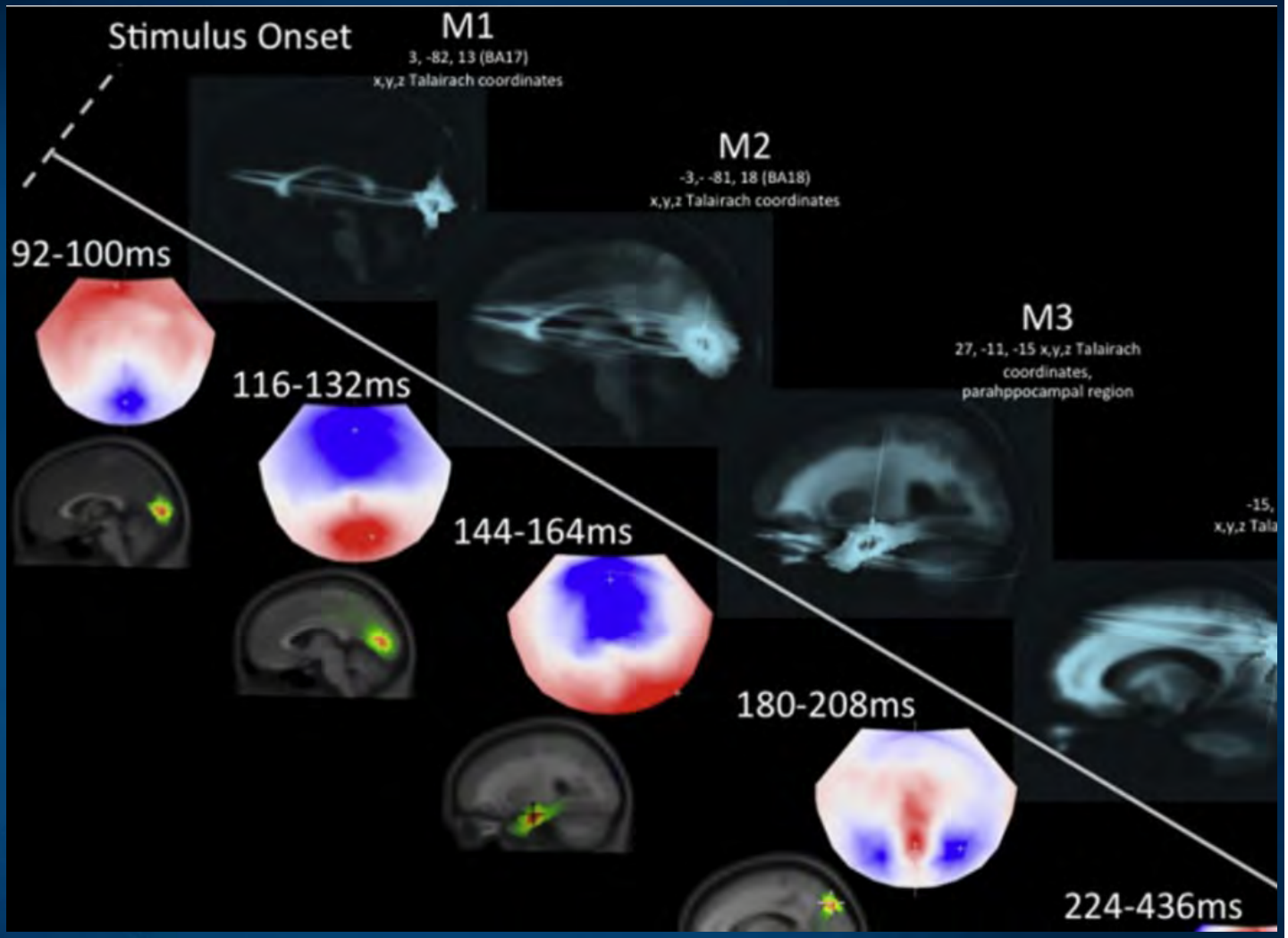

Cacioppo, S., Weiss, R. M., Runesha, H. B., & Cacioppo, J. T. (2014). Dynamic spatiotemporal brain analyses using high performance electrical neuroimaging: Theoretical framework and validation. *J. of Neuroscience Methods*, *238*, 11–34.

EEG localization and reconstruction

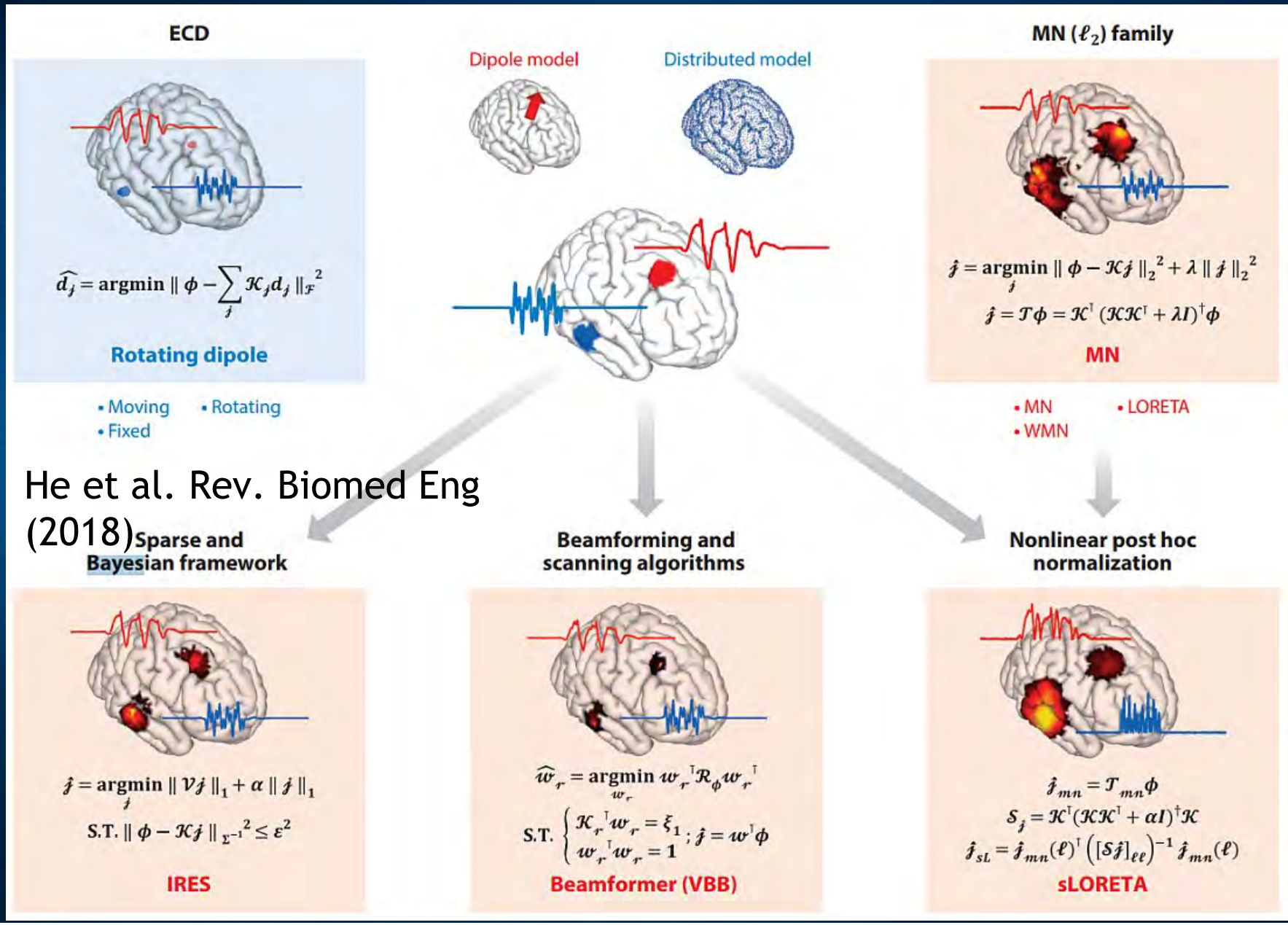

He et al. Rev. Biomed Eng (2018)

Spatial filters

LCMV (Linearly Constrained Minimum Variance), classical reconstruction filter is a solution to the following problem:

$$\Phi = K(\theta)j + n,\ j \approx W\Phi,\ WK(\theta) \approx \mathrm{I}$$

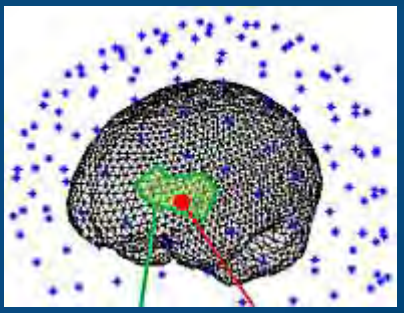

LCMV has large error if:

- sources are correlated,
- SNR (signal to to noise ratio) is low, or
- forward problem is ill-conditioned.

Minimum variance pseudo-unbiased reduced-rank (MV-PURE, Piotrowski, Yamada, IEEE Transactions on Signal Processing **56**, 3408-3423, 2008)

$$W = \bigcap_{j \in \Upsilon} \arg\min_{\hat{W} \in X_r} \left\| \hat{W}K(\theta) - \mathrm{I}_j \right\|_j^2$$

where X_r is a set of all matrices of rank at most r, and set Υ denotes all unitary norms. We use 15000 vertex FreeSurfer brain tessellation together with brain atlases that provide parcellation of the mesh elements into 100-240 cortical patches (regions of interest, ROIs).

SupFunSim

SupFunSim: our library/Matlab /tollbox, direct models for EEG/MEG.

Provides many spatial filters for reconstruction of EEG sources: linearly constrained minimum-variance (LCMV), eigenspace LCMV, nulling (NL), minimum-variance pseudo-unbiased reduced-rank (MV-PURE) …

Source-level directed connectivity analysis: partial directed coherence (PDC), directed transfer function (DTF) measures.

Works with FieldTrip EEG/ MEG software. Modular, object-oriented, using Jupyter notes, allowing for comments and equations in LaTex.

$$A := H_{Src,R} := R^{-1/2} H$$
$$B := H_{Src,N} := N^{-1/2} H$$

```
%%file calculate_H_Src.m
function model = calculate_H_Src(MODEL)
    model = MODEL;

    model.H_Src_R = pinv(sqrtm(model.R)) * model.H_Src;
```

Rykaczewski, K., Nikadon, J., Duch, W., & Piotrowski, T. (2019). *BioRxiv*, 618694

Functional connectivity changes

Influence of brain games on functional connectivity: **Phase Locking Value** (Burgess, 2013; Lachaux 1999), phase differences between signals measured at each electrode. PLV => synchronization maps, info flow.

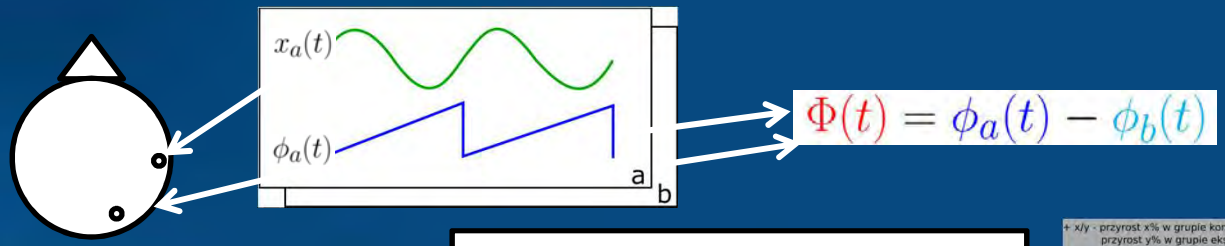

$$PLV(a,b) = \frac{1}{T}\left|\sum_{t}^{T} e^{i\Phi(t)}\right|$$

PLV channel vs channel

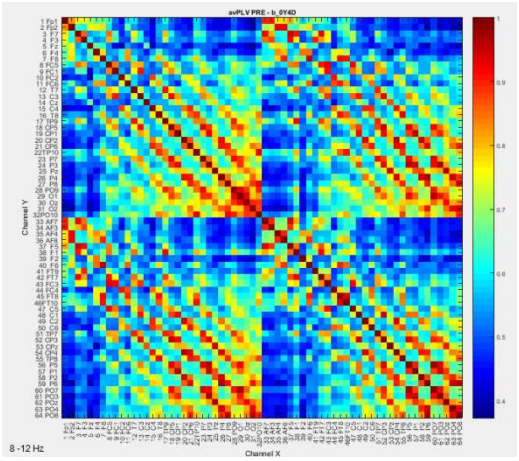

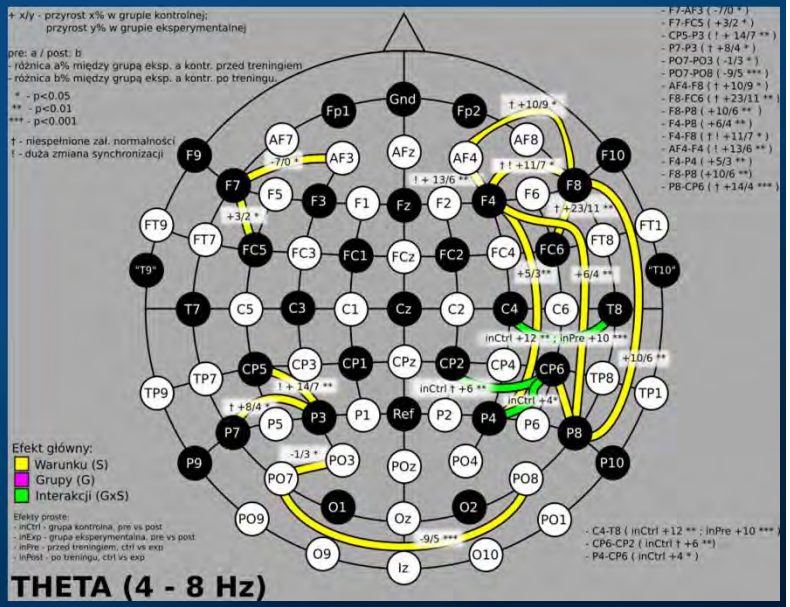

Spectral Fingerprints

Spectral fingerprints

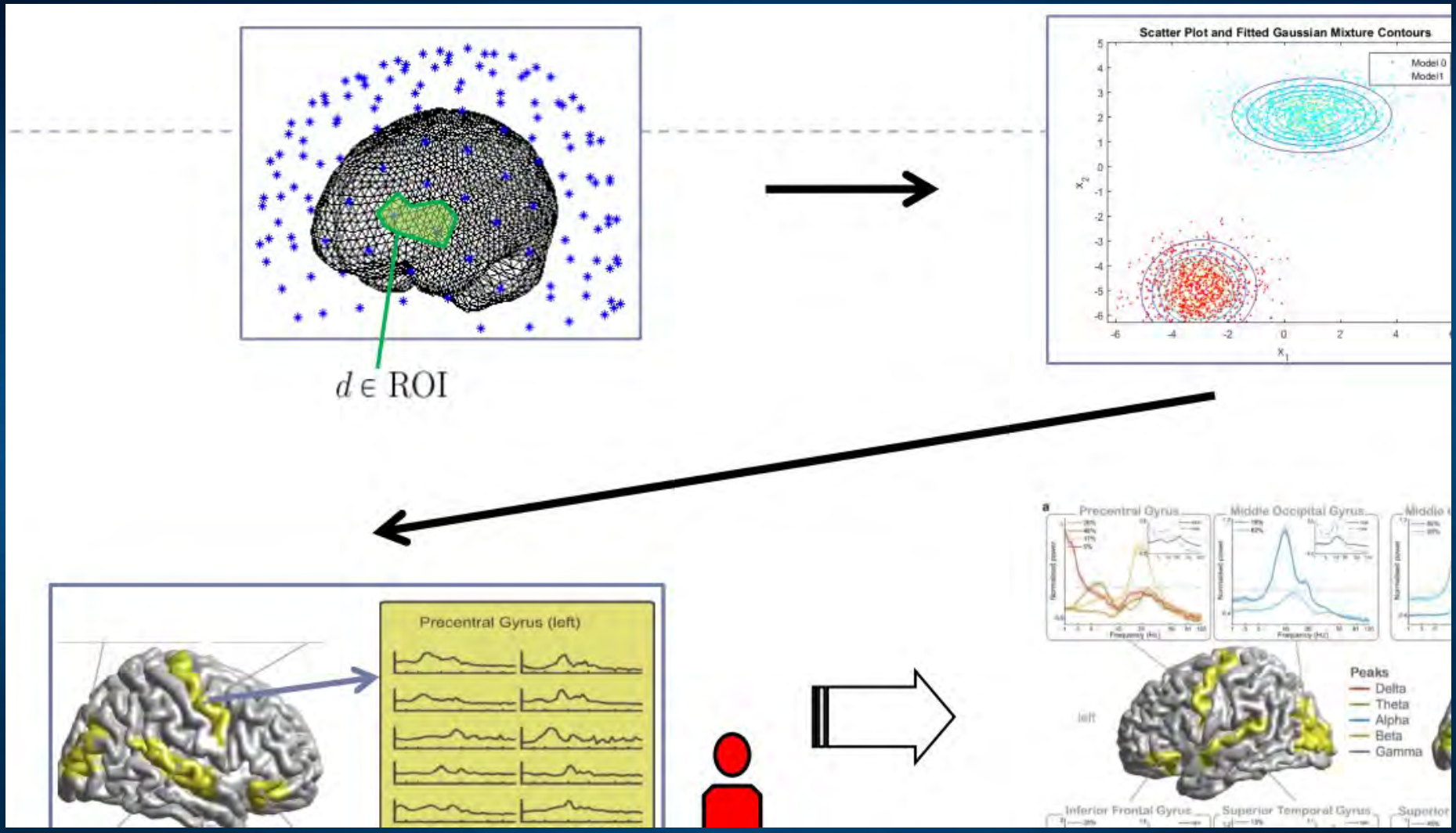

A. Keitel i J. Gross, „Individual human brain areas can be identified from their characteristic spectral activation fingerprints”, *PLoS Biol* 14(6), e1002498, 2016

Spectral fingerprints

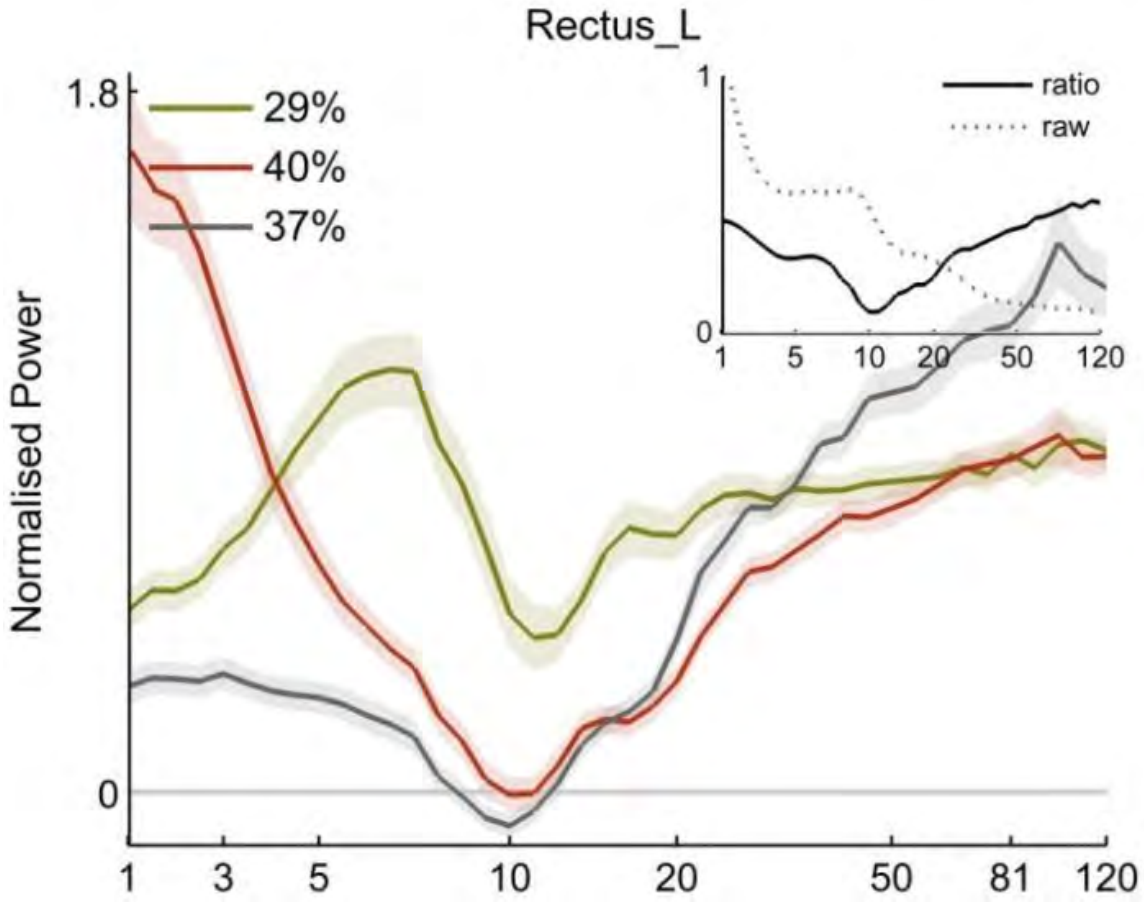

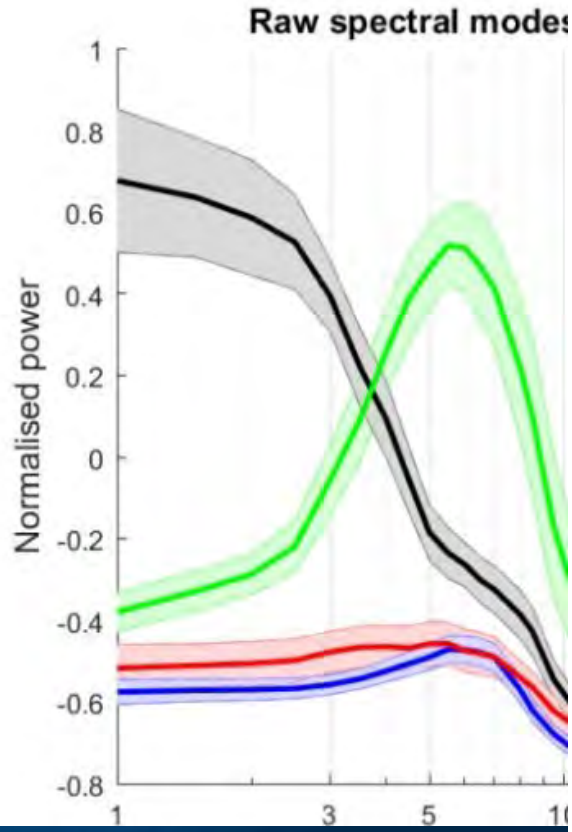

A. Keitel i J. Gross, „Individual human brain areas can be identified from their characteristic spectral activation fingerprints”, *PLoS Biol* 14, e1002498, 2016

Reliability of ROI identification

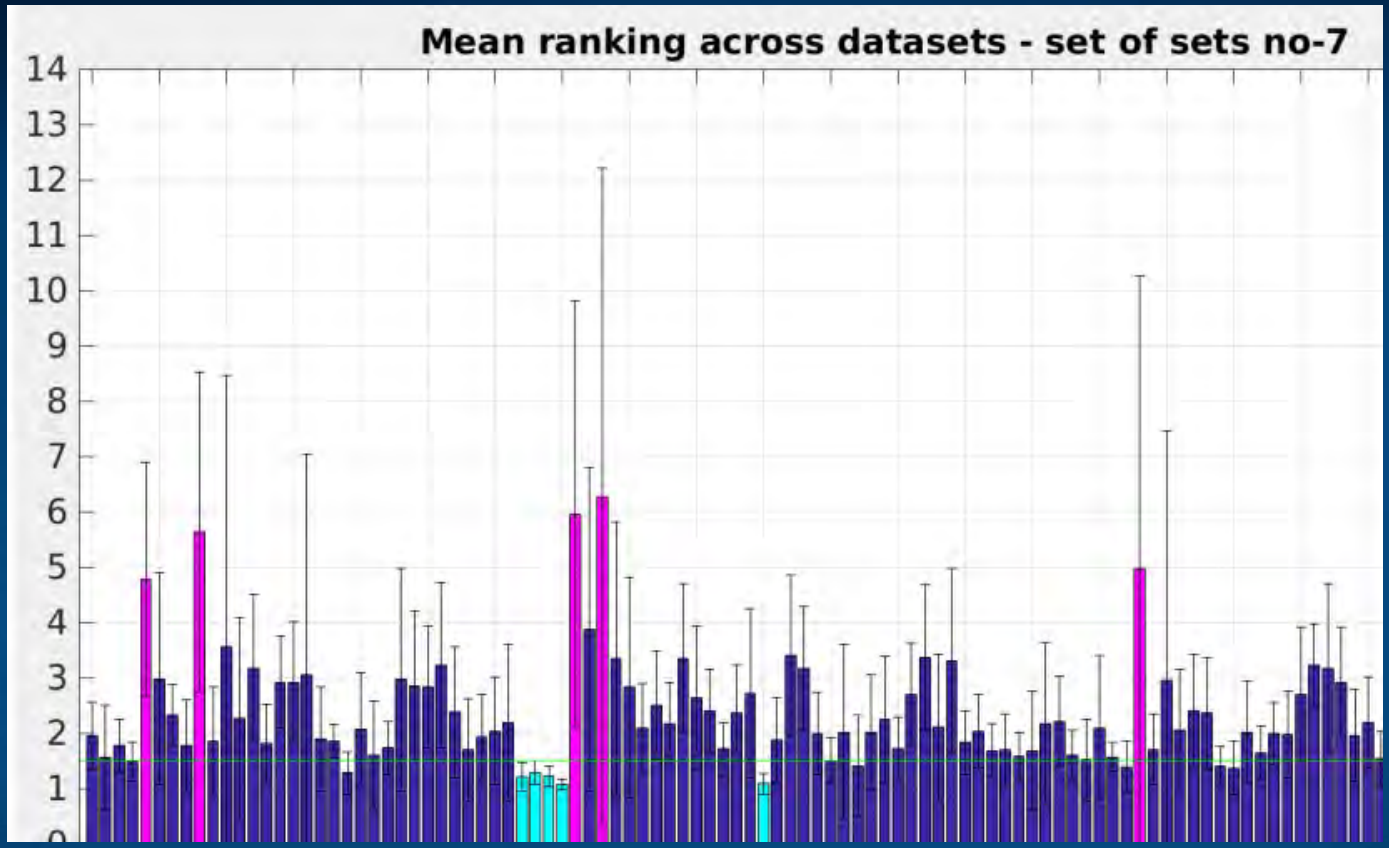

Rank one means that ROI is uniquely identified (blue).

Some errors are due to homologous ROIs (left-right) and have mean rank <2.

Most reliable ROI, midline structures

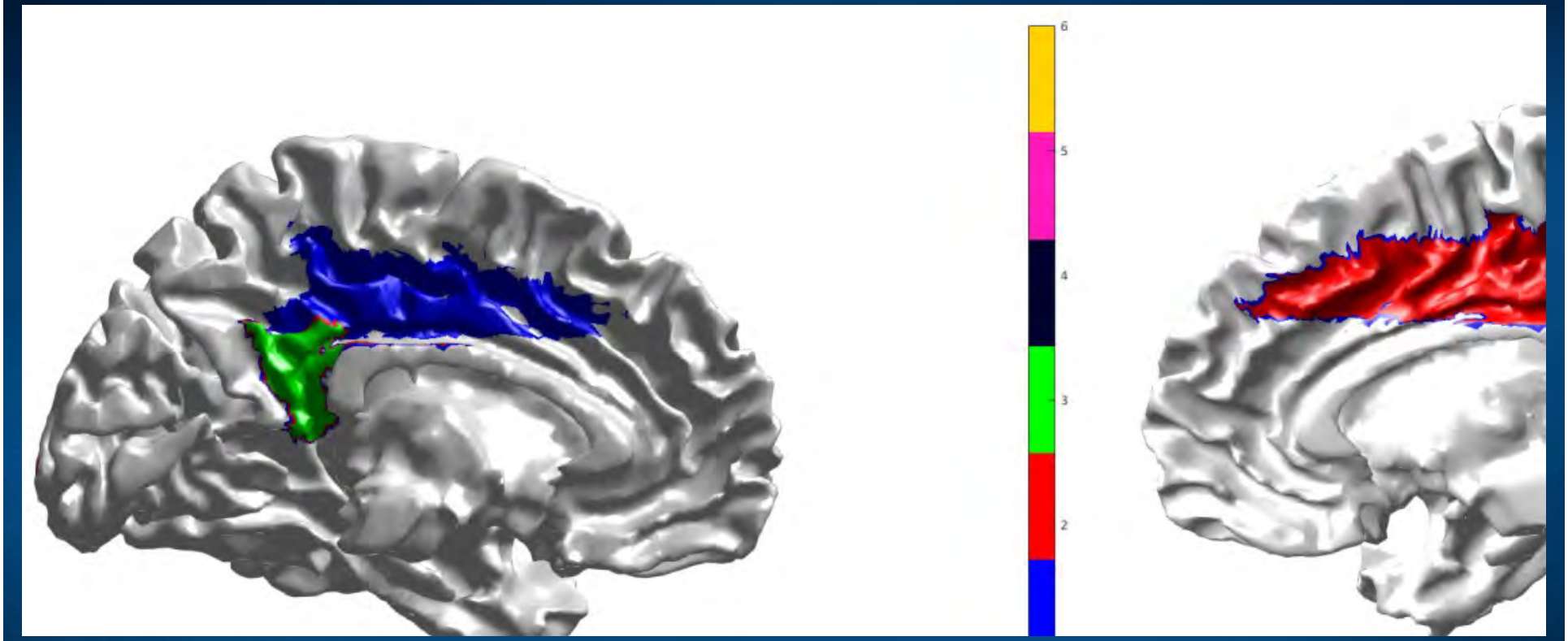

MEG data from the Human Connectome Project (HCP) for 1200 subjects.

ROI that we can recognize quite reliably. Colors – ROI 1-6
33 1 Cingulum_Mid_L, 34 2 Cingulum_Mid_R, 35 3 Cingulum_Post_L,
36 4 Cingulum_Post_R, 51 5 Occipital_Mid_L, 110 6 Vermis_3

Most reliable ROI, midline structures

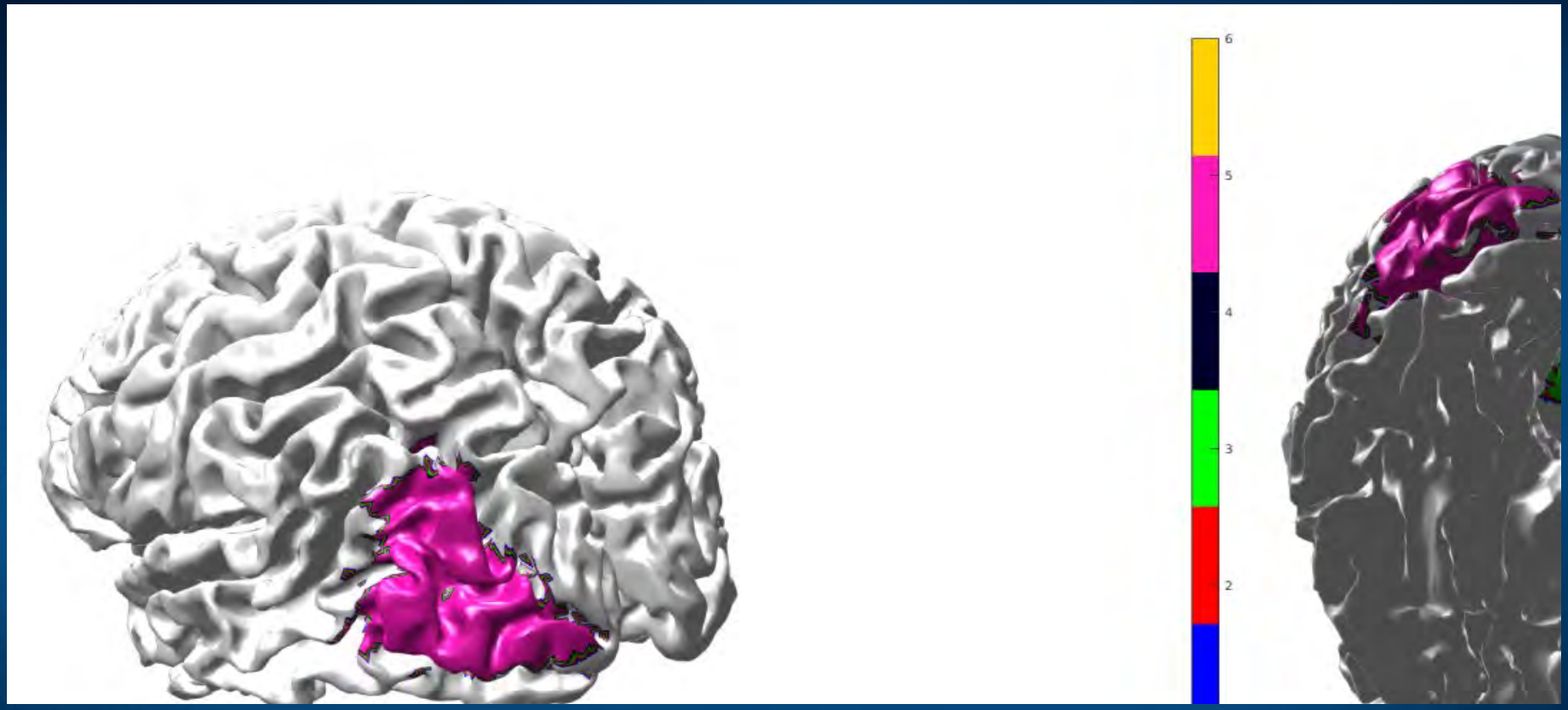

MEG data from the Human Connectome Project (HCP) for 1200 subjects.

ROI that we can recognize quite reliably. Colors – ROI 1-6

3 Cingulum_Post_L,

5 Occipital_Mid_L

Reliability of ROI identification

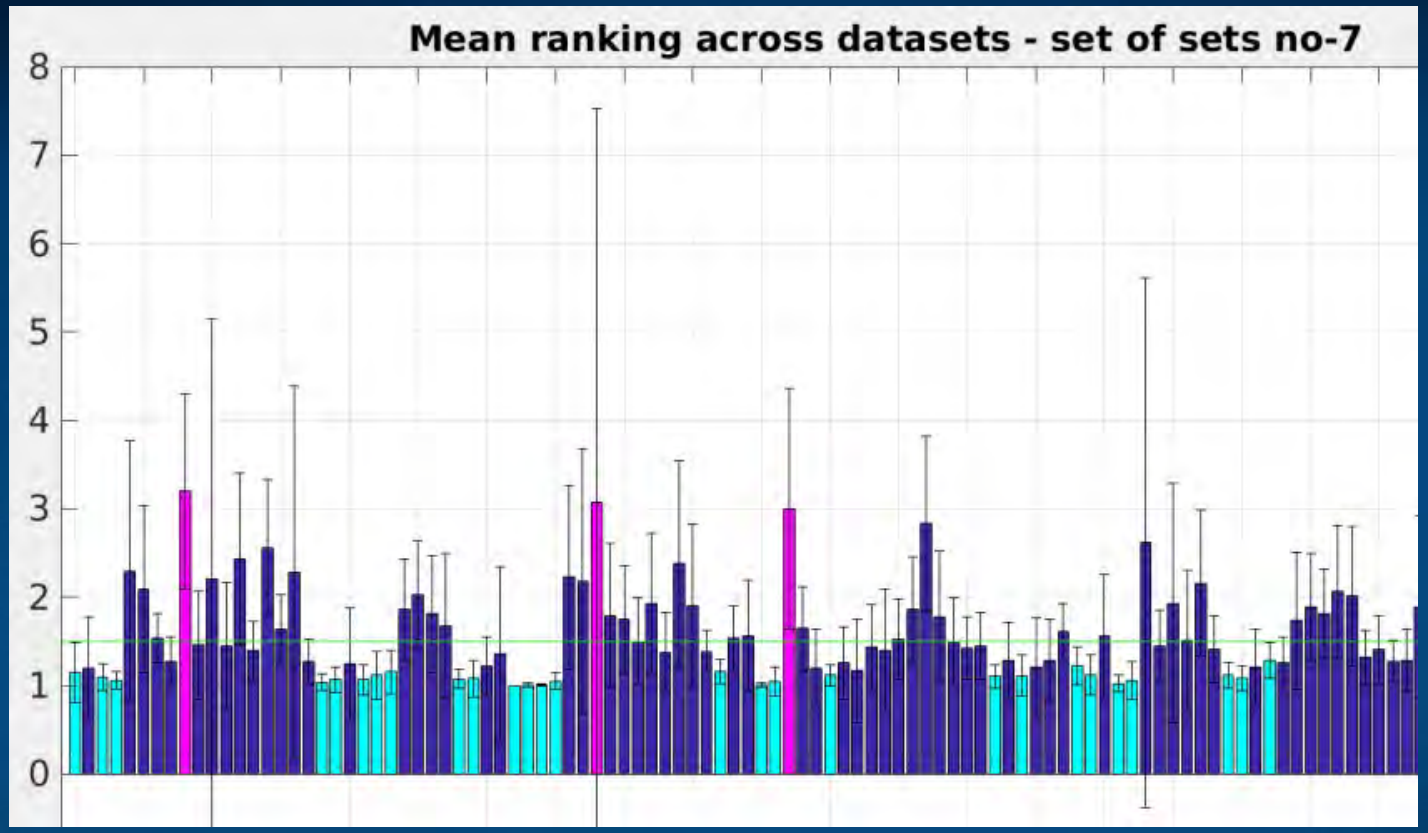

Some errors are due to homologous ROIs (left-right) and have mean rank <2.

Number of ROIs that can be reliably identified this way is much larger.

Some regions are hard to identify: S/N is different depending on cortex folding and MEG/EEG measures. MEG can see cingulate cortex activity, EEG is better for flat cortex on the surface.

Most reliable ROI, homologous ≤ 1.5

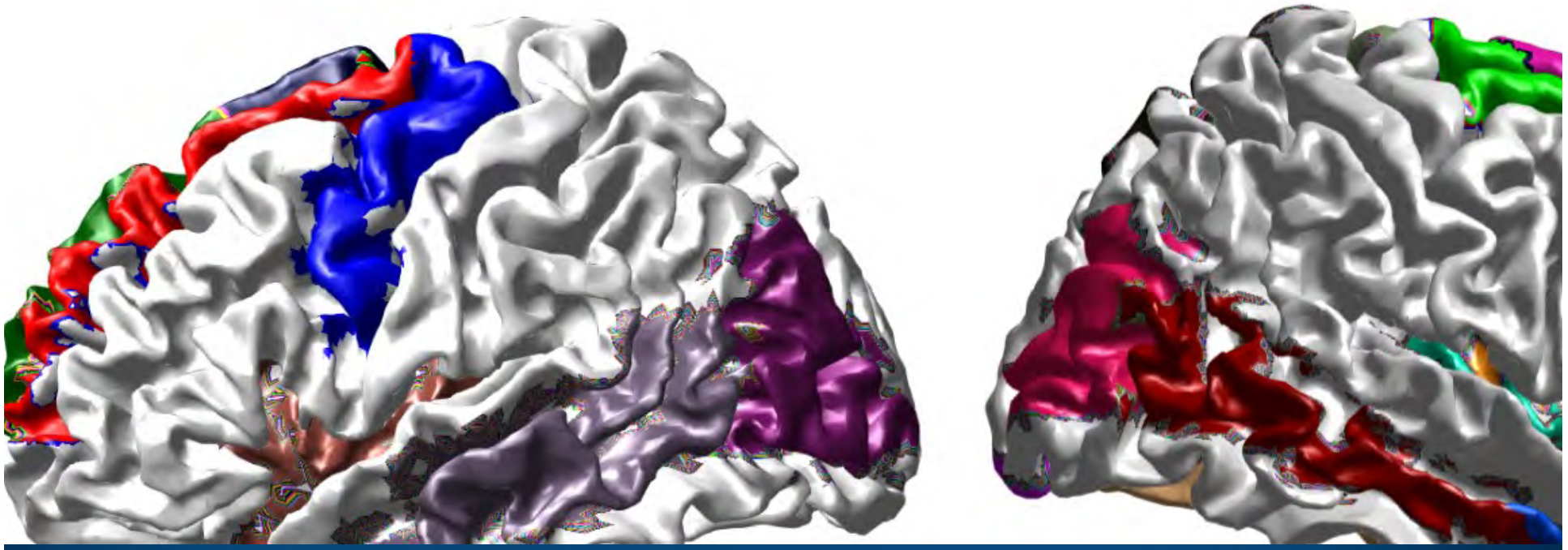

MEG data from the Human Connectome Project (HCP) for 1200 subjects.

Some ROI can be recognized quite reliably.

If homologues are not distinguished we have 29 ROIs, many sub-cortical.

Least reliable ROI

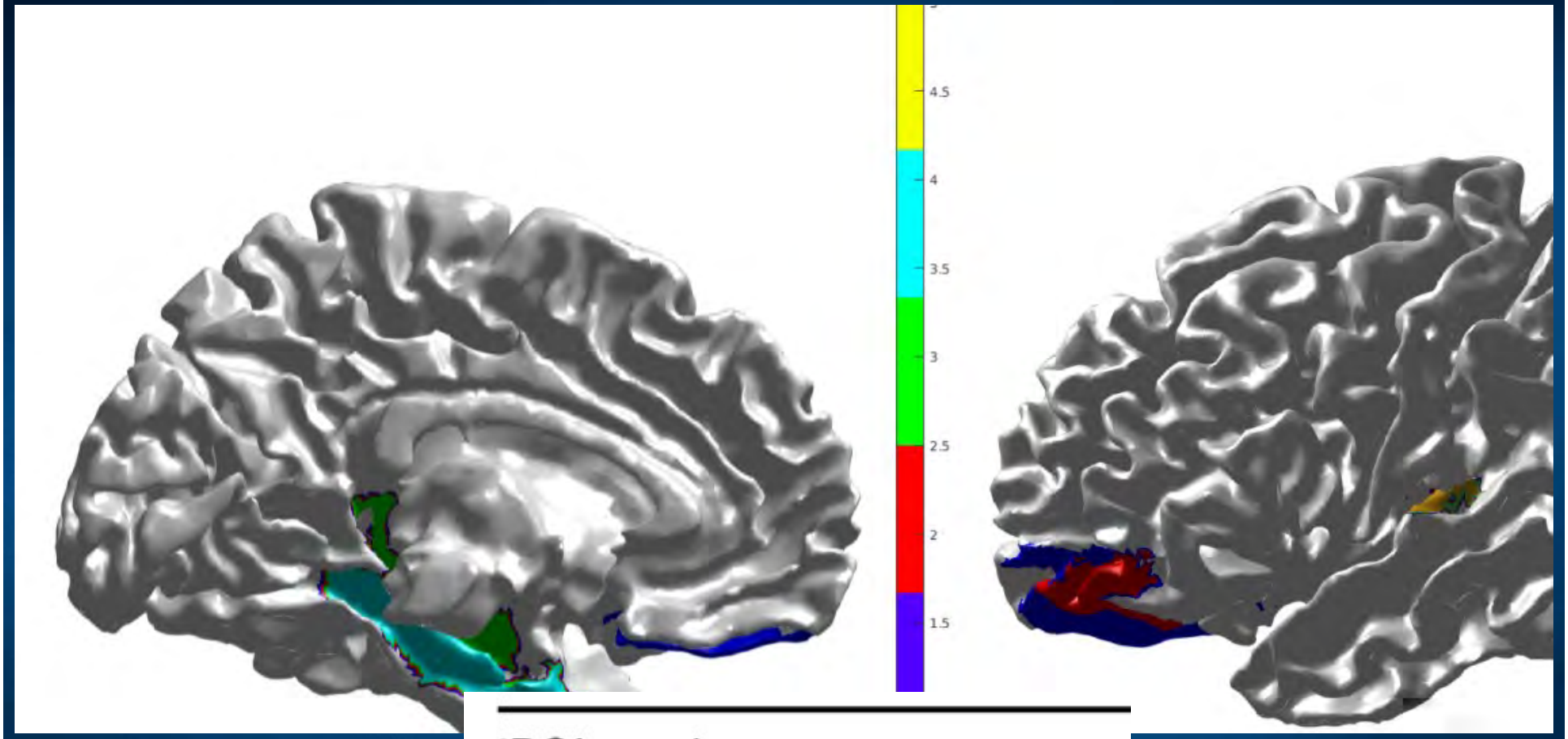

iROI	key	
5	1	Frontal_Sup_
9	2	Frontal_Mid_
37	3	Hippocampus_
39	4	ParaHippocam

Simulations of brain networks

Neuropsychiatric phenomics

2008: The Consortium for Neuropsychiatric Phenomics

"… categories, based upon presenting signs and symptoms, may not capture fundamental underlying mechanisms of dysfunction" (Insel et al., 2010).

New approach: RDOC NIMH.

Description of organisms at different levels will help to answer different types of questions.
Network level is in the middle and can be connected to the mental level via computational models.

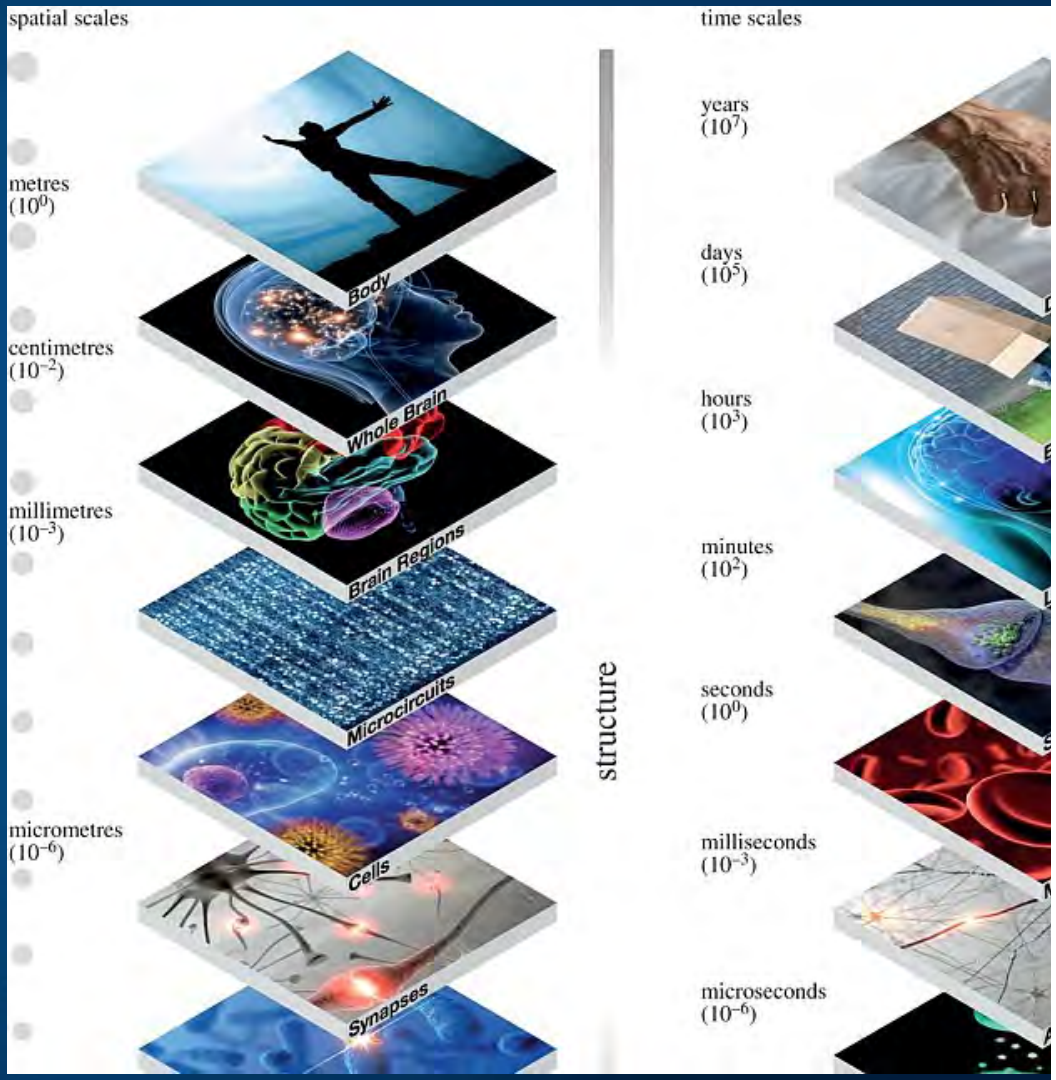

Model of reading & dyslexia

Emergent neural simulator:

Aisa, B., Mingus, B., and O'Reilly, R. The emergent neural modeling system. Neural Networks, 21, 1045, 2008.

3-layer model of reading:

orthography, phonology, semantics, or distribution of activity over
140 microfeatures defining concepts.

In the brain: microfeature=subnetwork.
Hidden layers OS/OP/SP_Hid in between.

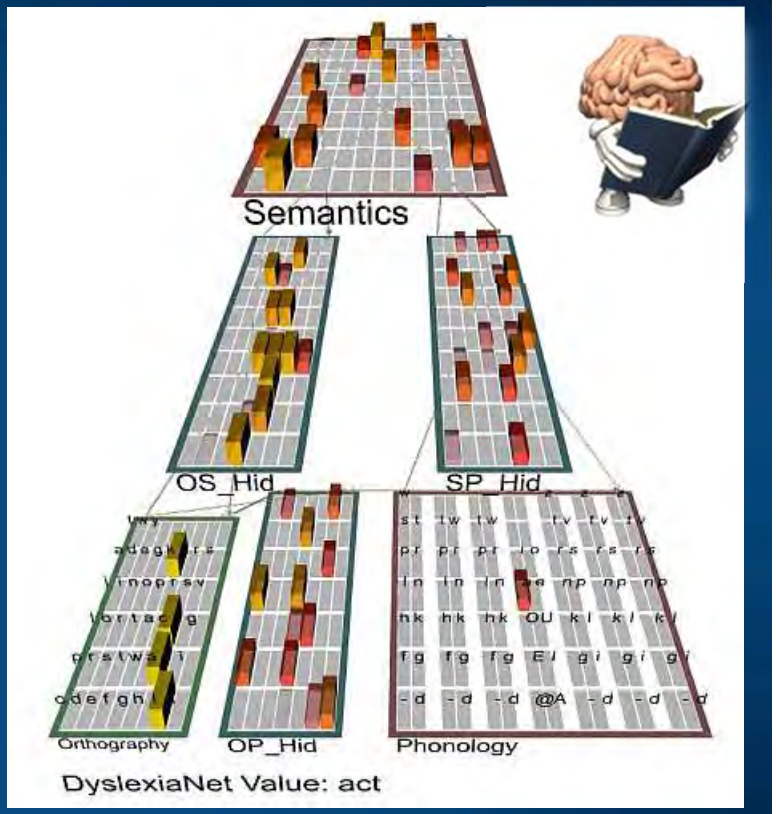

Learning: mapping one of the 3 layers to the other two.

Fluctuations around final configuration = attractors representing concepts.

How to see properties of their basins, their relations?
Model in **Genesis**: more detailed neuron description.

Computational Models

Models at various level of detail.

- Minimal model includes neurons with 3 types of ion channels.

Models of attention:

- Posner spatial attention;
- attention shift between visual objects.

Models of word associations:

- sequence of spontaneous thoughts.

Models of motor control.

Critical: control of the increase in intracellular calcium, which builds up slowly as a function of activation. Initial focus on the leak channels, 2-pore K^+, looking for genes/proteins.

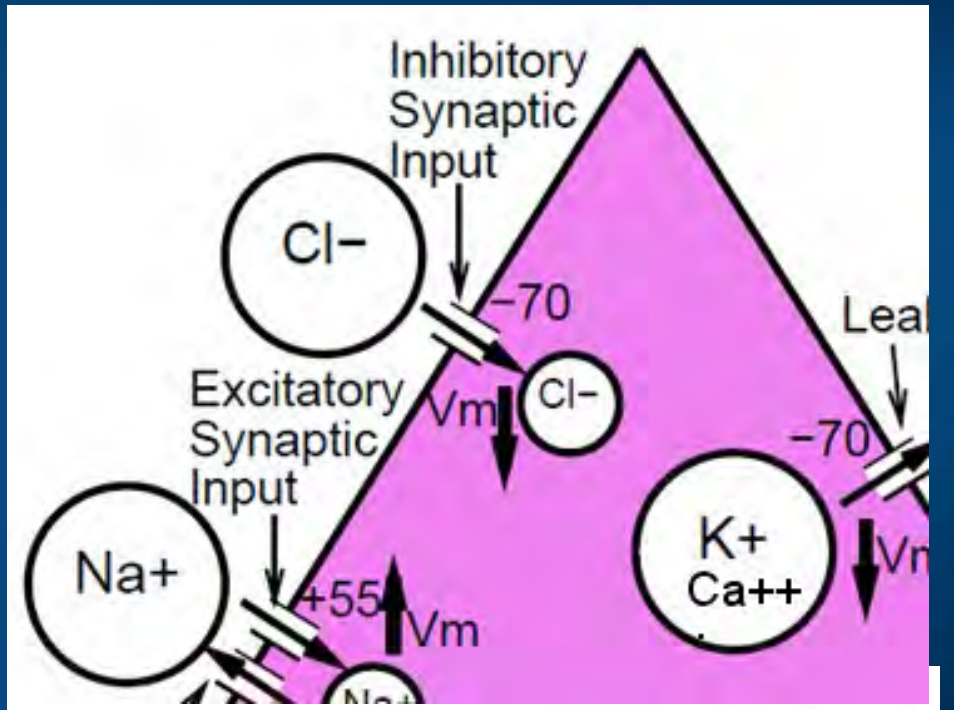

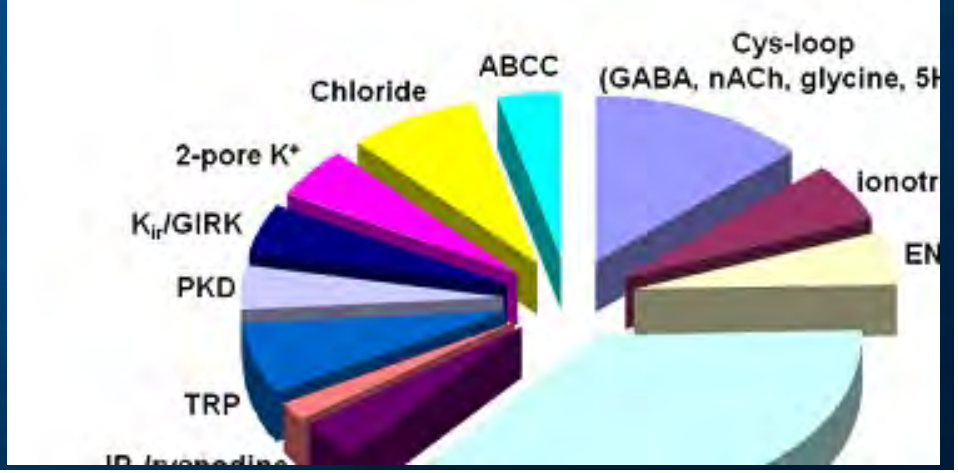

Viser toolbox

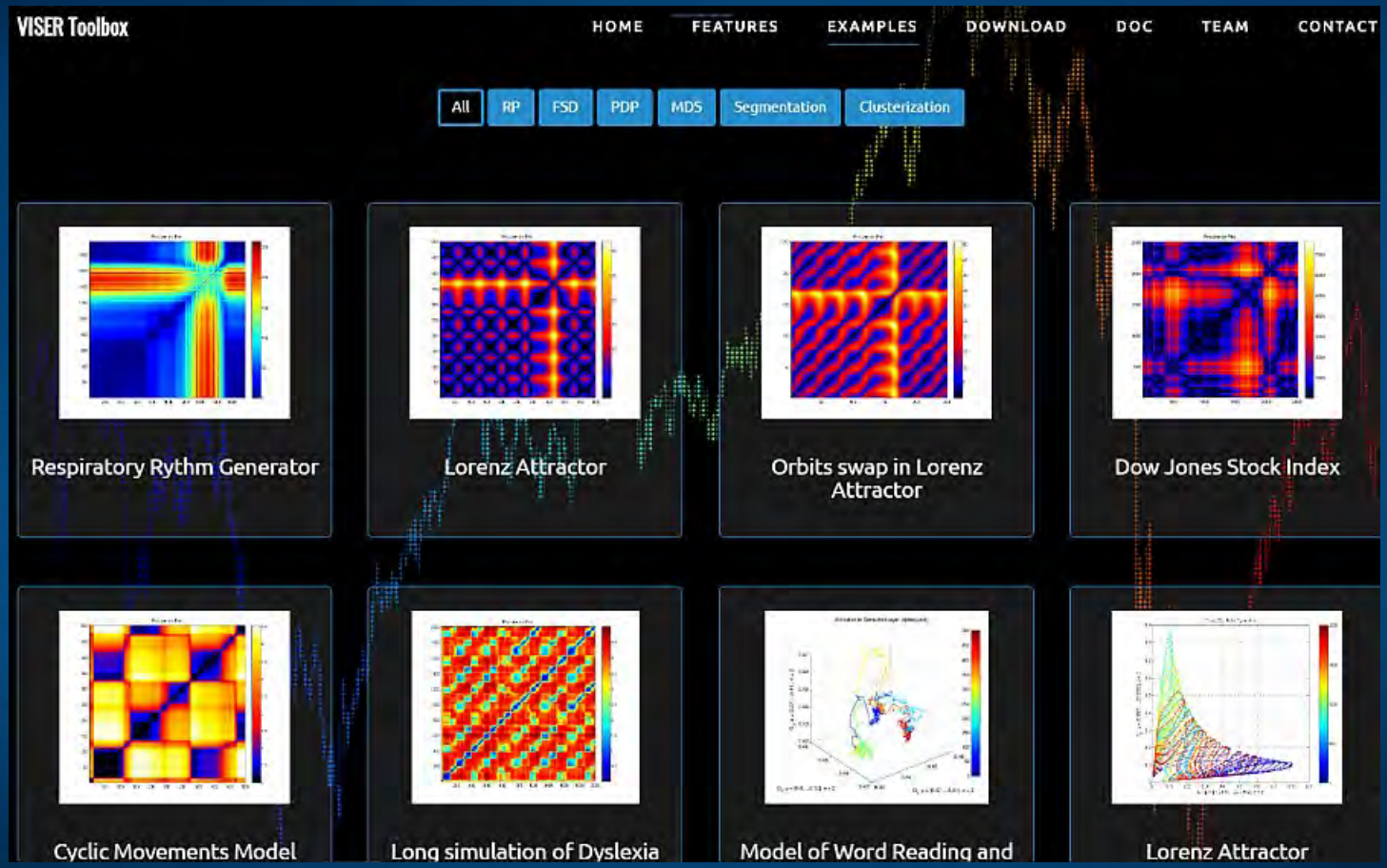

Nasz Viser toolbox (Dobosz, Duch) do wizualizacji szeregów czasowych w wielu wymiarach różnymi technikami.

rope

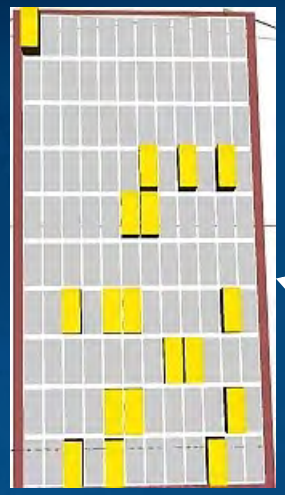

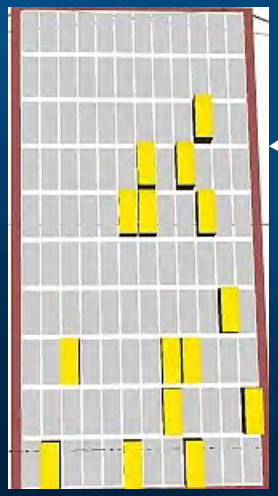

flag

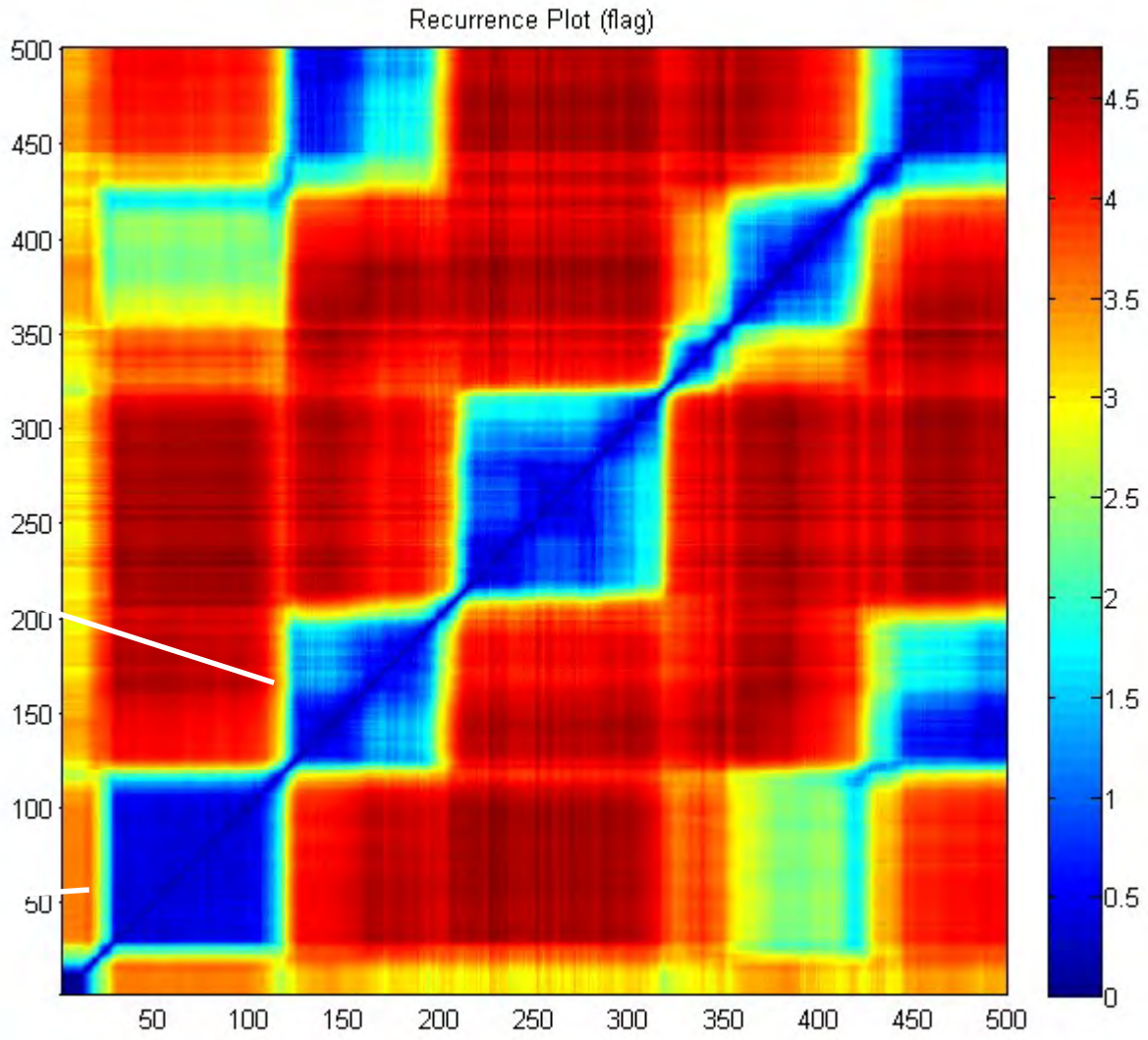

Transitions to new patterns that share some active units (microfeatures) shown in recurrence plots.

Probability of recurrence

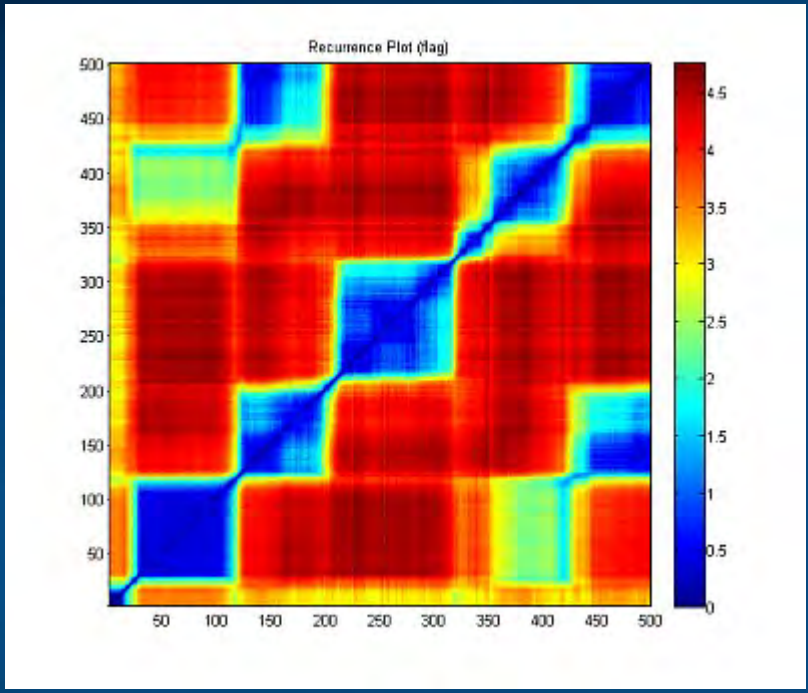

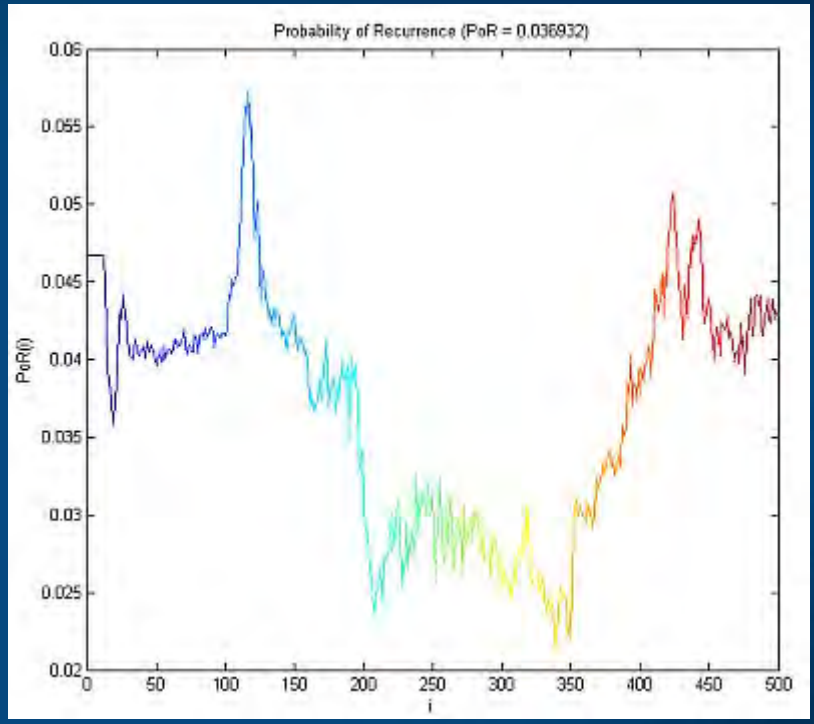

Probability of recurrence may be computed from recurrence plots, allowing for evaluation how strongly some basins of attractors capture neurodynamics.

Fast transitions

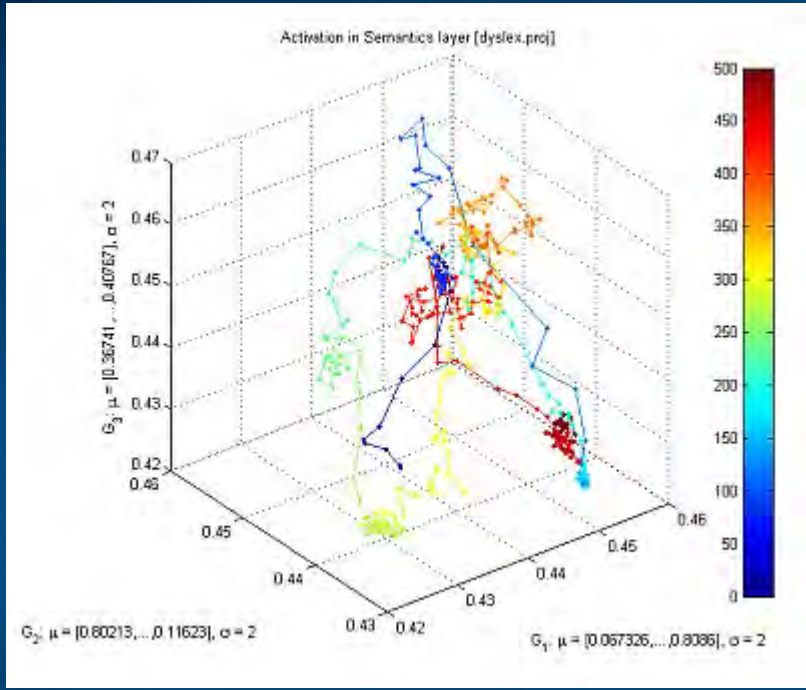

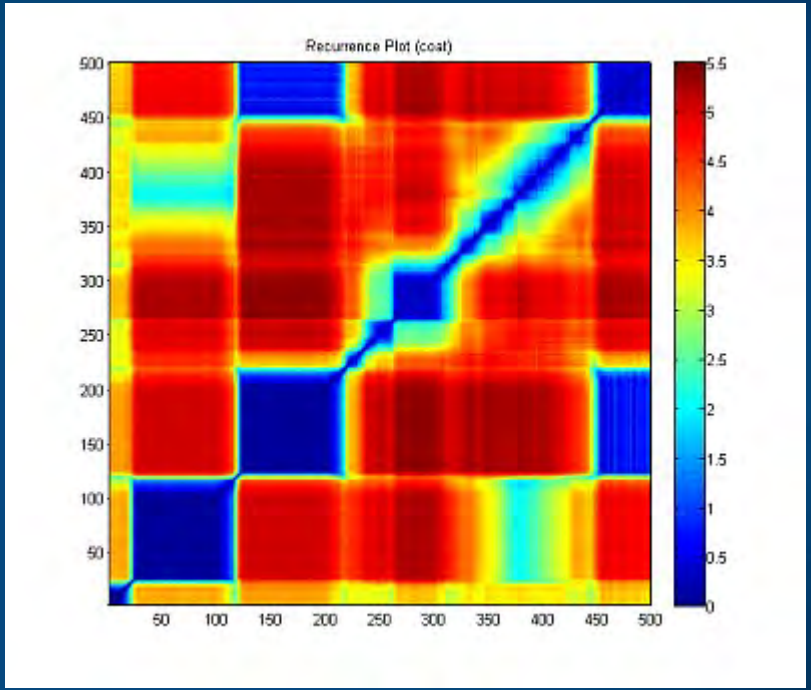

Attention is focused only for a brief time and than moved to the next attractor basin, some basins are visited for such a short time that no action may follow, corresponding to the feeling of confusion and not being conscious of fleeting thoughts.

Trajectory visualization

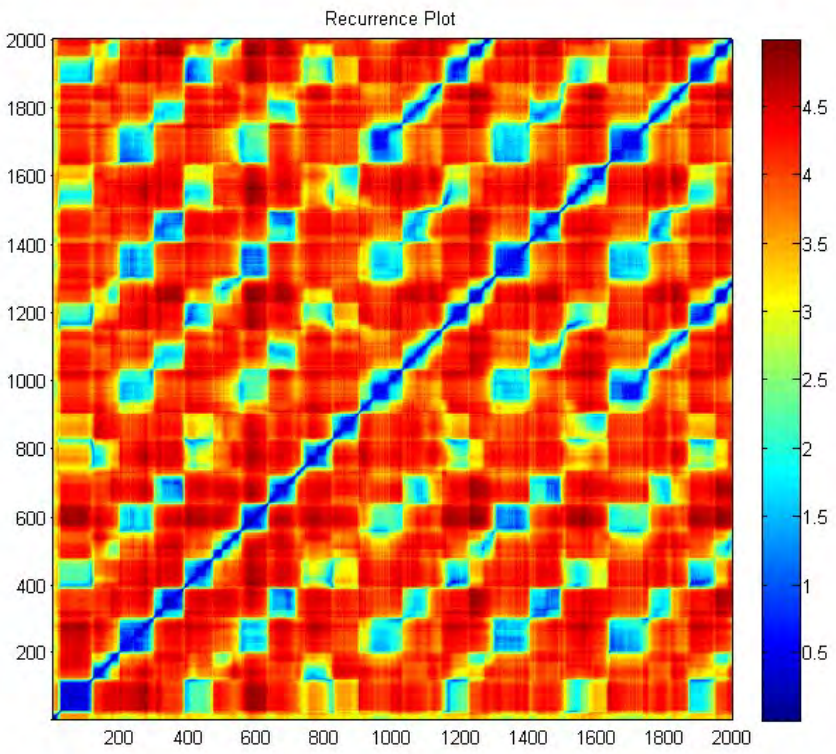

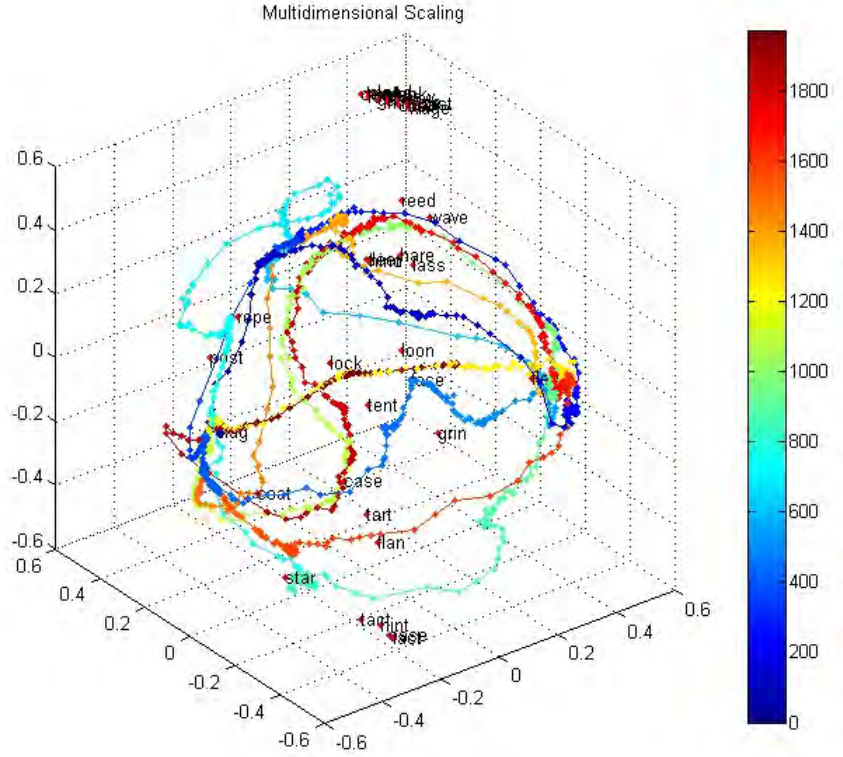

Recurrence plots and MDS/FSD/SNE visualization of trajectories of the brain activity. Here data from 140-dim semantic layer activity during spontaneous associations in the 40-words microdomain, starting with the word “flag”.

Our toolbox: http://fizyka.umk.pl/~kdobosz/visertoolbox/

ASD EEG SVM Classification

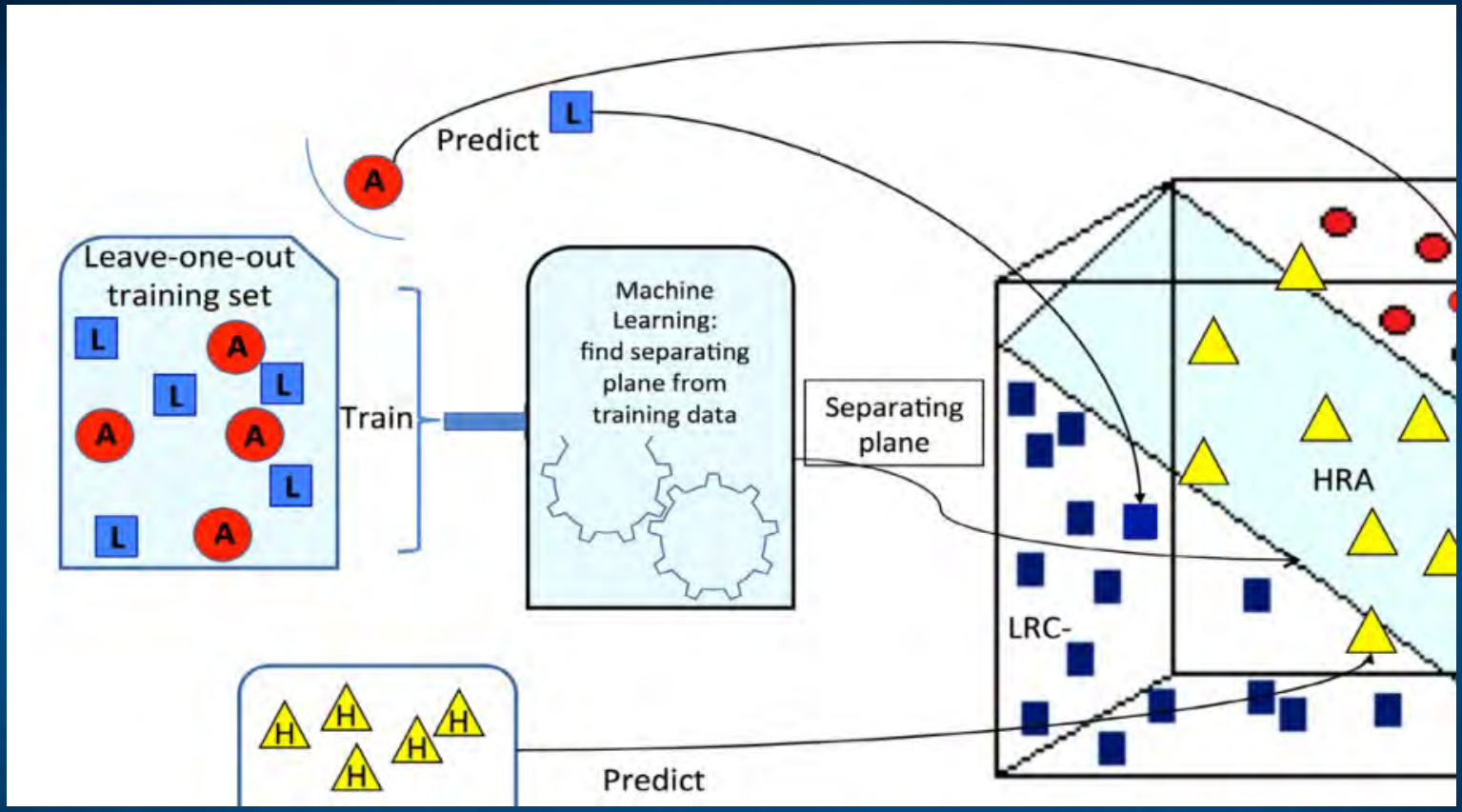

Wavelet decomposition, Recurrent Quantification Analysis, feature ranking and machine learning. Nonlinear features are critical to achieve good results, and their correlated with ASD depends on age.

EEG early ASD detection

Bosl, W. J., Tager-Flusberg, H., & Nelson, C. A. (2018). EEG Analytics for Early Detection of Autism Spectrum Disorder: A data-driven approach. Scientific Reports, 8(1), 6828.

EEG of 3 to 36-month old babies, 19 electrodes selected from 64 or 128.

Daubechies (DB4) wavelets transform EEG signal into 6 bands.

7 features from Recurrence Quantitative Analysis (RQA): RP entropy, recurrence rate, laminarity, repetition, max/mean line length, trapping time.

In addition sample entropy and Detrended Fluctuation Analysis was used.

Nonlinear features were computed from EEG signals and used as input to statistical learning methods. Prediction of the clinical diagnostic outcome of ASD or not ASD was highly accurate.

SVM classification with 9 features gave high specificity and sensitivity, exceeding 95% at some ages. Prediction using only EEG data taken as early as 3 months of age was strongly correlated with the actual measured scores.

EEG non-linear features

Features: not only structure, but also dynamics.

Nonlinear invariant measures of a time series and their physical interpretation, recurrence quantification analysis (RQA).

For example:

1. Sample Entropy (SampE)
2. Entropy derived from recurrence plot (L_entr).
3. Recurrence rate (RR), probability of recurrence.
4. Determinism (DET), repeating patterns in the system.
5. Laminarity (LAM), frequency of transitions between states.
6. Trapping time (TT), time in a given state.

Probability of recurrence

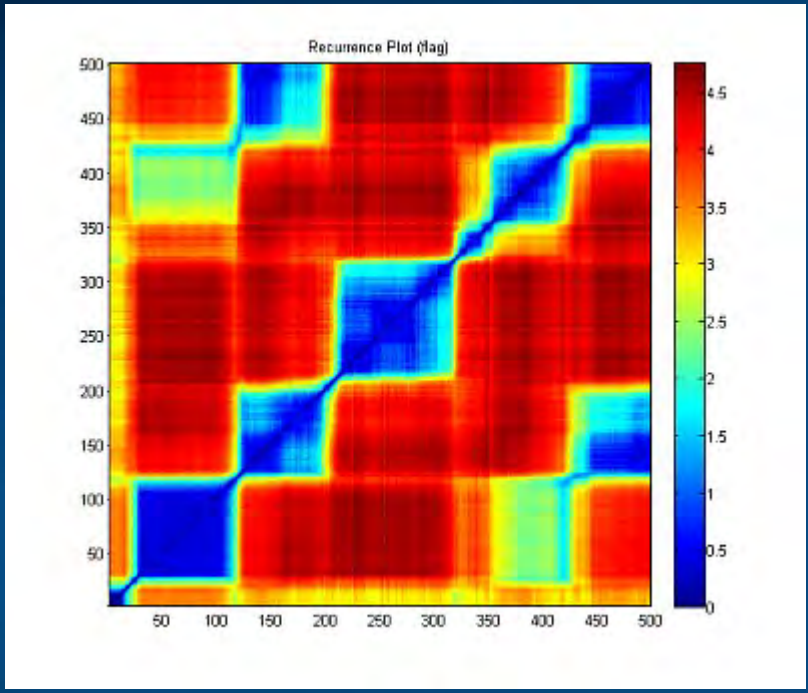

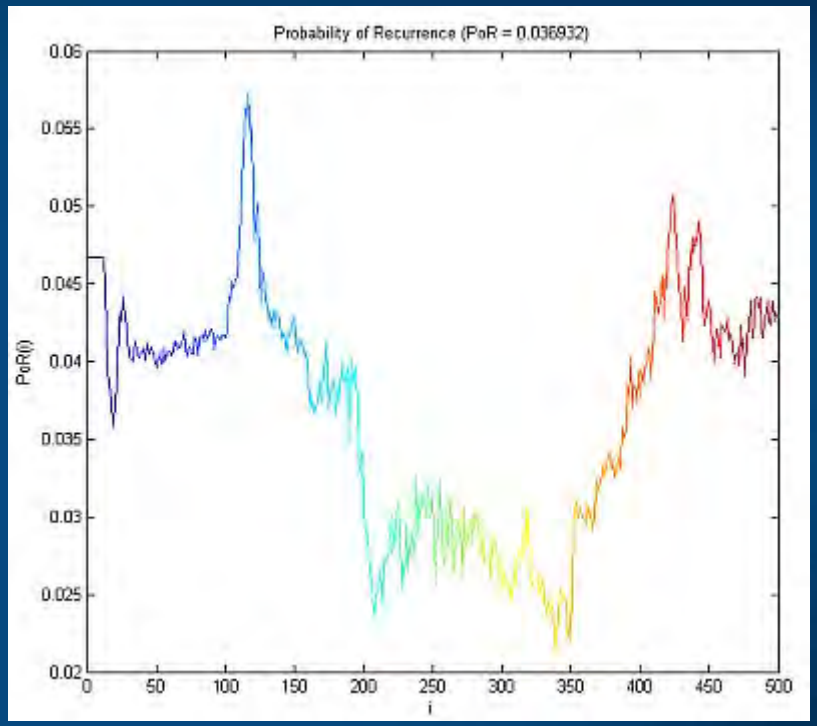

Probability of recurrence may be computed from recurrence plots, or from clusterization of trajectory points, allowing for evaluation how strongly some basins of attractors capture neurodynamics.

Our Viser Toolbox is used for all visualizations

ASD vs Low Risk Healthy

RR = recurrence rate

L_max = max line length, related to Lyapunov exponent

TT = trapping time

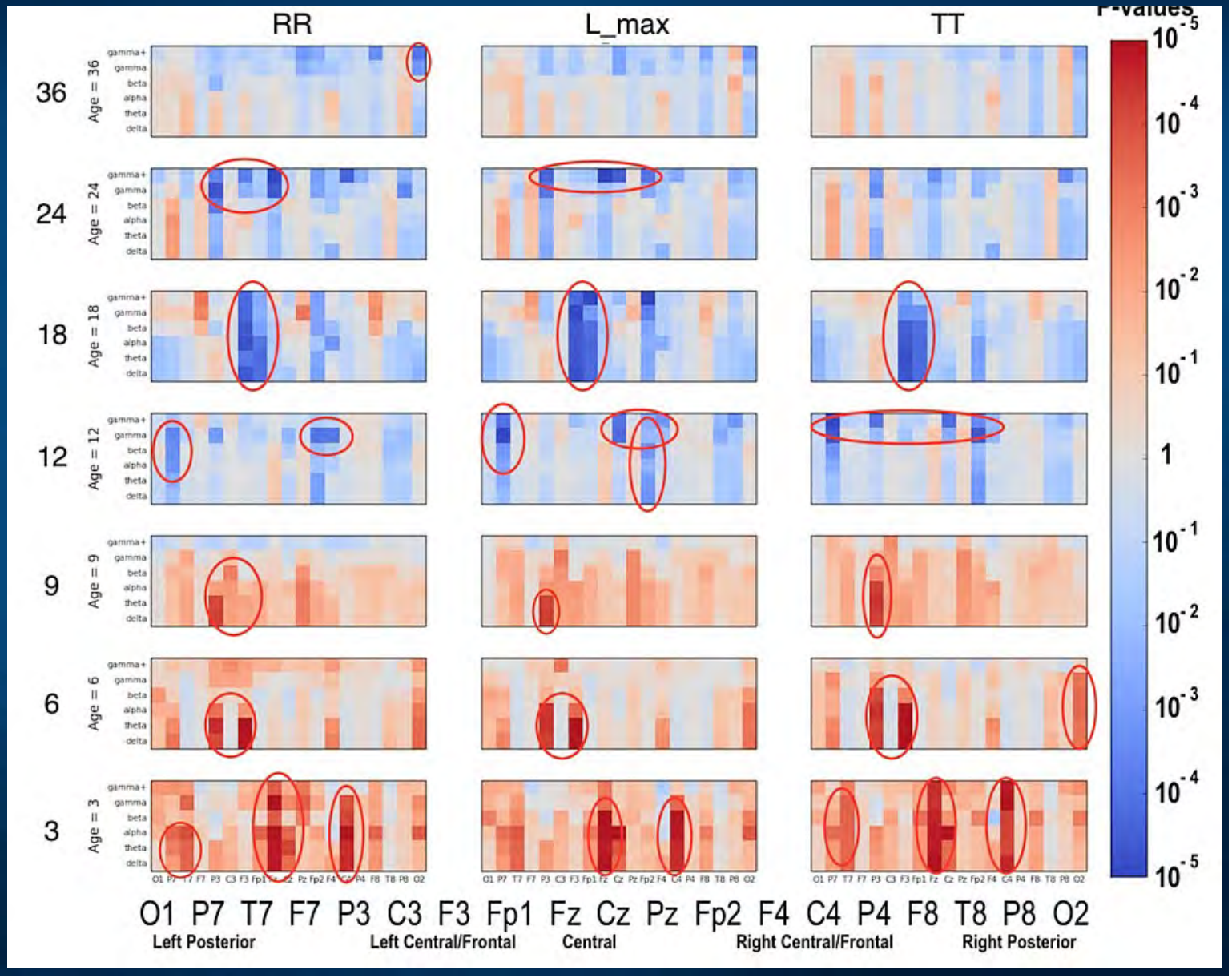

ASD EEG SVM Classification

Developmental trajectories for SampE in the left temporal region (T7 sensor) in higher frequencies (beta+gamma) for ASD, LRC-, and HRA-

LRC low risk controls

HRA high risk for ASD - no ASD

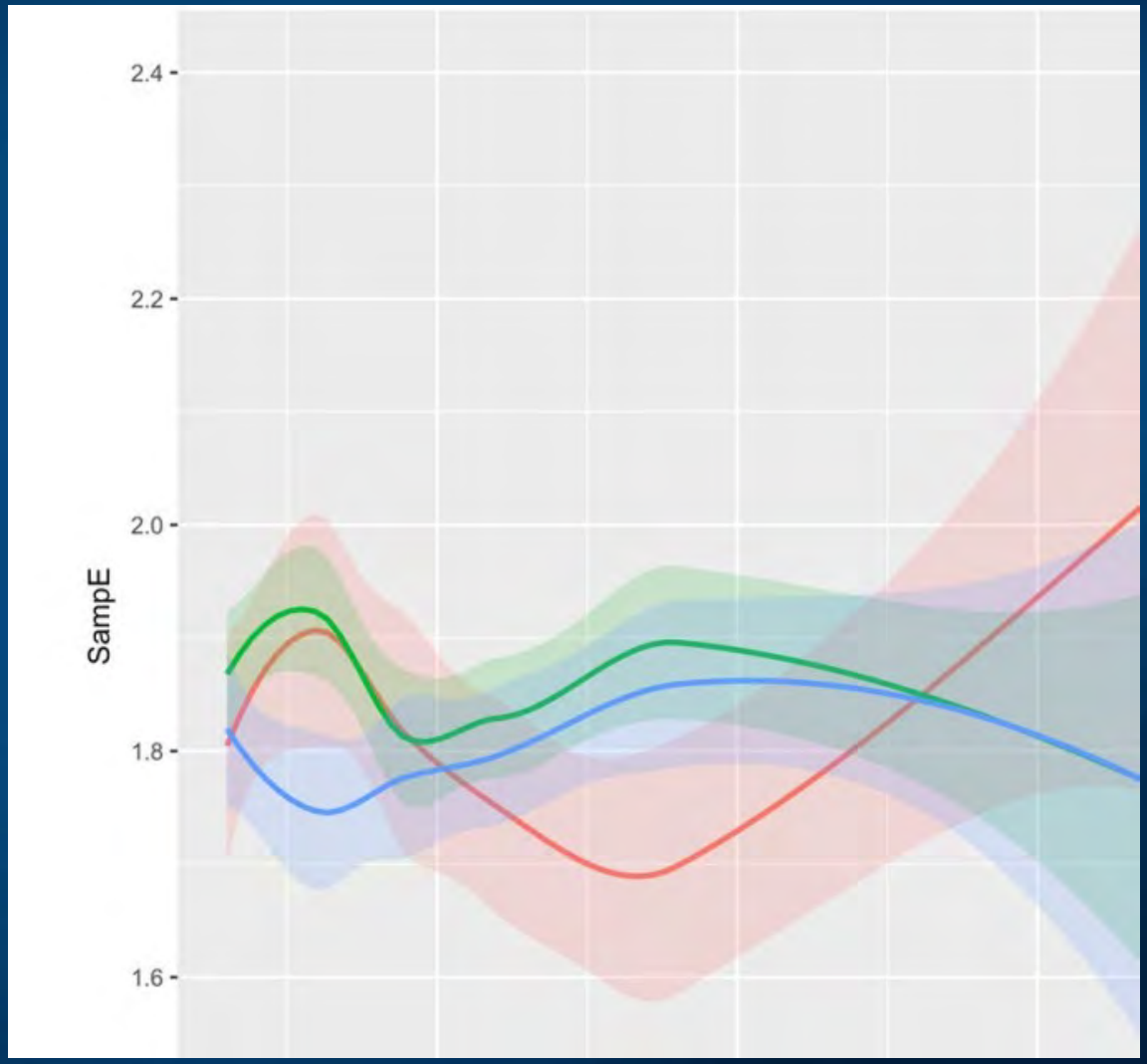

ASD EEG SVM Classification

Developmental trajectories for SampE in the right temporal-parietal region

(T8 +P4+P8 sensors) in frequencies theta through gamma for ASD, LRC-, and HRA-.

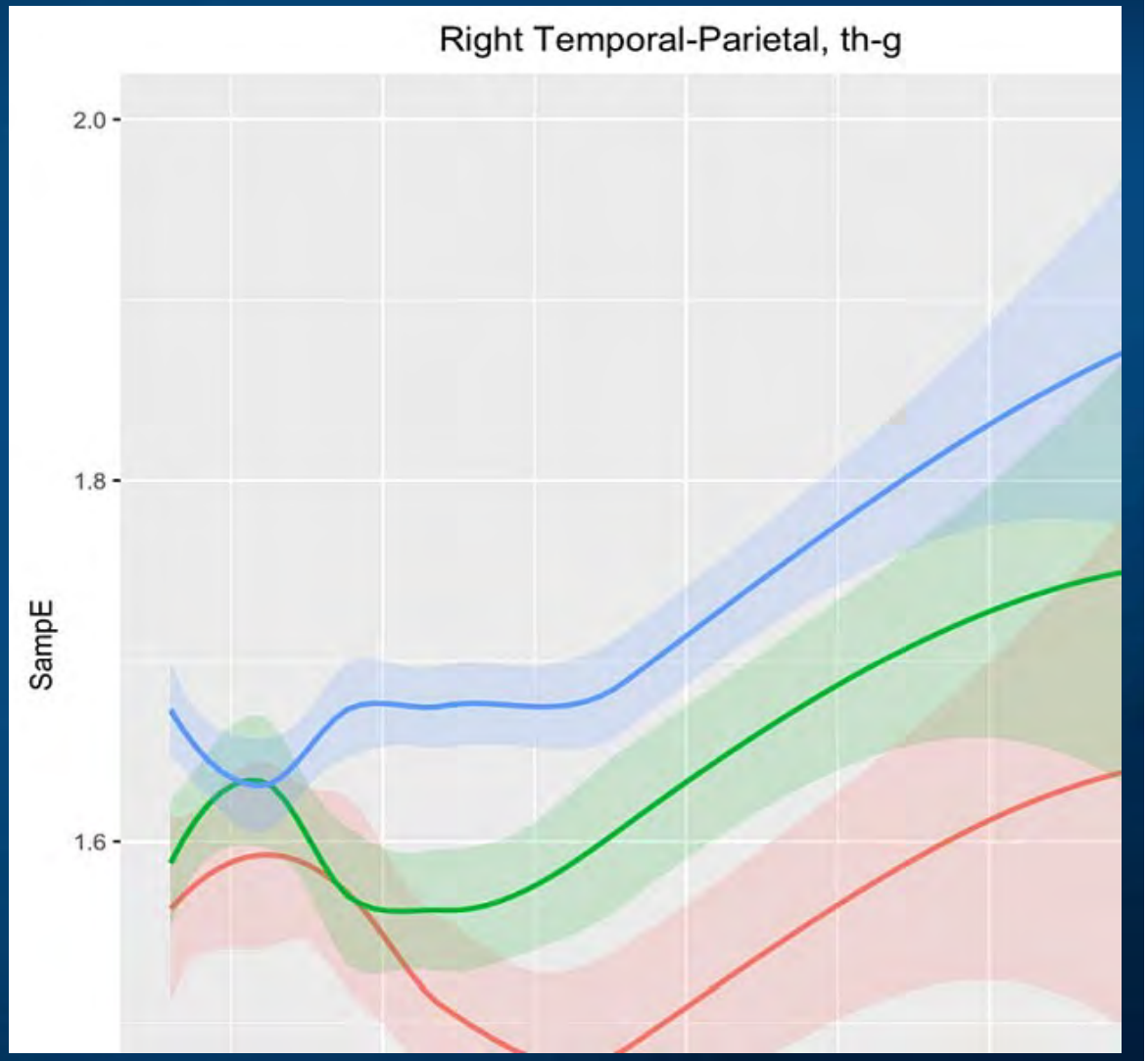

Trajectory visualization

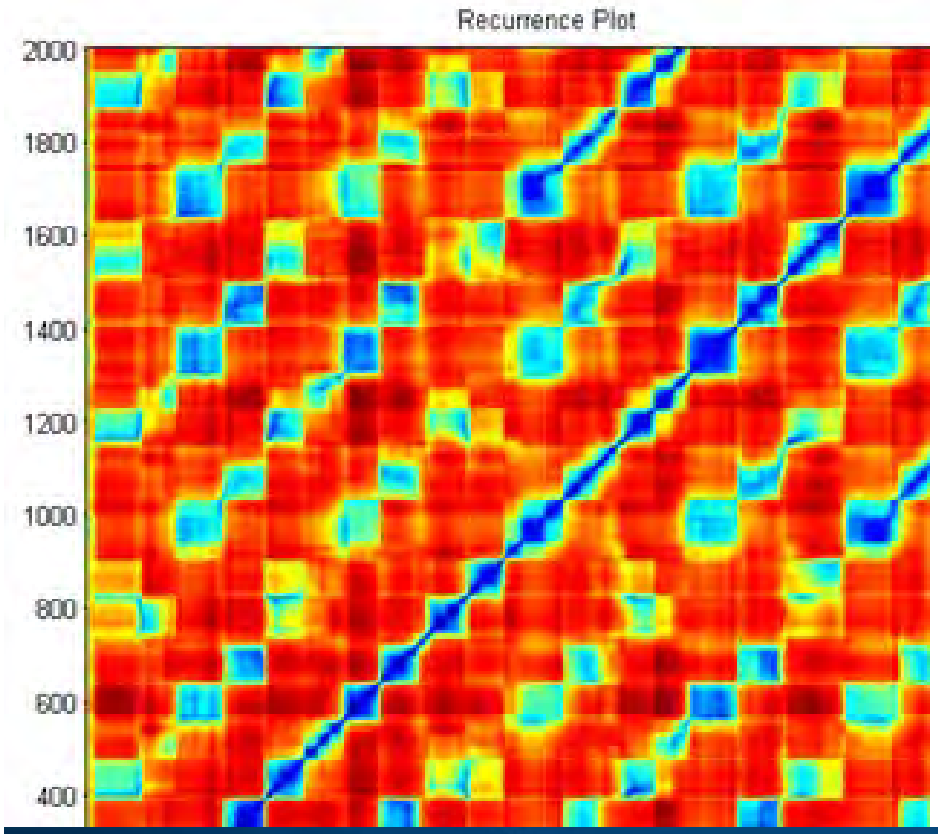

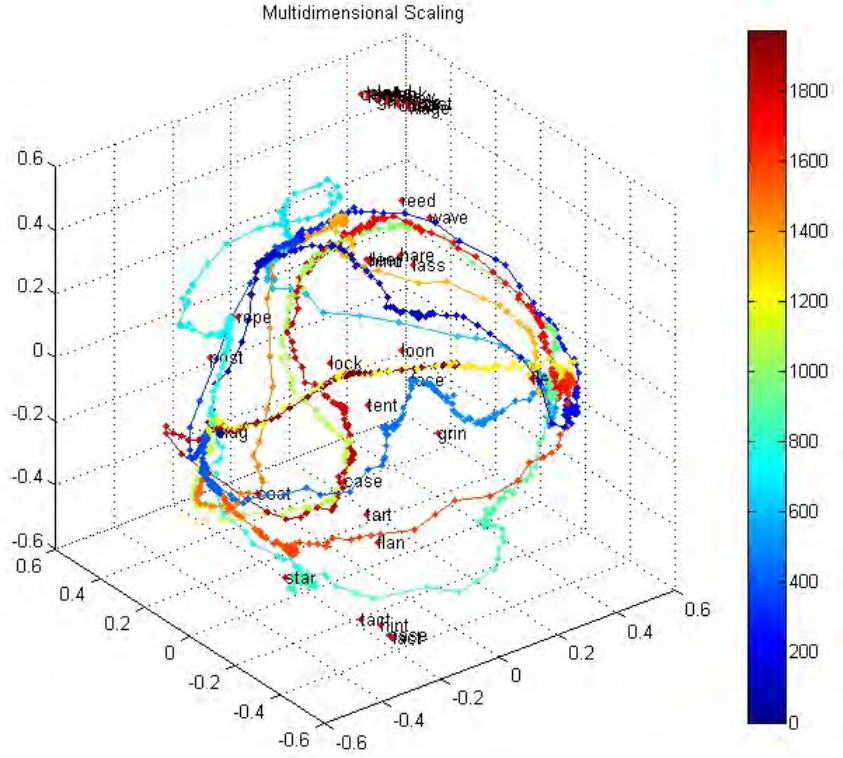

Trajectories may be visualized either using recurrence plots that shows relative changes of the trajectory or some form of visualization showing absolute positions of points on trajectories (MDS/FSD/SNE). Visualization shows transitions between microstates, or attractor states.

Depth of attractor basins

Variance around the center of a cluster grows with synaptic noise; for narrow and deep attractors it will grow slowly, but for wide basins it will grow fast.

Jumping out of the attractor basin reduces the variance due to inhibition of desynchronized neurons.

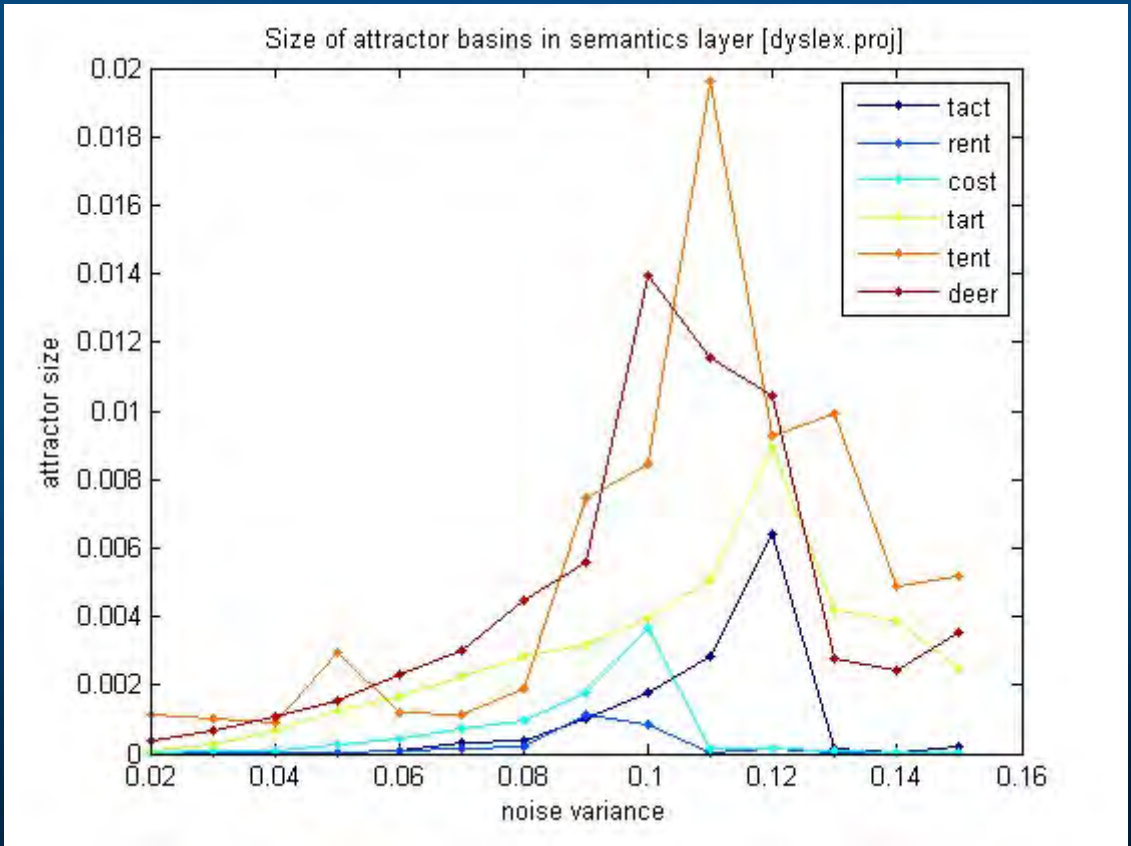

Typical Development vs. Autism

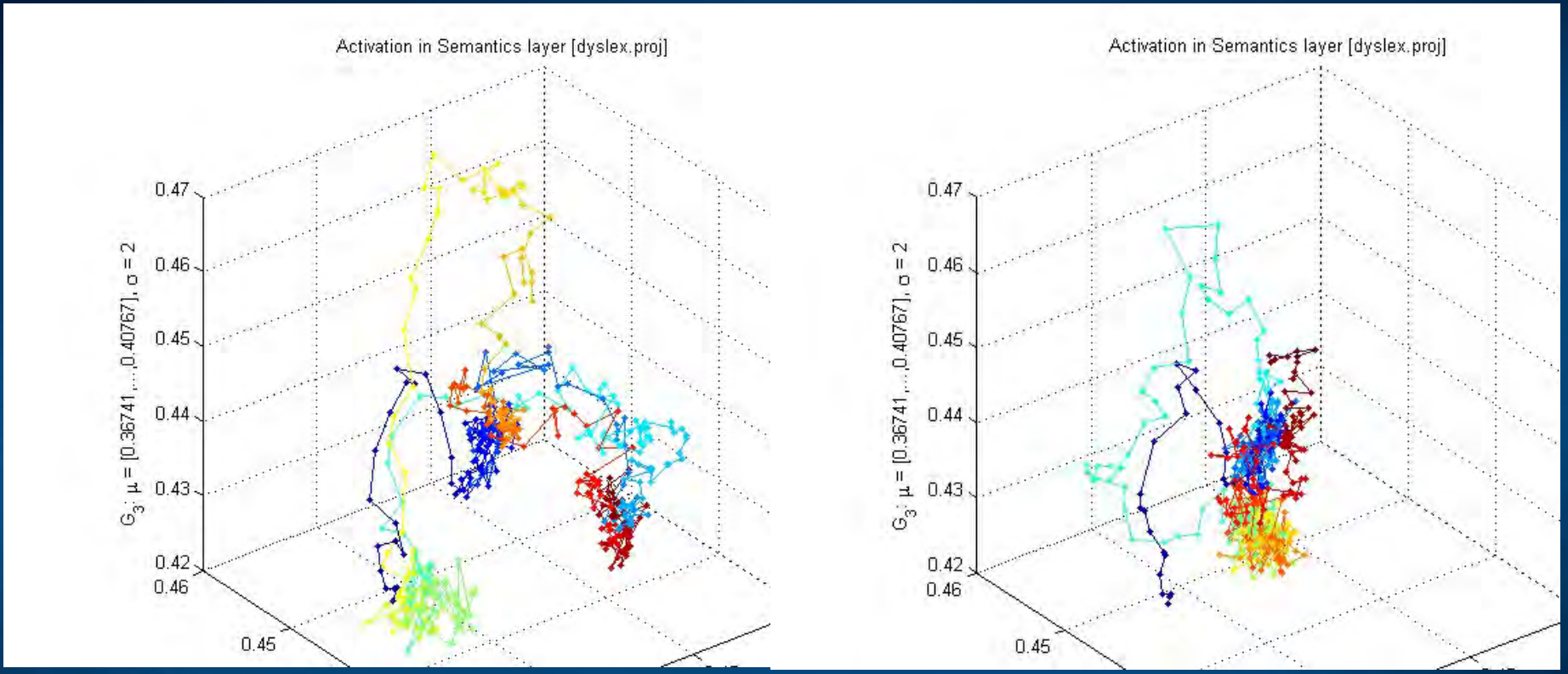

All plots for the flag word, different values of b_inc_dt parameter in the accommodation mechanism. b_inc_dt = 0.01 & b_inc_dt = 0.005

b_inc_dt = time constant for increases in intracellular calcium building up slowly as a function of activation, controls voltage-dependent leak channels.

http://kdobosz.wikidot.com/dyslexia-accommodation-parameters

Typical Development vs ADHD

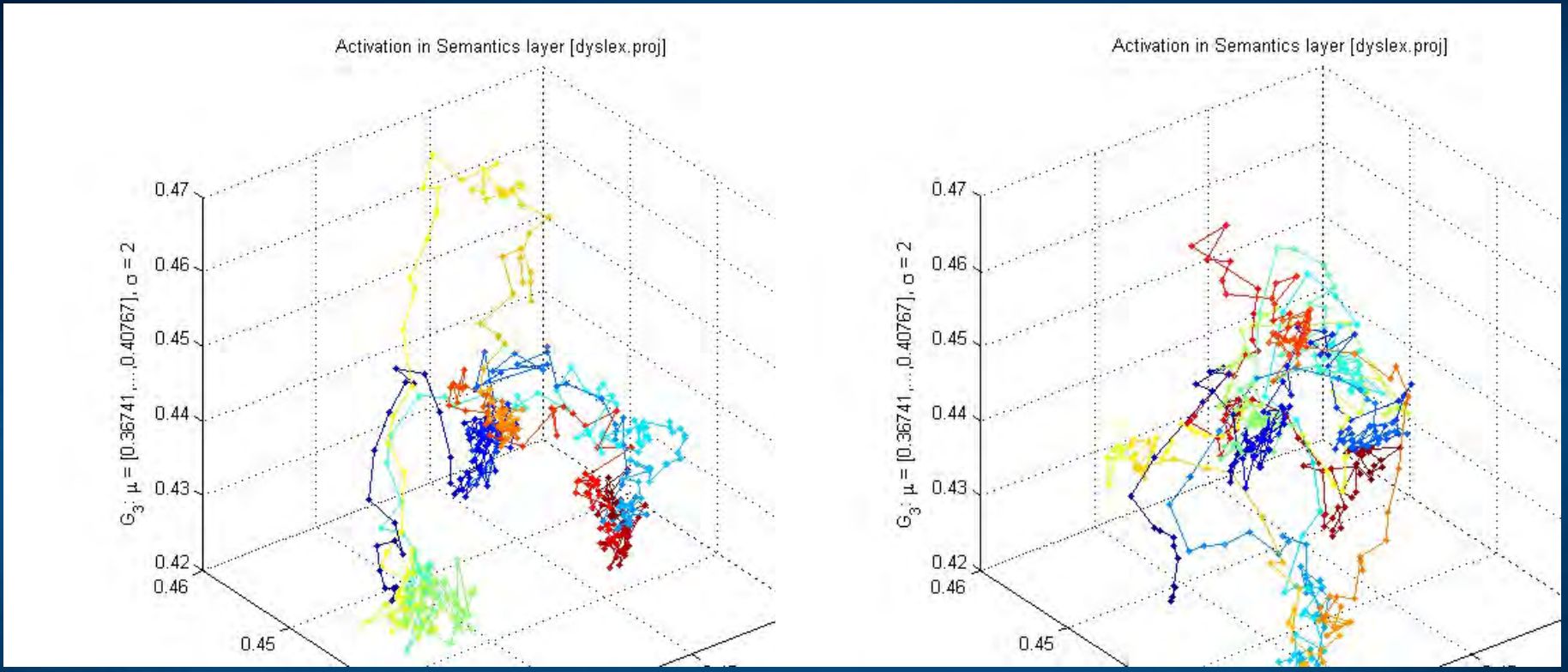

All plots for the flag word, different values of b_inc_dt parameter in the accommodation mechanism. b_inc_dt = 0.01 & b_inc_dt = 0.02.

b_inc_dt = time constant for increases in intracellular calcium which builds up slowly as a function of activation.

http://kdobosz.wikidot.com/dyslexia-accommodation-parameters

Rapid Serial Visual Presentation

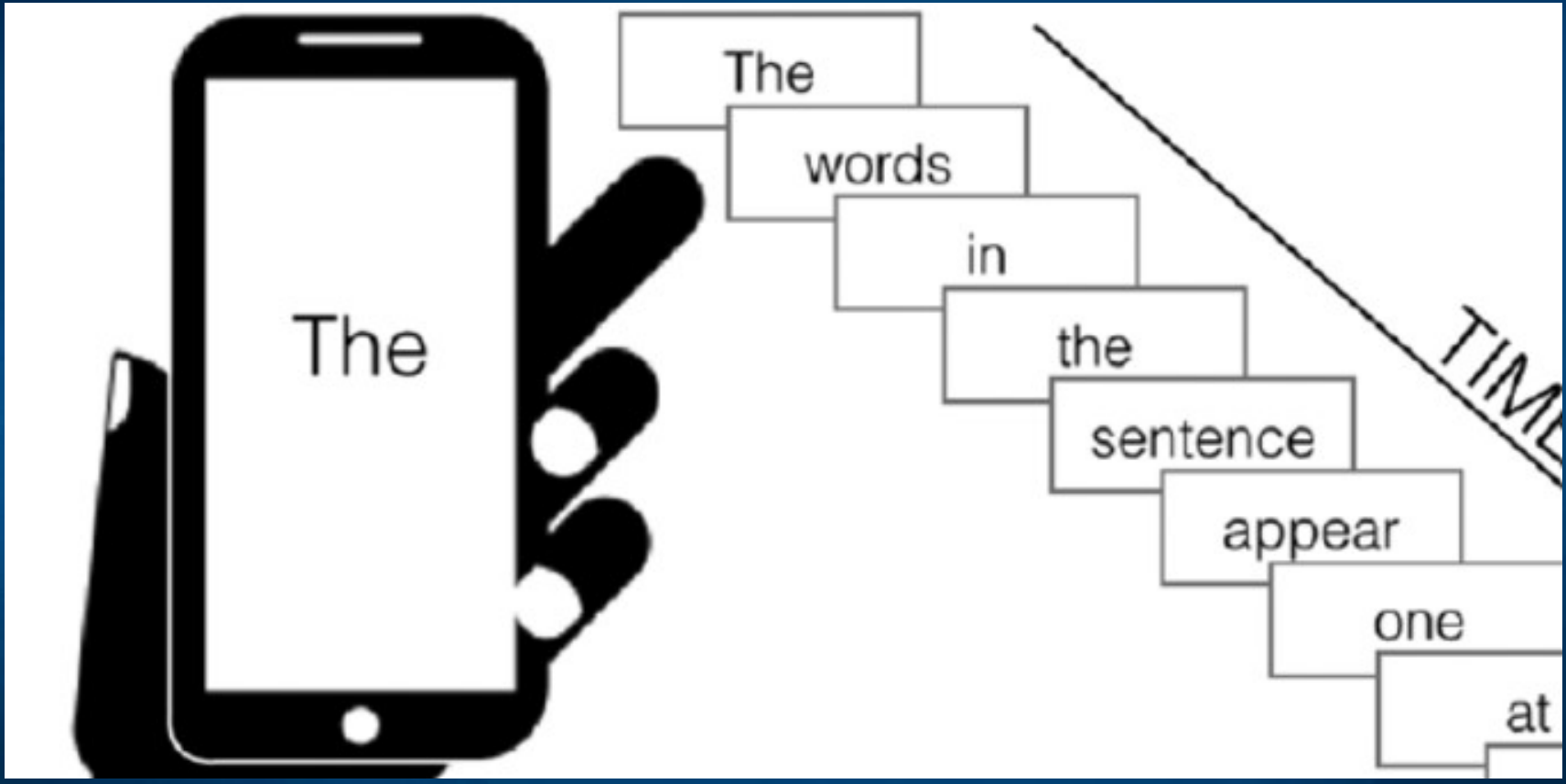

Any RSVP applications for fast reading.

Simulation: showing series of words, looking for attention/associations.
star => flea => tent => lock => tart => hind

RSVP: typical brain

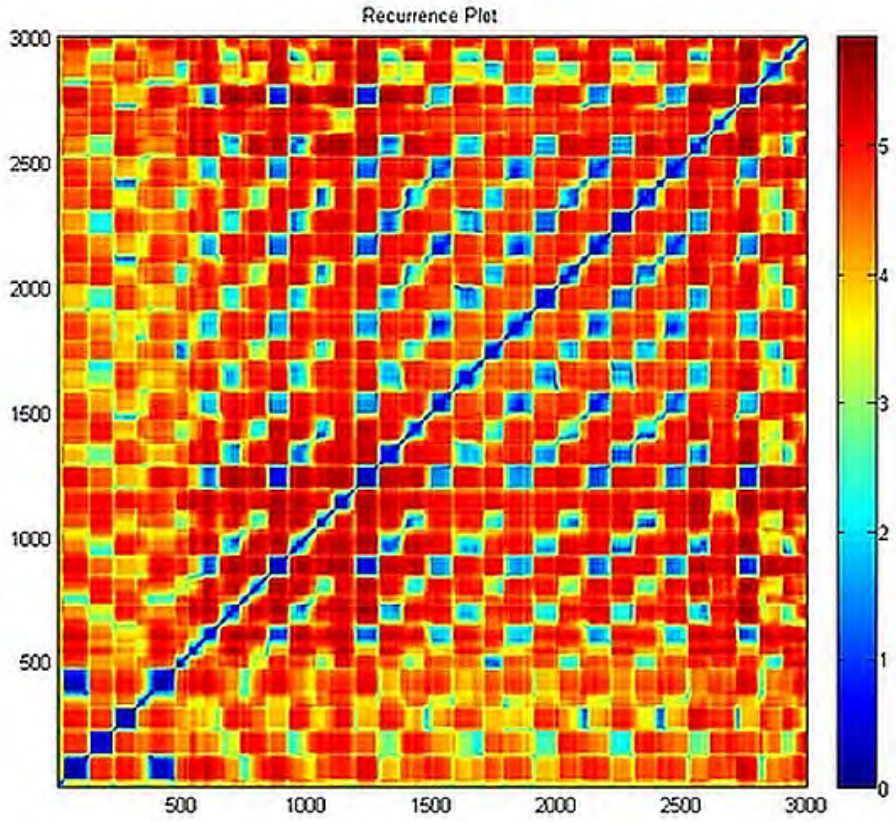

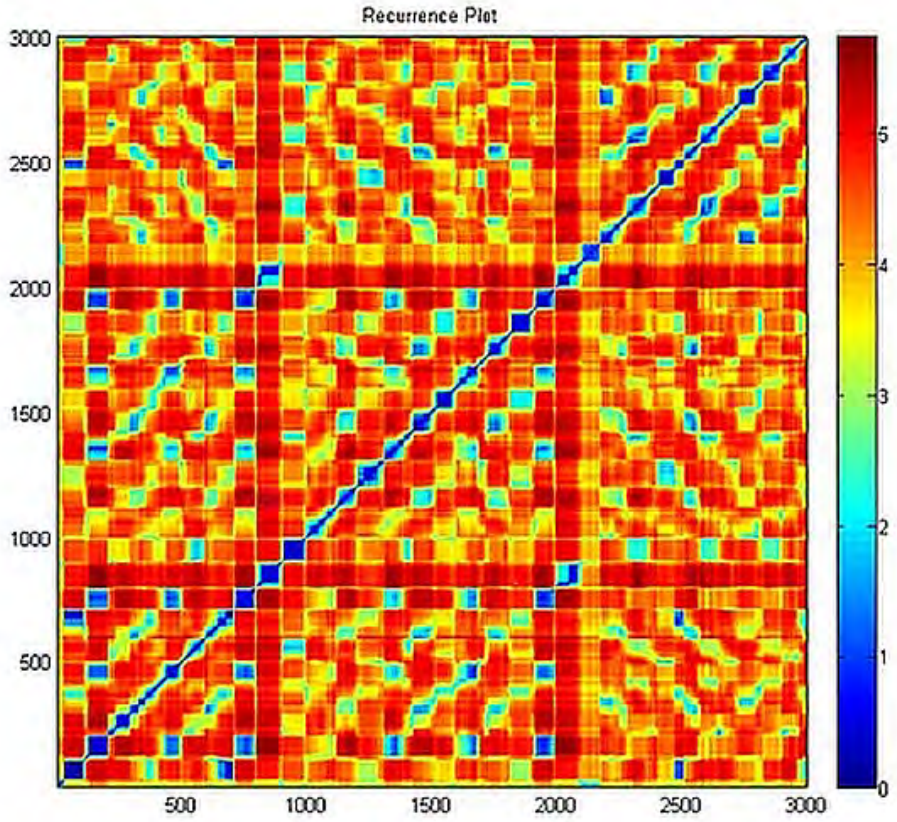

Normal speed
associations, context=>understanding

Some shallow microstates, no associations

too fast, speed 5x
microstates get blurred,

few associations

RSVP simulations: HFA

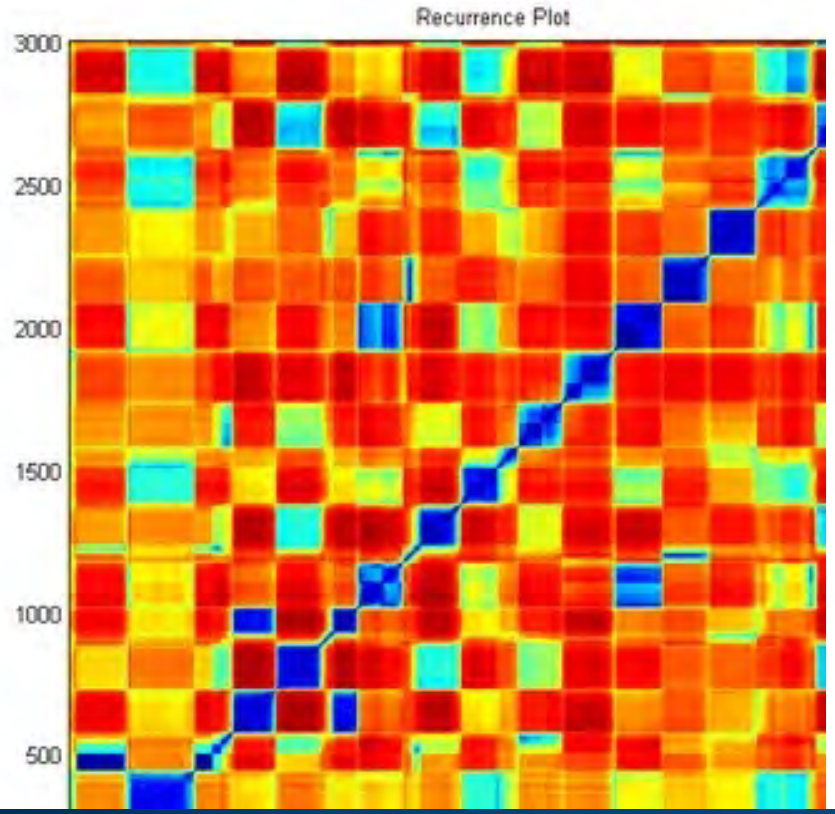

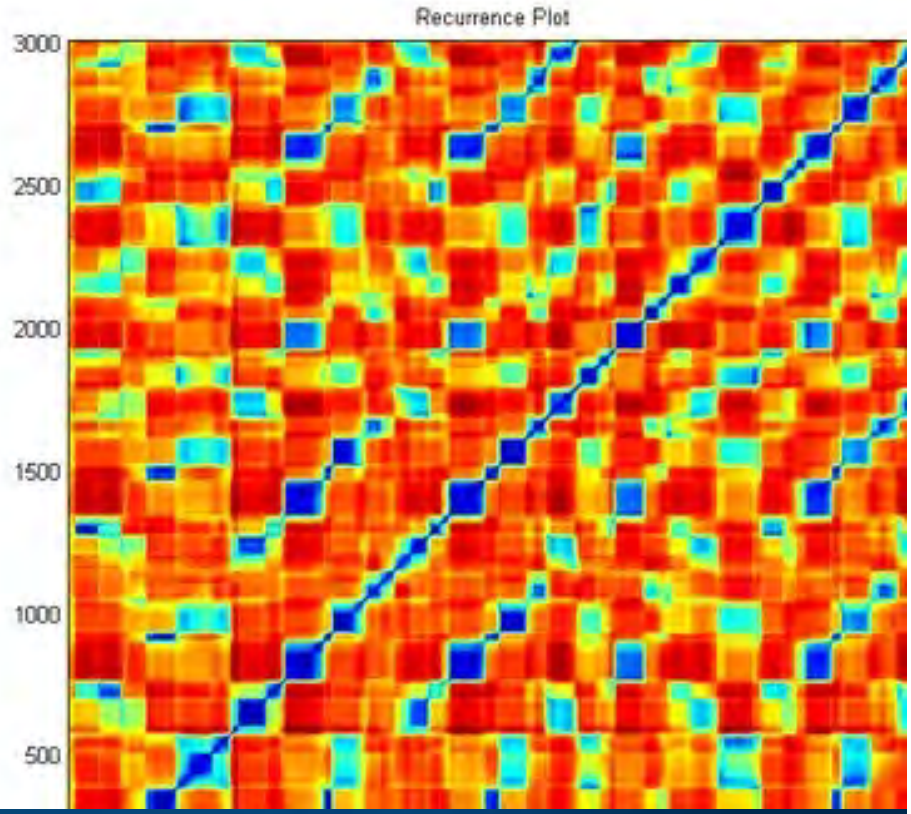

High functioning ASD case (HFA):

normal presentation
long dwelling times

fast presentation
enforced quick resynchronization
more internal stimuli.

RSVP simulations in deep autism

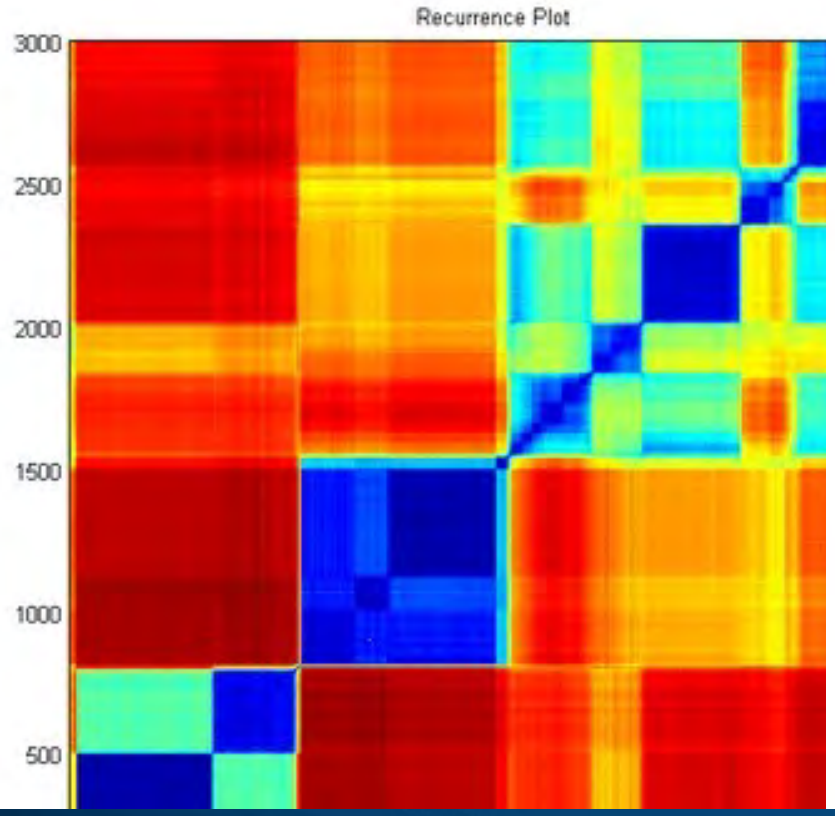

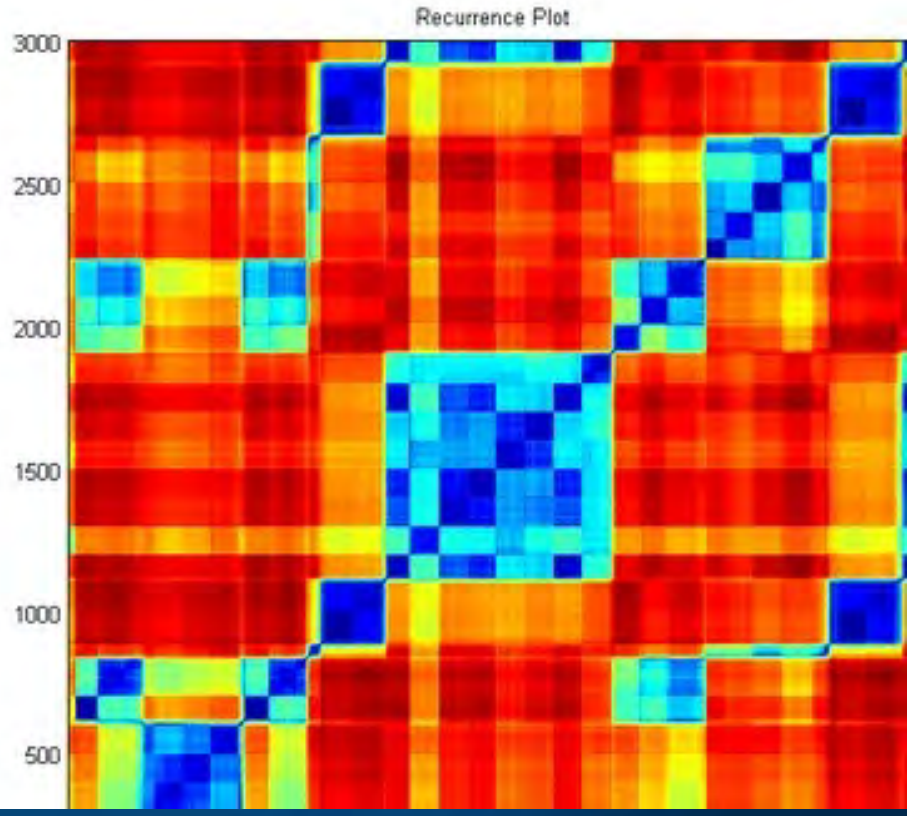

Normal speed
skipping some words,
no associations

fast presentation
more internal states
some associations arise

Conclusions

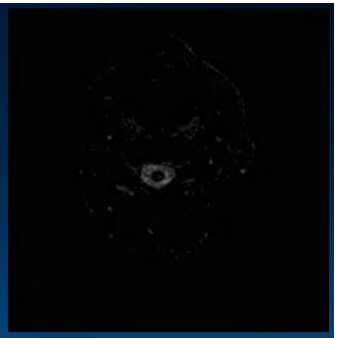

- Many brain states are now linked to specific mental states, and can be transformed into signals that we can understand: motor intentions, plans, images, inner voices …
- Neuroimaging ⇔ models of whole brain (TVB) ⇔ networks, neurodynamics ⇔ interpretation, mental states: S(B) ⇔ S(M).
- Neurodynamics is the key to understanding mental states; it creates dynamical forms, changing states of functional connectomes without re-arranging physical elements. Influence of other phenomics levels on mental states may be understood indirectly, via changes in neurodynamics.
- AI/ML draws inspirations from brain research, but also neural network models and learning algorithms (CNN, recurrence networks, reinforcement learning) help to interpret information processing in the brain.
- Many neurocognitive technologies are coming, helping to diagnose, repair and optimize brain processes.

International Ne

analyze diverse

brain and positi

Polish INCF Nod

Nicolaus Coperr

12th INCF Cong

Neuroimaging,

al: integrate and

understand the

.

nce 2017 at the

Warsaw 9/2019.

ce.

NE

Sessi 9

• G

infrastructure interoperabilit

• Data management and workfl

• Future of a

• Comparative and pred

incf | Neuro Informatics 2019

Warsaw, Poland | September 1-2

Join the global INCF community for

keynotes | panel discussions | posters | demos | socials

Speakers

Jan Bjaalie, *University of Oslo*
Rafal Bogacz, *University of Oxford*
Andrzej Cichocki, *RIKEN CBS*
Maureen Clerc, *Inria*
Carole Goble, *University of Manchester*
William Grisham, *UCLA*
Michael Hawrylycz, *Allen Institute for Brain Science*
Henry Kennedy, *INSERM*
Naomi Penfold, *ASAPbio*
Ariel Rokem, *University of Washington*
Frances Skinner, *University of Toronto*
Pedro Valdes-Sosa, *Cuban Neuroscience Center, University of Electronic Science and Technology China*
Kirstie Whitaker, *University of Cambridge*
Alexander Woodward, *RIKEN CBS*

Thank you for synchronization of your neurons

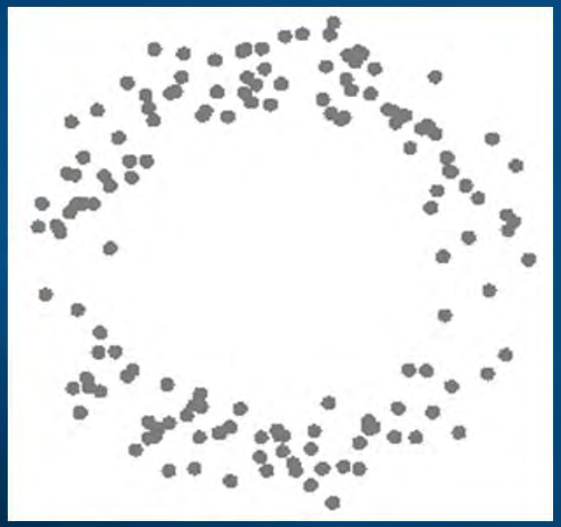

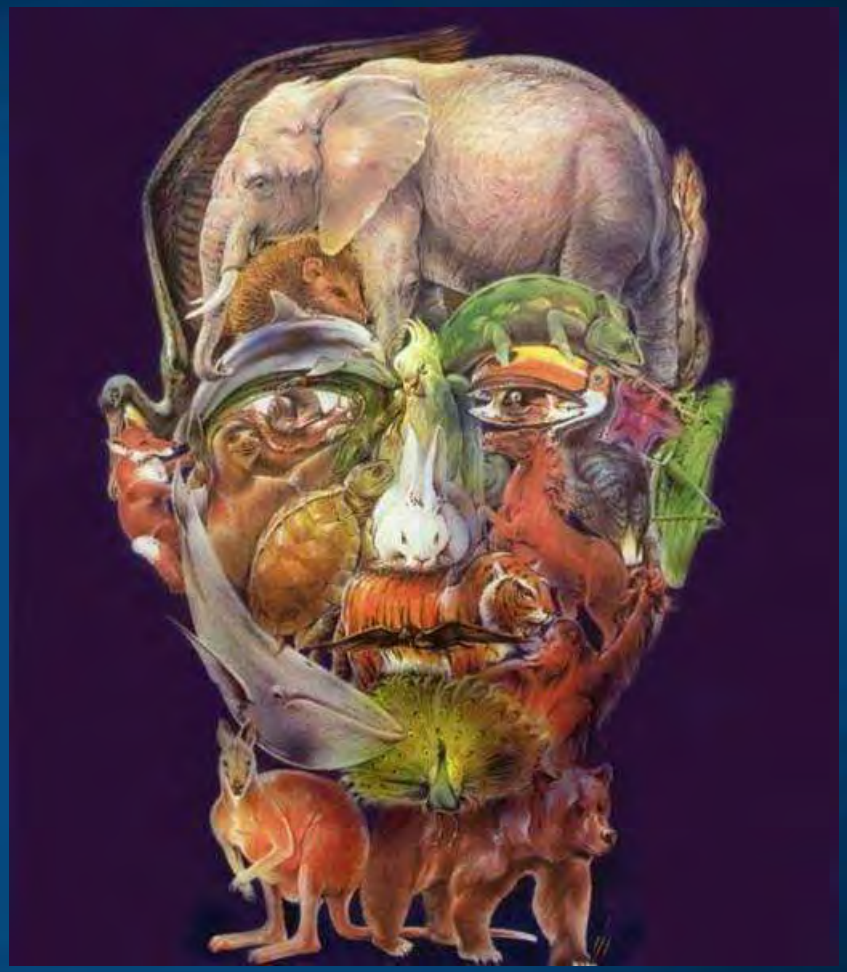

Google: W. Duch

=> talks, papers, lectures, Flipboard …